

**THE INVOLVEMENT OF IONOTROPIC AMPA RECEPTORS IN THE
PATHOGENESIS OF NEUROLOGICAL DISEASES**

A thesis submitted for the degree of Doctor of Philosophy in the Faculty of Science,
University of London

By

--OXO--

ANTHONY J. GROOM

--OXO--

Department of Pharmacology

Eisai London Research Laboratories

affiliated to -

Department of Anatomy and Developmental Biology

University College London

London

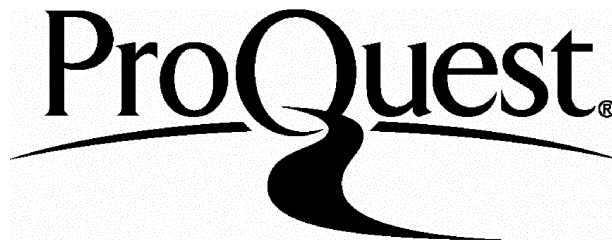
ProQuest Number: U642442

All rights reserved

INFORMATION TO ALL USERS

The quality of this reproduction is dependent upon the quality of the copy submitted.

In the unlikely event that the author did not send a complete manuscript and there are missing pages, these will be noted. Also, if material had to be removed, a note will indicate the deletion.



ProQuest U642442

Published by ProQuest LLC(2015). Copyright of the Dissertation is held by the Author.

All rights reserved.

This work is protected against unauthorized copying under Title 17, United States Code.
Microform Edition © ProQuest LLC.

ProQuest LLC
789 East Eisenhower Parkway
P.O. Box 1346
Ann Arbor, MI 48106-1346

Abstract

The interest in glutamate in the pathogenesis of neurodegenerative disorders has rapidly expanded since the early descriptions of the excitotoxic properties of amino acids in the central nervous system. With the identification of the numerous glutamate receptors, the contribution of the various ionotropic and metabotropic receptor subclasses to excitotoxicity has been intensely studied. A wealth of data support a role for AMPA receptor in acute neurodegeneration, exemplified by neuronal loss during stroke. More recently, however, the importance of low level glutamate exposure in the evolution of chronic neurodegenerative conditions has begun to emerge.

This thesis describes two aspects of AMPA receptor pathogenesis *in vivo*. (i.) The possible role for AMPA receptor activation and subsequent neurodegeneration within the context of acute and chronic rodent models of the inflammatory, demyelinating disorder, multiple sclerosis, and (ii.) the neurodegenerative phenotype associated with a, putatively, AMPA-mediated, spontaneous development of spasticity in the Han/Wistar *spa/spa* rat.

Experimental autoimmune encephalomyelitis in rodents reproduces physiological and pathological features of multiple sclerosis, including CNS inflammation, myelin breakdown and axonal loss. In two acute experimental autoimmune encephalomyelitis models, both competitive and non-competitive AMPA-receptor antagonists were effective in ameliorating disease severity. The efficacy *in vivo* correlated with the potency of the compounds in an *in vitro* AMPA receptor assay. The protective effects were independent of immunosuppressive or anti-inflammatory effects, as assessed by quantification of CNS inflammation and an *in vitro* T-cell proliferation assay.

Ultrastructural and immunohistochemical analysis revealed markers of axonal damage and a selective neurodegeneration of ventral horn motor neurons which had a direct T-cell-mediated component. The reduction in neuronal density was prevented by an AMPA receptor antagonist.

Glutamate-mediated neuronal cell death within the mature CNS is reported to occur via both necrosis and apoptosis, however, classification of the latter is often based on little more than TUNEL staining. More recently, several investigators have employed ultrastructural analysis to describe an additional form of cell death in neurons of the adult CNS. The Han/Wistar *spa/spa* rat shows chronic neurodegeneration beginning around 3-4 weeks of age. The CNS location of damage correlates with the presentation of motor deficits. The selective neurodegeneration in these animals is due, at least in part to, AMPA receptor activation, since the neuronal loss is reversed by AMPA receptor antagonists *in vivo*. Using ultrastructural analysis, neurodegeneration was revealed in discrete brain regions and whilst certain elements of apoptosis were preserved, such as reduction of cell volume and chromatin condensation with maintenance of organelles and cellular and nuclear membrane integrity, others like chromatin margination, membrane blebbing, or formation of apoptotic bodies were not observed. In addition, biochemical assessment of cell death showed that DNA breakdown occurred in many regions associated with known degeneration and at time points that were consistent with the onset of degeneration in these areas. However, whilst the crucial executor caspase, caspase-3, was active in the olfactory bulb where apoptosis of glial cells is known to be ongoing, activity was not observed in the other regions of neurodegeneration. This may suggest that this neuronal death in adult neurons is caspase-3 independent which would argue against classical apoptosis.

These studies open up a hitherto unexplored area of research and therapeutics within the field of multiple sclerosis and also question the role of classical neuronal apoptosis within the context of the adult central nervous system.

Table of Contents

Abstract	2
Table of Contents	5
List of Figures	10
List of Tables	13
Abbreviations	15
Acknowledgements	18
CHAPTER I - Glutamate	19
1.1 Glutamate receptors	20
1.1.1 Ionotropic glutamate receptors	20
1.1.1.1 NMDA receptors	21
<i>i. Conductivity</i>	22
<i>ii. Modulation</i>	23
1.1.1.2 AMPA receptors	25
<i>i. Conductivity</i>	26
<i>ii. Modulation</i>	26
1.1.1.3 Kainate receptors	28
<i>i. Conductivity</i>	29
<i>ii. Modulation</i>	30
1.1.2 Metabotropic glutamate receptors	31
1.2 Physiological function of glutamate receptors in the brain and spinal cord	32
1.3 Involvement of glutamate receptors in neuronal degeneration	33

1.4 Aims of thesis	35
CHAPTER 2 - AMPA and Multiple Sclerosis	37
2.1 Epidemiology and prevalence of multiple sclerosis	37
2.2 Pathogenesis of multiple sclerosis	40
2.2.1 Demyelination in the pathogenesis of multiple sclerosis	40
2.2.2 Neuronal degeneration in the pathogenesis of multiple sclerosis	42
2.3 Current therapies	44
2.4 Involvement of glutamate in the pathogenesis of multiple sclerosis.....	48
2.4.1 Oligodendrocyte protection in multiple sclerosis	48
2.4.2 A role for neuroprotection in multiple sclerosis?	49
2.5 Experimental autoimmune encephalomyelitis	51
2.6 Pathogenesis of experimental autoimmune encephalomyelitis	53
2.7 Evidence for the glutamatergic system in the pathogenesis of experimental autoimmune encephalomyelitis	55
2.8 Models of experimental autoimmune encephalomyelitis	57
2.9 Materials and methods	59
2.9.1 Animals	59
2.9.2 Induction of experimental autoimmune encephalomyelitis in Lewis rats	59
2.9.3 Adoptive transfer experimental autoimmune encephalomyelitis in Lewis rats	60
2.9.4 Neurological assessment.....	60
2.9.5 Induction of chronic relapsing experimental autoimmune encephalomyelitis	61
2.9.6 Compounds and dosing regimens	62
2.9.6.1 Actively-induced acute experimental autoimmune encephalomyelitis.....	63
2.9.6.2 Adoptive transfer acute experimental autoimmune encephalomyelitis	64
2.9.6.3 Chronic experimental autoimmune encephalomyelitis in Biozzi mice	64

2.9.7 Quantification of neuroinflammation.....	64
2.9.8 Evaluation of immunosuppression in a T-cell proliferation assay <i>in vitro</i>	65
2.9.9 Quantification of neuronal density in the spinal cord.....	66
2.9.10 Light microscopy.....	67
2.9.11 Electron microscopy.....	68
2.9.12 Immunohistochemistry	69
2.9.13 Statistics	70
2.10 Results	71
2.10.1 The effects of AMPA modulation on the progression of experimental autoimmune encephalomyelitis in the Lewis rat	71
2.10.1.1 NBQX in acute Lewis rat experimental autoimmune encephalomyelitis.....	71
2.10.1.2 MPQX in acute Lewis rat experimental autoimmune encephalomyelitis.....	74
2.10.1.3 GYKI52466 in acute Lewis rat experimental autoimmune encephalomyelitis	75
2.10.1.4 GYKI53773 in acute Lewis rat experimental autoimmune encephalomyelitis	76
2.10.1.5 BIIR561 in acute Lewis rat experimental autoimmune encephalomyelitis	77
2.10.1.6 CP465022 in acute Lewis rat experimental autoimmune encephalomyelitis	78
2.10.1.7 Aniracetam in acute Lewis rat experimental autoimmune encephalomyelitis.....	79
2.10.1.8 NBQX in Lewis rat adoptive transfer experimental autoimmune encephalomyelitis	80
2.10.2 AMPA antagonism ameliorates chronic Biozzi mouse experimental autoimmune encephalomyelitis	82
2.10.2.1 Acute phase treatment with NBQX and long term outcome in chronic mouse experimental autoimmune encephalomyelitis.....	82
2.10.2.2 NBQX treatment during the secondary phase of disease in chronic mouse experimental autoimmune encephalomyelitis.....	84
2.10.3 AMPA antagonism and perivascular inflammation in Lewis rat experimental autoimmune encephalomyelitis	84
2.10.4 The effects of AMPA antagonism on <i>in vitro</i> T-cell proliferation	85
2.10.5 Morphological analysis of lumbar spinal cord from Lewis rats with acute experimental autoimmune encephalomyelitis.	88

2.10.6 Change in neuronal density in the lumbar spinal cord of Lewis rats with experimental autoimmune encephalomyelitis	96
2.10.7 Demyelination in the lumbar spinal cord of Biozzi mice with experimental autoimmune encephalomyelitis	97
2.11 Discussion.....	99
2.11.1 AMPA receptor antagonist <i>in vivo</i> efficacy.....	99
2.11.2 Immunosuppressive and anti-inflammatory profiles of AMPA receptor antagonists	102
2.11.3 Oligodendrocyte protection in Lewis rat acute experimental autoimmune encephalomyelitis .	104
2.11.4 Neuronal and axonal pathology in the Lewis rat model of acute experimental autoimmune encephalomyelitis	105
2.11.5 NBQX in Biozzi mouse experimental autoimmune encephalomyelitis	113
2.11.6 Conclusions.	114
CHAPTER 3 - AMPA and Chronic Neurodegeneration	116
3.1 Glutamate and neurodegeneration	116
3.2 AMPA and neurodegeneration	118
3.3 Mechanism of AMPA receptor pathogenesis.....	119
3.3.1 Increase in AMPA receptor density.....	119
3.3.2 Q/R editing in the GluR2 subunit	120
3.3.3 Absence of GluR2 expression within the AMPA receptor channel complex	121
3.4 The <i>spa/spa</i> rat.....	122
3.4.1 Involvement of AMPA in the pathophysiology	123
3.5 Mechanism of cell death	124
3.6 Neuronal death in <i>spa/spa</i> rat.....	127
3.7 Materials and methods	129
3.7.1 Animals	129
3.7.2 Light microscopy.....	129

3.7.3 Electron microscopy.....	130
3.7.4 Sample preparation for caspase activity assay and nucleosome ELISA.....	131
3.7.5 Nucleosome enzyme-linked immunosorbent assay (ELISA).....	132
3.7.6 Caspase-3 activity assay.....	132
3.7.7 TdT-mediated dUTP nick end labelling (TUNEL).....	133
3.7.8 Statistics.....	134
3.8 Results.....	135
3.8.1 Verification of the cell death detection ELISA and caspase-3 activity assay sensitivity.....	135
3.8.2 Regional distribution of DNA damage in <i>spa/spa</i> rats at 4 weeks.....	136
3.8.3 Regional distribution of caspase-3 activity in 4 week old <i>spa/spa</i> rats.....	138
3.8.4 Comparison of DNA cleavage in selected brain regions at 4 and 8 weeks in <i>spa/spa</i> rats.....	140
3.8.5 TUNEL staining in the cerebellum of <i>spa/spa</i> rats.....	142
3.8.6 Light microscopy in <i>spa/spa</i> CNS tissue.....	144
3.8.7 Electron microscopy in <i>spa/spa</i> rats.....	147
3.8.7.1 Purkinje cell degeneration in the cerebellum of <i>spa/spa</i> rats.....	148
3.8.7.2 Motor neuron degeneration in the ventral horn of the lumbar spinal cord in <i>spa/spa</i> rats..	150
3.8.7.3 Pyramidal cell death in the hippocampal CA3 subfield of <i>spa/spa</i> rats.....	152
3.9 Discussion.....	155
3.9.1 Conclusions.....	163
CHAPTER 4 - Final Conclusions.....	165
References.....	170
Publications Relevant to Thesis.....	210
Peer Reviewed Articles.....	210
Abstracts.....	210

List of Figures

Figure 1.1.1 General structure of the glutamate receptor subunit showing the hydrophobic membrane domains (M1-4) and the glutamate binding domains (S1 and S2).	21
Figure 1.1.1.1 Comparison of amino acid sequences in the pore lining membrane domain, M2, of the glutamate receptor subunits.	23
Figure 2.1 Worldwide distribution of multiple sclerosis for 1994.....	39
Figure 2.9.9 Schematic of lumbar spinal cord depicting the areas defined as ventral, intermediate and dorsal for neuronal density estimations.	67
Figure 2.10.1.1 The effect of NBQX on motor disability induced by experimental autoimmune encephalomyelitis in Lewis rats.....	73
Figure 2.10.1.2 Dose-dependent effect of MPQX on motor disability induced by experimental autoimmune encephalomyelitis in Lewis rats.	74
Figure 2.10.1.3 The effect of GYKI52466 on motor disability induced by experimental autoimmune encephalomyelitis in Lewis rats.....	75
Figure 2.10.1.4 The effect of GYKI53773 on motor disability induced by experimental autoimmune encephalomyelitis in Lewis rats.....	76
Figure 2.10.1.5 The effect of BIIR561 on motor disability induced by experimental autoimmune encephalomyelitis in Lewis rats.....	77
Figure 2.10.1.6 The effect of CP465022 on motor disability induced by experimental autoimmune encephalomyelitis in Lewis rats.....	78
Figure 2.10.1.7 The effect of aniracetam on motor disability induced by experimental autoimmune encephalomyelitis in Lewis rats.....	80
Figure 2.10.1.8 The effect of NBQX on motor disability induced by adoptive transfer experimental autoimmune encephalomyelitis in Lewis rats.	81
Figure 2.10.2.1 The effect of NBQX on motor disability induced by experimental autoimmune encephalomyelitis in Biozzi mice.....	83

Figure 2.10.4.1 Dose response relationship for AMPA antagonists against mitogen-induced <i>in vitro</i> T-cell proliferation. NBQX, MPQX, GYKI52466 and GYKI53773	86
Figure 2.10.4.2 Dose response relationship for AMPA antagonists against mitogen-induced <i>in vitro</i> T-cell proliferation. BIIR561, CP465022 and dexamethasone	87
Figure 2.10.5.1 Electron micrograph of myelin debris contained within a macrophage.	88
Figure 2.10.5.2 Electron micrograph of perineuronal satellitosis of oligodendrocytes in the ventral horn of a Lewis rat spinal cord.	89
Figure 2.10.5.3 Electron micrographs depicting different stages of degeneration of motor neurons associated with lymphocyte entry.....	91
Figure 2.10.5.4 Neuronal vacuoles in the lumbar spinal cord ventral horn of a peak score experimental autoimmune encephalomyelitis Lewis rat.....	92
Figure 2.10.5.5 Electron micrograph depicting the invasion and subsequent death of lymphocytes in an axon of a ventral horn motor neuron.	93
Figure 2.10.5.6 Chromatolysis and neuronal swelling in the ventral horn of the lumbar spinal cord from experimental autoimmune encephalomyelitis Lewis rats.	94
Figure 2.10.5.7 Immunohistochemistry depicting the invasion of ventral horn motor neurons in the lumbar spinal cord by T-lymphocytes, but not macrophage/microglia, or astrocytes.....	95
Figure 2.10.5.8 Electron micrograph of a ventral horn motor neuron from the lumbar spinal cord of a Lewis rat with experimental autoimmune encephalomyelitis	96
Figure 2.10.7 Toluidine blue sections taken from the lumbar spinal cord, ventral commissure of Biozzi mice with experimental autoimmune encephalomyelitis.	98
Figure 3.8.1 Change in DNA degradation and caspase-3 activity in the olfactory bulbs of <i>spa/spa</i> rats and age-matched littermates at 4 weeks.	136
Figure 3.8.2.1 Increased DNA degradation in discrete brain regions of <i>spa/spa</i> rats at 4 weeks of age. .	137
Figure 3.8.2.2 Increased DNA degradation in the hindbrain and spinal cord of <i>spa/spa</i> rats at 4 weeks of age.	138

Figure 3.8.3.1 Caspase-3 activity in discreet brain regions of 4 week old <i>spa/spa</i> rats.....	139
Figure 3.8.3.2 Caspase-3 activity in the hindbrain and spinal cord of 4 week old <i>spa/spa</i> rats.	140
Figure 3.8.4.1 Change in DNA degradation in discreet brain regions of <i>spa/spa</i> rats between 4 and 8 weeks of age. Cerebellum and spinal cord.	141
Figure 3.8.4.2 Change in DNA degradation in the hippocampus of <i>spa/spa</i> rats between 4 and 8 weeks of age.....	142
Figure 3.8.5.1 TUNEL staining in the cerebellum of 4 week old <i>spa/spa</i> rats.....	143
Figure 3.8.5.2 TUNEL staining controls in phenotypically normal <i>spa/spa</i> littermates, demonstrating the specificity of staining in normal rat brain.....	143
Figure 3.8.6.1 Purkinje cell degeneration in the cerebellum of <i>spa/spa</i> rats at 4 weeks of age.....	145
Figure 3.8.6.2 Motor neuron degeneration in the lumbar spinal cord, ventral horn of 4 week old <i>spa/spa</i> rats.....	146
Figure 3.8.6.3 Hippocampal CA3 pyramidal neurons exhibit normal morphology in a 4 week old <i>spa/spa</i> rat.	146
Figure 3.8.6.4 Degeneration in the hippocampal CA3 subfield of an 8 week old <i>spa/spa</i> rat.....	147
Figure 3.8.7.1 Electron micrographs depicting the stages of Purkinje cell degeneration in 4 week old <i>spa/spa</i> rats.....	149
Figure 3.8.7.2 Electron micrographs depicting the process of α -motor neuron degeneration in the ventral horn of the lumbar spinal cord in 4 week old <i>spa/spa</i> rats.	151
Figure 3.8.7.3.1 Neurodegeneration in the CA3 subfield of <i>spa/spa</i> rat hippocampus at 8 weeks of age. Stages of degeneration.	153
Figure 3.8.7.3.2 Degeneration of the hippocampal CA3 region in an 8 week old <i>spa/spa</i> rat. An overview.	154

List of Tables

Table 2.10.1.1 Parameters of disease activity during experimental autoimmune encephalomyelitis in Lewis rats. NBQX.	72
Table 2.10.1.2 Parameters of disease activity during experimental autoimmune encephalomyelitis in Lewis rats. MPQX.	75
Table 2.10.1.3 Parameters of disease activity during experimental autoimmune encephalomyelitis in Lewis rats. GYKI52466.	76
Table 2.10.1.4 Parameters of disease activity during experimental autoimmune encephalomyelitis in Lewis rats. GYKI53773.	77
Table 2.10.1.5 Parameters of disease activity during experimental autoimmune encephalomyelitis in Lewis rats. BIIR561.	78
Table 2.10.1.6 Parameters of disease activity during experimental autoimmune encephalomyelitis in Lewis rats. CP465022.	79
Table 2.10.1.7 Parameters of disease activity during experimental autoimmune encephalomyelitis in Lewis rats. Aniracetam.	80
Table 2.10.1.8 Parameters of disease activity during adoptive transfer experimental autoimmune encephalomyelitis in Lewis rats. NBQX.	81
Table 2.10.2.1 Parameters of disease activity during experimental autoimmune encephalomyelitis in Biozzi mice between 10-25 days post immunisation (d.p.i.). NBQX.	83
Table 2.10.3 Quantification of CNS inflammation in experimental autoimmune encephalomyelitis Lewis rats. NBQX.	85
Table 2.10.6 Neuronal density in the lumbar spinal cord of rats subjected to experimental autoimmune encephalomyelitis and the effect of NBQX at 30 mg/kg i.p. on cell loss in the ventral horns.	97
Table 2.11.1 IC ₅₀ values at AMPA receptors compared with the corresponding minimum effective dose (ED) in Lewis rat experimental autoimmune encephalomyelitis for the AMPA antagonists used in these studies.	100

Table 3.5 Comparison of the main morphological and biochemical criteria identifying apoptotic and necrotic cell death 125

Abbreviations

3-NP	3-nitropropionic acid
ACTH	adrenocorticotropic hormone
ALS	amyotrophic lateral sclerosis
AMPA	α -amino-3-hydroxy-5-methyl-4-isoxazole propionate
ANOVA	analysis of variance
APC	antigen presenting cell
ATPO	phosphorylated AMPA analogue
BBB	blood-brain barrier
BIIR561	5-(2-[N,N-dimethylamino]oxy-phenyl)-3-phenyl-1,2,4-oxadiazol
BOAA	β -N-oxalylamino- <i>L</i> -alanine
C	cysteine
CAMKII	calcium/calmodulin kinase II
CFA	complete Freund's adjuvant
CGS19755	1-(cis-2-carboxypiperazine-4-yl)methyl-1-phosphonate, (Selfotel)
CNS 1102	Guanidine, N-(3-ethylphenyl)-N-methyl-N'-1-naphthalenyl- [CAS], (Cerestat)
CNS	central nervous system
Copaxone	Copolymer-1, Glatiramer acetate
COX-2	cyclooxygenase 2
CP465022	3-(2-chlorophenyl)-2-[2-[6-[(diethylamino)methyl]-2-pyridinyl]ethenyl]-6-fluoro-4(3H)-quinazolinone
cpm	counts per minute
<i>D</i> -AP5	<i>D</i> -2-[³ H]amino-5-phosphonopentanoate
<i>D</i> -CPP-ene	3-((+)-2-carboxypiperazine-4-yl)propyl-1-phosphonate
CSF	cerebrospinal fluid
d.p.i.	days post immunisation
DEVD-AMC	Aspartate-Glutamine-Valine-Aspartate-aminomethylcoumarin
DEVD-CHO	Aspartate-Glutamine-Valine-Aspartate-aldehyde
DNA	deoxyribonucleic acid
dUTP	d-uridine triphosphate
EAAT-2	excitatory amino acid transporter 2

EAE	experimental autoimmune encephalomyelitis
EBSS	Earle's balanced salt solution
ED	effective dose
ELISA	enzyme-linked immunosorbent assay
ERK	extracellular signal-related kinase
GDH	glutamate dehydrogenase
GFAP	glial fibrillary acidic protein
GS	glutamine synthetase
GYKI52466	1-(4-aminophenyl)-4-methyl-7,8-methylene-dioxy-5H-2,3-benzodiazepine
GYKI53773	(-)-1-(4-aminophenyl)-4-methyl-7,8-methylene-dioxy-4,5-dihydro-3-methylcarbamoyl-2,3-benzodiazepine, (LY300164)
HEPES	N-[2-hydroxyethyl]piperazine-N'-[2-ethanesulfonic acid]
I	isoleucine
i.c.v.	intracerebroventricular
i.p.	intraperitoneal
IFA	incomplete Freund's adjuvant
IFN- β	interferon- β
IFN- γ	interferon- γ
ISNEL	<i>in situ</i> nick end labelling
KA	kainate
LTP	long term potentiation
MAG	myelin-associated glycoprotein
MAPK	mitogen-activated protein kinase
MBP	myelin basic protein
mGluR	metabotropic glutamate receptor
MHC	major histocompatibility complex
MK-801	(+)-5-methyl-10,11-dihydro-5H-dibenzo[a,d] cyclohepten-5,10-imine maleate, (Dizocilpine)
MNQX	5,7-dinitro-quinoxaline-2,3-dione
MOG	myelin oligodendrocyte glycoprotein
MPQX	[1,2,3,4-tetrahydro-7-morpholinyl-2,3-dioxo-6-(trifluoromethyl)quinoxalin-1-yl]methylphosphonate, (ZK200775)
MRI	magnetic resonance imaging
MRS	magnetic resonance spectroscopy

N	asparagine
NAA	<i>N</i> -acetylaspartate
NAAG	<i>N</i> -acetyl-aspartyl-glutamate
NAALADase	<i>N</i> -acetylated- α -linked-acidic dipeptidase
NAWM	normal appearing white matter
NBQX	2,3-dihydroxy-6-nitro-7-sulfamoylbenzo(f)quinoxaline
NMDA	<i>N</i> -methyl- <i>D</i> -aspartate
N_v	numerical density
PBS	phosphate-buffered saline
PCP	phencyclidine
PGE ₂	prostaglandin E ₂
PKA	protein kinase A
PLP	proteolipid protein
PNS	peripheral nervous system
PPMS	primary progressive multiple sclerosis
Q	glutamine
R	arginine
RRMS	relapsing remitting multiple sclerosis
s.c.	subcutaneous
s.e.m.	standard error of mean
SDF-1	stromal-derived factor-1
SOD-1	superoxide dismutase
SPMS	secondary progressive multiple sclerosis
TdT	terminal deoxynucleotidyl transferase
Th2	type 2 helper T-cells
TNF α	tumour necrosis factor- α
TNFR1	tumour necrosis factor receptor 1
TUNEL	TdT-mediated dUTP nick end labelling
V	valine
Y	tyrosine

Acknowledgements

Firstly, I would like to thank my supervisors, Prof. Dr. Les Turski, for his guidance and unerring ability to inspire and motivate and Dr. Terence Smith for helping me realise that sanity is not a prerequisite for ground-breaking science.

I am indebted to Dr. Chrissanthy Ikonomidou for allowing me to carry out studies in her laboratories in Berlin and for her hospitality during my stay.

I would also like to thank Sarah, my family and friends, in particular Leanne, for their support and attempts at motivation which at times verged on abuse. I would not have survived without their patience.

Finally, I am grateful to Eisai and my co-supervisor, Dr Yoshiharu Yamanishi, in particular, for allowing me the opportunity to study for this degree and for supporting me and allowing me time to complete my studies.

CHAPTER I - Glutamate

Glutamic acid is an acidic amino acid which is widely distributed throughout the central nervous system (CNS). Originally studied for its role in metabolism, it is now widely investigated as the major excitatory neurotransmitter of the CNS involved in both normal brain function and in the aetiology of many neurodegenerative disorders. The neuroexcitatory actions of glutamate were originally described by Hayashi almost fifty years ago. He described the production of convulsions when sodium glutamate was administered into the gray matter of dogs and monkeys and suggested these effects were the result of direct stimulation of nerve cells by glutamate (Hayashi, 1954). By 1959 following observations in crustaceans, Robbins and Van Harreveld and Mendelson (Robbins, 1959; Van Harreveld and Mendelson, 1959) proposed glutamate as a putative neurotransmitter, a view that was largely rejected until the early 1970's when calcium-dependent release from axon terminals (Roberts and Mitchell, 1972; Bradford, *et al.*, 1973) and clearance of glutamate from the synaptic cleft by a high affinity uptake system (Wofsey *et al.*, 1971; Roberts and Keen, 1973) were demonstrated.

Paralleling these research developments into the physiological role of glutamate, was an expanding body of evidence concerning the pathological consequences of glutamate exposure. In 1957, two years before glutamate was proposed as a neurotransmitter, Lucas and Newhouse demonstrated that subcutaneous administration of glutamate to new born mice lead to degeneration of the inner neural layers of the developing retina (Lucas and Newhouse, 1957). Later Olney showed that not only did retinal neurons degenerate (Olney, 1969a), but several other regions were also vulnerable to glutamate exposure (Olney, 1969b). These data and the central toxicity of glutamate food additives gave rise to the concept of excitotoxicity, that is, the ability of glutamate to

destroy neurons through the activation of post synaptic excitatory amino acid receptors (Olney *et al.*, 1971).

1.1 Glutamate receptors

Glutamate exerts its effects through its actions at pre- and post-synaptic receptors. These receptors are divided into two distinct classes, those forming cation channels, the ionotropic glutamate receptors, and a second group of G-protein coupled receptors, the metabotropic glutamate receptors. The first functional ionotropic glutamate receptor was isolated and cloned in 1989 (Hollmann *et al.*, 1989). There are now some 29 recombinant glutamate receptors, and many more splice variants, 23 members of the ionotropic glutamate family and 8 metabotropic receptors (reviewed in Hollmann and Heinemann, 1994).

1.1.1 Ionotropic glutamate receptors

Unlike many other classes of ionotropic receptors, the glutamate receptors consist of only three transmembrane domains, M1, M3 and M4 with an additional re-entrant loop on the cytoplasmic surface, M2. Thus, the N-terminus is extracellular and the C-terminus intracellular (Fig. 1.1.1). Receptor subunits form heteromeric transmembrane pores which are selective for monovalent and/or divalent cations. The channels themselves are composed of four, or five glutamate receptor subunits forming a central pore lined by the M2 domain of each subunit. For reviews of transmembrane topology and subunit stoichiometry see Dingledine *et al.*, 1999; Bigge, 1999; and Hollmann and Heinemann, 1994. Ionotropic glutamate channels are named according to their pharmacological selectivity for particular ligands and are divided into three groups, N-

methyl-*D*-aspartate (NMDA), α -amino-3-hydroxy-5-methyl-4-isoxazole propionate (AMPA) receptors and kainate (KA) receptors

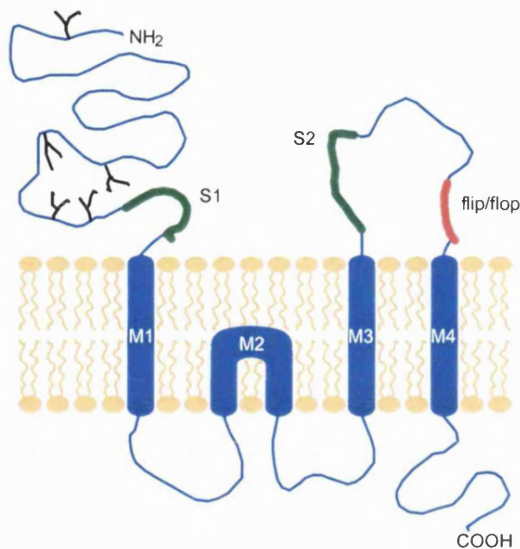


Figure 1.1.1 General structure of the glutamate receptor subunit showing the hydrophobic membrane domains (M1-4) and the glutamate binding domains (S1 and S2). Also shown in red is the flip/flop alternative splice region found in AMPA receptors. Glycosylation sites are shown as black branches in the N-terminal region.

1.1.1.1 NMDA receptors

The most intensely studied of all the glutamate receptors, NMDA receptors have long been implicated in the physiological and pathological roles of glutamate. NMDA receptors are assembled through combination of six possible glutamate receptors subunits originating from three gene families. NR1, the first cloned NMDA receptor, present in all NMDA channels, is able to form functional homomeric ion channels (Moriyoshi K *et al.*, 1991), although the current amplitudes are smaller than those observed for native channels *in vivo*, indicating that other subunits are required for a fully functional *in vivo* ion channel. The NR2 sub-family of NMDA subunits has four members, NR2A-D, which are unable to form homomeric channels, or heteromeric channels with each other (Ikeda *et al.*, 1992; Kutsuwada *et al.*, 1992; Meguro *et al.*, 1992; Monyer *et al.*, 1992). However, when combined with NR1 subunits they form functional channels with a large conductance similar to the conductance of NMDA channels *in vivo* (Momiyaama *et al.*, 1996). A third gene family has recently been

identified, NR3. NR3A, the only member of this family currently identified, is co-immunoprecipitated with both NR1 and NR2 in mouse cortical brain homogenates (Ciabarra *et al.*, 1995). The function of NR3A is unknown, however, co-expression of NR3 leads to a reduction in whole cell (Ciabarra *et al.*, 1995) and single channel (Das *et al.*, 1998) conductance of NMDA-evoked currents and NR3A knockouts show a 3-fold increase in NMDA-induced currents in cortical neurons (Das *et al.*, 1998), suggesting NR3A may have a regulatory role in controlling the amplitude and conductance of NMDA channels.

i. Conductivity

The native NMDA receptors are ligand gated cation channels which, as with all glutamate ion channels, conduct Na^+ and K^+ in equal measures. In addition, NMDA receptors show a higher permeability to Ca^{++} ions than non-NMDA channels (Burnashev *et al.*, 1995) due to an asparagine (N) residue at the critical glutamine/arginine (Q/R) site of the M2 membrane domain of receptor subunits (Fig. 1.1.1.1; Burnashev *et al.*, 1992b). It is this calcium conductivity of glutamate receptors, and NMDA channels in particular, that is thought to contribute to the delayed neuronal toxicity of glutamate (Choi, 1987).

	M2												M3																											
GluR1	T	T	S	D	Q	S	N	E	F	G	I	F	N	S	L	W	F	S	L	G	A	F	M	Q	Q	G	C	.	D	I	S	P	R	S	L	S	G	R	I	
GluR2	S	.	S	E	S	R	N	E	F	G	I	F	N	S	L	W	F	S	L	G	A	F	M	R	Q	Q	G	C	.	D	I	S	P	R	S	L	S	G	R	I
GluR3	S	P	P	D	P	P	N	E	F	G	I	F	N	S	L	W	F	S	L	G	A	F	M	Q	Q	G	C	.	D	I	S	P	R	S	L	S	G	R	I	
GluR4	S	.	D	Q	P	P	N	E	F	G	I	F	N	S	L	W	F	S	L	G	A	F	M	Q	Q	G	C	.	D	I	S	P	R	S	L	S	G	R	I	
GluR5	S	.	D	V	V	E	N	N	F	T	L	L	N	S	F	W	F	G	V	G	A	L	M	Q	Q	G	S	.	E	L	M	P	K	A	L	S	T	R	I	
GluR6	S	.	D	V	V	E	N	N	F	T	L	L	N	S	F	W	F	G	V	G	A	L	M	R	Q	Q	G	S	.	E	L	M	P	K	A	L	S	T	R	I
GluR7	S	.	E	V	V	E	N	N	R	T	L	L	N	S	F	W	F	G	M	G	S	L	M	Q	Q	G	S	.	E	L	M	P	K	A	L	S	T	R	I	
KA1	R	C	N	L	L	V	N	Q	Y	S	L	G	N	S	L	W	F	P	V	G	G	R	M	Q	Q	G	S	.	T	I	A	P	R	A	L	S	T	R	C	
KA2	R	P	H	I	L	E	N	Q	Y	T	L	G	N	S	L	W	F	P	V	G	G	F	M	Q	Q	G	S	.	E	I	M	P	R	A	L	S	T	R	C	
NMDA1	S	E	E	E	E	E	D	A	L	T	L	S	S	A	M	W	F	S	W	G	V	L	L	N	S	G	I	.	G	E	G	A	P	R	S	F	S	A	R	I
NMDA2A	G	K	A	P	T	G	L	L	F	T	I	G	K	A	I	W	L	L	W	G	L	V	F	N	N	S	V	.	P	V	Q	N	P	K	G	T	T	S	K	I
NMDA2B	G	R	E	P	G	G	P	S	F	T	I	G	K	A	I	W	L	L	W	G	L	V	F	N	N	S	V	.	P	V	Q	N	P	K	G	T	T	S	K	I
NMDA2C	G	K	K	P	G	G	P	S	R	T	I	G	K	S	V	W	L	L	W	A	L	V	F	N	N	S	V	.	P	I	E	N	P	R	G	T	T	S	K	I
NMDA2D	G	K	R	P	G	G	S	T	R	T	I	G	K	S	I	W	L	L	W	A	L	V	F	N	N	S	V	.	P	V	E	N	P	R	G	T	T	S	K	I

Figure 1.1.1.1 Comparison of amino acid sequences in the pore lining membrane domain, M2, of the glutamate receptor subunits. Periods represent gaps inserted to maintain sequence alignment. The glutamine/arginine (Q/R) editing site for GluR1-7 is shown in red (adapted from a figure in Hollmann and Heinemann, 1994).

ii. Modulation

The many studies investigating the modulation of the NMDA receptor have led to the identification of a number of modulatory sites and pharmacological agents. The channel is unusual in that its function is dependent on both agonist binding and membrane potential. *L*-Glutamate is the primary agonist at NMDA and non-NMDA receptors *in vivo*, although NMDA receptors are also exclusively responsive to *L*-aspartate (Patneau and Mayer, 1990), an important consideration for NMDA activity in the spinal cord. In addition, NMDA receptors require the presence of the co-agonist glycine for receptor activation (Kleckner and Dingeldine, 1988). Analysis of mutants of NR1 and NR2 has led to the proposal that the glycine binding site is contained within NR1 and that the glutamate binding site is in the NR2 subunit (Anson *et al.*, 1998). Recent evidence suggests that the endogenous co-agonist may actually be *D*-serine rather than glycine (Wolosker *et al.*, 1999; Mothet *et al.*, 2000)

The voltage-dependence of NMDA channels comes from the presence of Mg^{++} ions in the extracellular face of the channel pore (Nowak *et al.*, 1984; Mayer *et al.*, 1984; Jahr and Stevens, 1990a,b). At resting membrane potentials the NMDA channel is constitutively blocked by physiological Mg^{++} . In order to be activated the cell membrane must be depolarised. Under these conditions the magnesium block is relieved and the channel is opened by occupation of the agonist and co-agonist binding sites. Endogenous levels of Zn^{++} are also able to inhibit NMDA function. The binding site for Zn^{++} is contained within the channel pore as with Mg^{++} , but is a separate site. This was determined by mutational studies where mutation of the Q/R site in the M2 domain, from asparagine to glutamine, lead to a prevention of Mg^{++} blockade, but not of Zn^{++} (Mori *et al.*, 1992). Koh and Choi, suggest that co-release of Zn^{++} with glutamate would lead to inhibition of NMDA channels by Zn^{++} , driving the glutamate responses from NMDA to non-NMDA (Koh and Choi, 1988).

NMDA channels can also be modulated by other endogenous factors such as protons and polyamines. H^+ ions inhibit NMDA activity with an IC_{50} that corresponds to a pH of about 7.3 (Traynelis and Cull-Candy, 1990). This suggests that NMDA channels are only half maximally active at normal pH which has important implications for the activity of NMDA receptors during pathological events which alter pH (Siesjo, 1988). Polyamines, on the other hand, are able to potentiate NMDA receptor function. The mechanism of this modulation is thought to be through relief of the resting inhibition by H^+ ions (Traynelis *et al.*, 1995).

As well as endogenous modulators of NMDA function, there are a number of pharmacologically active compounds which are able to inhibit NMDA function. There are three main mechanisms of action for the currently available inhibitors. One class of

inhibitor is active through block within the channel pore. These compounds are non-competitive and include ketamine, phencyclidine (PCP/Angel dust), Dizocilpine (MK-801) and Cerestat (CNS 1102). The second class of agents are those which compete for glutamate/aspartate binding, the competitive antagonists, such as *D*-AP5, *D*-CPP-ene and Selfotel (CGS19755). The final class of agent are the glycine site antagonists. These compounds inhibit NMDA function by preventing binding of the co-agonist, glycine, which is essential for channel function. 5, 7-dichlorokynurenate and 5,7-dinitro-quinoxaline-2,3-dione (MNQX) both inhibit NMDA receptors at the glycine site.

1.1.1.2 AMPA receptors

The AMPA receptor subunits were the first glutamate subunits to be cloned. The cloning of glutamate receptors had proven incredibly difficult until 1989 when Hollmann and colleagues (Hollmann *et al.*, 1989) adopted a new cloning technique, developed by Masu *et al.* in 1987, to identify the first glutamate receptor, the AMPA receptor GluR1. This was followed shortly afterwards by the cloning of three more AMPA receptors, GluR2-4 (Boulter *et al.*, 1990; Keinänen *et al.*, 1990; Nakanishi *et al.*, 1990; Sakimura *et al.*, 1990). The receptor subunit has the transmembrane topology described earlier (Section 1.1.1) with the glutamate binding domain formed from the S1 and S2 domains (Fig. 1.1.1). The binding of glutamate causes a conformational change that puts tension on the M1 transmembrane domain and causes the channel to open (Armstrong *et al.*, 1998). Seven amino acid residues within the S1/S2 domains determine the ligand specificity of the glutamate receptors. The four AMPA receptor subunits, GluR1-4, are able to combine to form either heteromeric, or homomeric functional ion channels.

i. Conductivity

The AMPA ionotropic receptors differ from NMDA receptors in their conductivity. All AMPA receptor ion channels are able to conduct Na^+ and K^+ in equal measures as with the NMDA receptors, but the conduction of Ca^{++} ions is highly regulated and depends on a critical amino acid residue within the M2 cytoplasmic re-entrant loop (Hume *et al.*, 1991; Burnashev *et al.*, 1992a). The primary transcripts all contain a glutamine residue at the Q/R site, but the GluR2 subunit undergoes RNA editing to transform this glutamine residue to an arginine. An arginine residue at the Q/R site renders any channel containing a GluR2 subunit impermeable to Ca^{++} ions (Hollmann *et al.*, 1991) and results in a linear I/V relationship (Verdoorn *et al.*, 1991).

Desensitisation of AMPA channels is affected by alternate splicing of a 115-base pair region preceding the M4 transmembrane region (Sommer *et al.*, 1990). This results in two splice variants termed flip and flop. The two forms are equally abundant in the adult brain, but have differing patterns of distribution. Channels containing the flip spliced variant demonstrate a higher efficacy for glutamate activation and slower desensitisation following stimulation than flop channels. In addition, there is developmental regulation, with the flip variant predominant before birth and changing to flop postnatally. This may reflect a requirement for increased efficiency of glutamate signalling during synaptogenesis.

ii. Modulation

The primary factor regulating AMPA channel function is the control of expression of GluR2. Any AMPA receptor channel not expressing GluR2 is able to conduct Ca^{++} ions

due to the absence of an arginine residue in the channel pore (1.1.1.2i). In addition, calcium-permeable AMPA channels are subject to voltage-dependent block by intracellular polyamines (Kamboj *et al.*, 1995) and as with Mg^{++} ion blockade of NMDA receptors, are blocked at resting membrane potentials by polyamines (Bowie *et al.*, 1998).

AMPA channels also contain a number of intracellular phosphorylation sites for protein kinase A (PKA; Greengard *et al.*, 1991), calcium/calmodulin kinase II (CAMKII; McGlade-McCulloh *et al.*, 1993) and other, as yet unidentified, kinases. Phosphorylation at these sites potentiates AMPA receptor activation by increasing the open frequency and mean open time.

The desensitisation of AMPA receptors is dependent on the structure of the ligand involved. When the ligand is AMPA there is a rapid desensitisation of the AMPA receptor. However, when activated by kainate, desensitisation does not occur. Both cyclothiazide and aniracetam are able to relieve desensitisation and thereby potentiate AMPA receptor activation. The effects of cyclothiazide in particular are also dependent on the splice variant, with cyclothiazide being able to almost completely prevent desensitisation of the flip splice variant.

There are a number of pharmacological agents which act at the AMPA channel. The first generation of competitive AMPA antagonists such as CNQX and NBQX show little selectivity for AMPA receptors over kainate receptors. However, later compounds such as MPQX (ZK200775) and ATPO, a phosphono analogue of AMPA, have better selectivity (10-100 fold). The first non-competitive AMPA antagonists to be synthesised were the 2,3-benzodiazepines. The prototype inhibitor was GYKI52466

which has subsequently been superseded by GYKI53773 (LY300164). This compound has a much higher potency than GYKI52466 with a sub-micromolar IC_{50} . (See Nikam and Kornberg, 2001 for review of AMPA receptor antagonists). The most potent antagonists are the polyamine amide toxins, active in the nanomolar concentration range. These toxins bind in the channel pore from either face and include argiotoxin from the orb-web spider, Joro spider toxin and philanthotoxin from the digger wasp.

1.1.1.3 Kainate receptors

Unlike AMPA receptors, kainate receptors are formed from subunits derived from two sub-families of glutamate receptor. The first group are the low affinity kainate receptors which share a high homology with each other (75 – 80 %), but only 40 % homology with AMPA receptor GluR1-4. These three kainate receptors were named GluR5, GluR6 and GluR7 (Bettler *et al.*, 1990; Egeberg *et al.*, 1991; Bettler *et al.*, 1992; Sommer *et al.*, 1992). The second group of kainate receptors demonstrate high affinity binding for kainate, the two members of this family described to date being KA1 and KA2 (Werner *et al.*, 1991; Herb *et al.*, 1992; Kamboj *et al.*, 1992; Sakimura *et al.*, 1992). These receptors share 70 % homology with each other, but less than 40 % homology with GluR1-7. Kainate receptors share the same membrane topology as the other ionotropic glutamate receptor families (Fig. 1.1.1). The ligand binding domain is formed from the S1 and S2 domains in the extracellular loops of M1 and M3-4 and, similar to AMPA receptors, kainate receptors contain no co-agonist binding site. The five kainate subunits are able to combine to form functional heteromeric and homomeric channels. The molecular biology and pharmacology of kainate receptors is reviewed in greater detail in Hollmann and Heinemann (1994), Bleakman and Lodge (1998), Dingledine *et al.* (1999) and Chittajallu *et al.* (1999).

i. Conductivity

Kainate receptors share several similarities with AMPA receptors: Functional kainate receptors conduct Na^+ and K^+ ions in equal measures. GluR5 and GluR6 undergo post-translational modification (Egebjerg and Heinemann, 1993), the critical Q/R site residue in the M2 region undergoes RNA editing from glutamine to an arginine (Fig. 1.1.1.1) and consequently channels expressing edited GluR5 and GluR6 have a reduced permeability to Ca^{++} ions (Egebjerg and Heinemann, 1993; Burnashev *et al.*, 1996). However, the editing efficiency of the GluR5 and GluR6 Q/R site is much lower than that for GluR2, 35 % and 75 % for GluR5 and GluR6, respectively (Swanson *et al.*, 1997) in contrast to almost 100 % efficiency in the GluR2 subunit of the AMPA channel. Editing efficiency is also regulated throughout development with less editing of GluR5 and GluR6 in developing brain tissue than in the adult (Bernard and Khrestchatisky, 1994; Paschen *et al.*, 1994; Paschen *et al.*, 1995; Schmitt *et al.*, 1996). In addition to editing at the Q/R site in the channel pore, kainate receptor Ca^{++} permeability is also sensitive to mutations in the M1 transmembrane domain. An isoleucine (I) residue can be edited to a valine (V) residue and a tyrosine (Y) residue is edited to cysteine (C). Both changes result in alterations in ion permeability suggesting that at least in the kainate receptor channel, M1 is important in determining the properties of the channel (Köhler *et al.*, 1993).

The conductance of kainate receptor ion channels is more complex than that of the AMPA channel. Channel composition is a crucial determinant of conductance with kainate receptors demonstrating different conductance levels depending on which subunits are expressed. Channels expressing unedited GluR5(Q) or GluR6(Q) have a sub-picoSiemen conductance, whereas channels expressing edited GluR5(R) or

GluR6(R) and channels containing KA2 have a much higher conductance in the range of 5.4 - 8.6 pS or a higher state of 25 pS (Swanson *et al.*, 1996). As with AMPA receptors, expression of edited subunits results in a linear I/V relationship (Sommer *et al.*, 1992), but edited kainate receptor channels are also unusual in that they are permeable to anions such as Cl⁻ ions (Burnashev *et al.*, 1996).

ii. Modulation

The kainate channel rapidly desensitises in response to agonist stimulation, however, there is a certain amount of subunit specificity. GluR6 kainate receptors desensitise more rapidly in response to kainate than channels composed of GluR5 subunits (Swanson *et al.*, 1997). The desensitisation caused by agonist activation is relieved in GluR5 and GluR6 subunits, but not GluR7, by concanavalin A (Schiffer *et al.*, 1997) suggesting a conserved glycosylation site between GluR5 and GluR6 which is not present in GluR7. A number of potent agonists act at kainate receptors including ATPA, 5'-iodowillardine and SYM2081. All three agonists show good selectivity for kainate receptors over AMPA, and also have different selectivity for individual kainate receptor subunits.

Conversely, there are fewer antagonists of kainate receptors than for the other classes of ionotropic glutamate receptors as the kainate field of research is still quite young. The prototypical competitive kainate receptor antagonist, NS-102, which has poor solubility and selectivity, has been superseded by the GluR5-selective Ely Lilly compound, LY294486, for investigations into the role of kainate receptors *in vitro* and *in vivo*. To date, there are no known non-competitive antagonists for kainate receptors.

1.1.2 Metabotropic glutamate receptors

The existence of a second class of glutamate receptor became apparent following a report that glutamate stimulated phospholipase C in cultured striatal neurons via a receptor that did not belong to any of the ionotropic glutamate families (Sladeczek *et al.*, 1985). This observation was later confirmed in a number of other cell types, suggesting that glutamate could exert its effects through receptors coupled to GTP-binding proteins (G-proteins) in addition to its actions on ionotropic receptors. It was not until 1991 that the first of these G-protein-coupled, metabotropic glutamate receptors (mGluRs), was cloned (Houamed *et al.*, 1991; Masu *et al.*, 1991) as the very low sequence homology between mGluRs and all previously cloned G-protein-coupled receptors meant probing with recognised sequences was largely unsuccessful. However, following the cloning of the first receptor, mGluR1, seven more related receptors were cloned, mGluR2 to mGluR8 (Tanabe *et al.*, 1992; Abe *et al.*, 1992; Nakajima *et al.*, 1993; Saugstad *et al.*, 1994; Okamoto *et al.*, 1994; Duvoisin *et al.*, 1995; Saugstad *et al.*, 1997).

Amino acid sequencing of these receptors revealed they are much larger than any previously cloned G-protein-coupled receptors. The sequence contains seven closely linked hydrophobic regions in the centre of the molecule which form the seven transmembrane domains typical of G-protein-coupled receptors. However, unlike other receptors in this class, they possess an unusually large extracellular N-terminus and intracellular C-terminus. There are two regions which show the most conservation between mGluRs. A hydrophobic region in the extracellular domain, with adjacent amino acids, which is thought to represent the ligand binding domain, and the first and third intracellular loops which may account for G-protein binding.

Nakanishi proposed separation of the metabotropic glutamate receptors into three groups on the basis of the sequence homology between certain receptors (approximately 70 % homology within and 40 % between groups; Nakanishi, 1992). This classification based on sequence homology also holds true for the signal transduction mechanisms and pharmacology of these receptors. The group I mGluRs, mGluR1 and mGluR5, which are most sensitive to activation by quisqualate, stimulate phospholipase C resulting in an increase in phosphoinositide turnover and release of Ca^{++} from intracellular stores. Group II mGluRs include mGluR2 and mGluR3 and activation results in an inhibition of adenylyl cyclase and a decrease in cAMP production. They are most sensitive to *L*-CCG-I. Group III contains the remaining mGluRs, mGluR4 and mGluR6-8. Stimulation of these receptors is also coupled to a decrease in cAMP, but activation cannot fully inhibit forskolin-induced cAMP production (maximum 50 % inhibition) unlike group II receptors. Group III mGluRs are uniquely sensitive to activation by *L*-AP4. The pharmacology of the mGluR antagonists is extremely complex and outside the scope of this thesis. Further information on the pharmacology and function of metabotropic glutamate receptors can be found in reviews by Roberts (1995), Pin and Duvoisin (1995), Conn and Pin (1997) and Schoepp *et al.* (1999).

1.2 Physiological function of glutamate receptors in the brain and spinal cord

Glutamate is the major excitatory neurotransmitter in the brain. It is found in nearly all central nervous system neurons and is primarily responsible for fast excitatory neurotransmission. The anatomical distribution of the glutamatergic pathways demonstrate a crucial role for glutamate in cortical and hippocampal cognitive function, pyramidal and extrapyramidal motor function, cerebellar function and sensory function. The consequence of presynaptic release of glutamate is dependent on the post-synaptic

receptor expression. Fast synaptic transmission seen, for example, in monosynaptic reflexes is mediated through activation of AMPA receptors which results in membrane depolarisation and the opening of voltage operated cation channels (Collins and Buckley, 1989). Glutamate is also able to induce a biphasic response by stimulating NMDA receptors. The consequence of depolarisation of the cell membrane in response to AMPA is the relief of Mg^{++} blockade of NMDA receptors and a slower second phase of glutamate depolarisation (Nowak *et al.*, 1984). The NMDA receptor-mediated response is important in polysynaptic reflexes and in reinforcing synaptic transmission. This process of long term potentiation (LTP) is thought to underlie learning and memory (Collingridge and Bliss, 1995). The participation of AMPA receptors in motor reflexes is important in explaining the temporary functional deficits seen following AMPA receptor antagonist treatment. The physiology of glutamate receptors is reviewed further in Headley and Grillner (1990) and Greenamyre and Porter (1994).

1.3 Involvement of glutamate receptors in neuronal degeneration

Glutamate neurotransmission is essential for normal brain function, however, inappropriate glutamatergic activity is implicated in a host of central nervous system diseases. Whilst the relevance of original literature correlating ingestion of glutamate with neurotoxicity in species from rodents to primates is now contested (reviewed in Meldrum 1993), there are other situations where activation of the glutamatergic system is clearly involved. Domoic acid, synthesized by algae and concentrated in blue mussels or fish when they feed, produces confusion and occasionally seizures when subsequently ingested by mammals (Teitelbaum *et al.*, 1990; Scholin *et al.*, 2000). The primary pathological hallmarks of domoic acid toxicity are degeneration of neurons in the amygdala and hippocampus, in particular cells of the CA3 subfield, a consequence of

direct toxicity or secondary damage via seizure activity in other brain regions (Jarrard and Meldrum, 1993). The motor neuron loss observed in neuroleptosis is associated with the AMPA receptor antagonist, β -N-oxalylamino-L-alanine (BOAA), present in chick peas. BOAA becomes toxic when combined with vitamin and mineral deficiencies in malnourished humans (Spencer *et al.*, 1986). It is suggested that the deficiencies cause impaired mitochondrial function. Indeed, compromised mitochondrial function may lead to increased sensitivity to excitatory neurotransmitters. When ingested 3-nitropropionic acid (3-NP), synthesised by a fungus that grows on sugar cane, causes a loss of striatal GABA-ergic neurons in a pattern reminiscent of Huntington's disease pathology. This damage is prevented *in vivo* by NMDA antagonists (Schulz *et al.*, 1996).

There are two paradigms of endogenous glutamate toxicity in the CNS. Excess production, or potentiation of glutamate activity leads to a rapid excitotoxic, acute neurodegeneration (Olney, 1971) and is associated with neurodegeneration in epilepsy, stroke and traumatic brain injury. In this paradigm, increased flux of Na^+ , K^+ and Ca^{++} ions through glutamate ionotropic receptors and voltage-dependent ion channels causes a collapse of membrane potential, activation of a number of Ca^{++} -dependent enzymes and a disturbance of the osmotic gradient of the cell leading to water influx. The result is massive proteolysis, mitochondrial disruption and swelling of the cytosol. Ultimately, the cell membrane ruptures and the intracellular contents are released, initiating an inflammatory response. Conversely, chronic exposure to low levels of glutamate results in a more protracted cell death which has been implicated in the mechanisms underlying neuronal death in chronic neurodegenerative disorders.

Whilst the study of glutamate in the pathology of acute neurodegenerative diseases spans several decades, interest in the neuropathological consequences of chronic glutamate exposure is a relatively new field. Thus, glutamate has now been proposed as a key mediator in the pathogenesis of a number of chronic neurodegenerative diseases, including motor neuron disease (such as amyotrophic lateral sclerosis (ALS); Plaitakis, 1990; Leigh and Meldrum, 1996), Huntington's disease (Coyle and Schwarcz, 1976; DiFiglia, 1990), Parkinson's disease (Turski *et al.*, 1991), Alzheimer's disease (Maragos *et al.*, 1987; Greenamyre and Young, 1989), and more recently multiple sclerosis (Bolton and Paul, 1997; Smith *et al.*, 2000; Pitt *et al.*, 2000). Some less common neurological disorders such as Rasmussen's encephalitis (Rogers *et al.*, 1994), olivopontocerebellar degeneration (Gähring *et al.*, 1997) and paraneoplastic neurodegenerative syndrome (Gähring *et al.*, 1995) involve an antibody response against specific glutamate receptor subunits, intimating a glutamatergic component in their aetiology.

1.4 Aims of thesis

Glutamate is involved in many neurological disorders, through a number of different mechanisms. This thesis is concerned with two independent aspects of glutamate toxicity. Glutamate toxicity in rodent models of multiple sclerosis and in a model of spontaneous neurodegeneration in the *spa/spa* rat.

There have been a number of observations suggesting that the pathogenesis of multiple sclerosis and the animal models of the disease can be attributed in part to the glutamatergic system (Bolton and Paul, 1997; Werner *et al.*, 2001). Whilst Bolton and Paul suggest that glutamate acting via the NMDA receptors may be contributing to

disease through alterations in blood brain barrier (BBB) permeability, others indicate the AMPA/kainate system may be involved in the disease pathogenesis (Matute *et al.*, 1997; Matute, 1998; McDonald *et al.*, 1998). One aim of this thesis, therefore, was to determine the importance of AMPA receptors in animal models of multiple sclerosis and to examine the possible mechanism of protection of AMPA antagonists.

The second part of this thesis is concerned with the nature of glutamate-mediated cell death within the adult CNS. The excitotoxic theory of neuronal cell death associated with acute overexposure to glutamate is widely accepted. However, low levels of glutamate exposure have been postulated to induce a slower degeneration which is increasingly implicated in neuronal loss in chronic neurodegenerative diseases. Only recently have researchers started examining the mechanisms of neuronal death within the adult CNS. Here, I describe an assessment of the biochemical and ultrastructural changes following neuronal degeneration within the adult brain and spinal cord of a rat model of spontaneous neurodegeneration.

CHAPTER 2 - AMPA and Multiple Sclerosis

Multiple sclerosis is an inflammatory, demyelinating disease of the central nervous system. The progress of disease is unpredictable and, more than a century since its first description, very little is known of the aetiology or why there should be such variability in disease development between patients.

2.1 Epidemiology and prevalence of multiple sclerosis

Epidemiological studies of multiple sclerosis have revealed a very distinctive worldwide distribution for the disease (Fig. 2.1). There are clear areas of high incidence (>30 cases per 100,000) concentrated in northern Europe, North America and Australasia, which seemingly correlate with colonisation by European settlers, whilst there are other populations where the incidence of multiple sclerosis is extremely rare. The reason for the large variation in prevalence is not understood. Environmental and genetic explanations have been offered and both are likely to be important. Kurtzke (1997) argues against a genetic component, citing the spread of multiple sclerosis from an origin in Scandinavia as evidence for an acquired, exogenous, environmental cause of transmission. One of the primary investigations demonstrating the possible transmission of an environmental, infectious agent is the Faroe Islands study (Kurtzke and Hyllested, 1987). Prior to the occupation of the islands by British troops between 1941 and 1944, there were no reported cases of multiple sclerosis on the islands. Subsequently, a series of four epidemics occurred amongst the indigenous population. This series of studies are described in detail in Kurtzke (1997). Interestingly, the disease was not transmitted to residents who were under the age of eleven at the time of exposure. A threshold age for

acquisition of disease is also supported by a number of studies which suggest that an age at, or near puberty is the important cut off before which geographical region of origin is most relevant, a view upheld by studies of United States army veterans (Beebe *et al.*, 1967; Kurtzke *et al.*, 1979). Beebe *et al.*, in a study of veterans diagnosed with multiple sclerosis during their service in the US army, found that when disease incidence was compared with place of birth, there was a clear distribution of multiple sclerosis with a higher prevalence in northern USA compared with the south. These findings were in agreement with the distribution of disease associated with the general population. However, when the incidence was compared with place of residence at the time of entry into the armed forces, the relationship had disappeared completely indicating that the risk associated with changing residence had almost completely disappeared before the third decade of life.

Racial background is another important factor in determining the risk of developing multiple sclerosis. The incidence amongst non-whites is much lower, suggesting either an increased resistance to an unknown, environmental pathogen, or alternatively a higher genetic susceptibility amongst whites. The genetics of multiple sclerosis has been studied extensively and whilst no single risk factor has been identified (The Transatlantic Multiple Sclerosis Genetics Cooperative, 2001), some genetic links have been found. The incidence of multiple sclerosis between monozygotic twins is about six times greater than the rate among dizygotic twins and there is an increased risk of multiple sclerosis in populations expressing certain HLA alleles (reviewed in McFarland *et al.*, 1997). Many other genes of interest have been investigated, but as yet no strong link between a specific gene and multiple sclerosis has been observed (See McFarland *et al.*, 1997 for review).

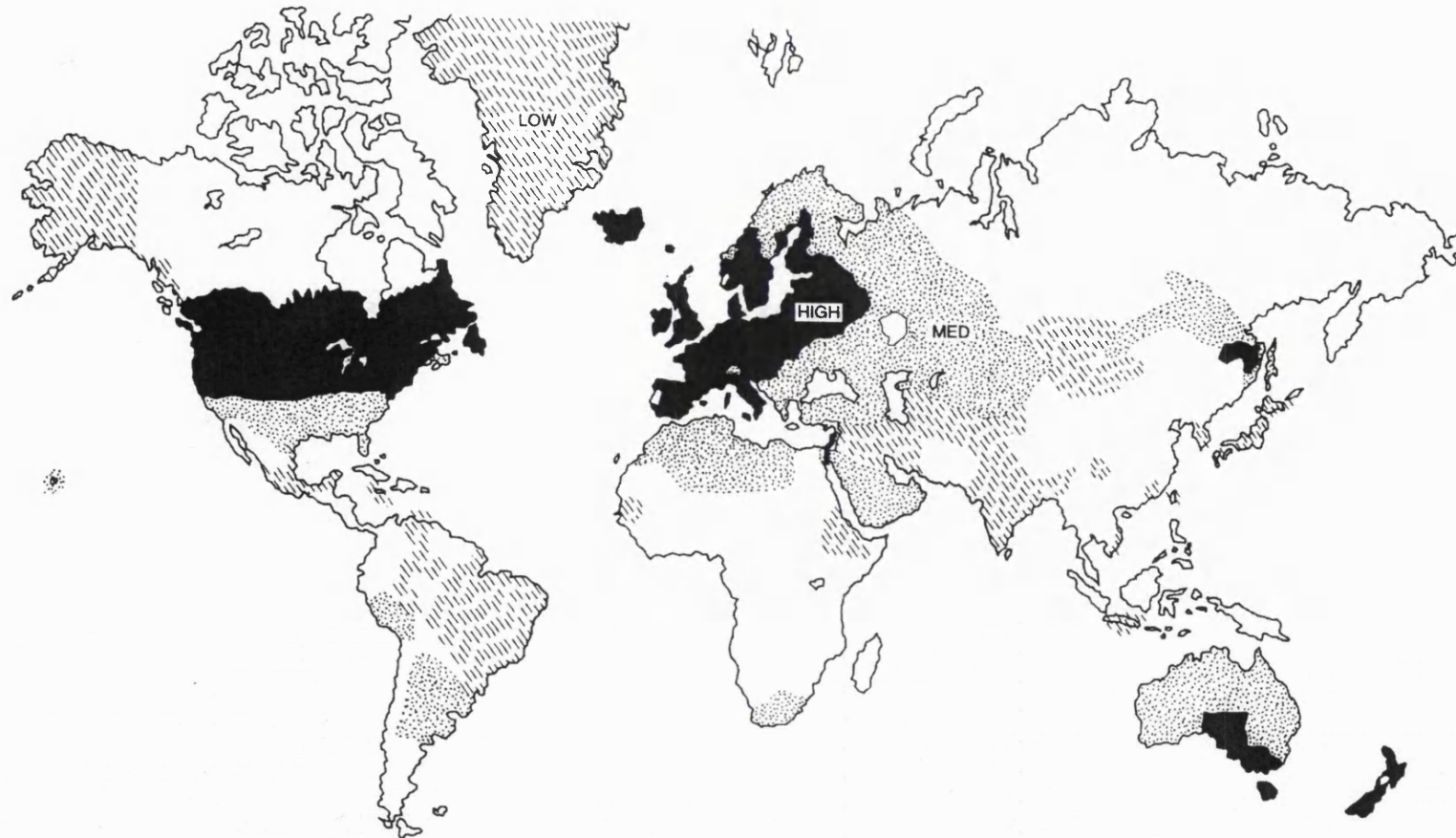


Figure 2.1 Worldwide distribution of multiple sclerosis for 1994. High frequency areas (>30 cases/100,000) are indicated in black, medium frequency areas (5-30 cases/100,000) by dots and low frequency areas (<5 cases/100,000) with diagonal dashes. Blank areas indicate regions for which there are no data. Reproduced from Kurtzke *et al.*, 1997.

2.2 Pathogenesis of multiple sclerosis

The actual triggering event or events for multiple sclerosis are still unknown. A number of viruses are able to recreate the symptoms and pathology of multiple sclerosis in animals (Dal Canto and Lipton, 1980; Fazakerley *et al.*, 1988), and in multiple sclerosis patients *Chlamydia pneumoniae* has been found in the CSF of 97 % of patients compared with 18 % of control patients with other neurological diseases (Sriram *et al.*, 1999). This association has placed viral and/or bacterial infections at the top of the list of potential environmental risk factors for multiple sclerosis. Despite the lack of knowledge concerning the aetiology of multiple sclerosis, much progress has been made towards understanding the mechanisms of damage and progression of the disease. Multiple sclerosis is most commonly referred to as an inflammatory, demyelinating disease of the central nervous system, a description that goes only part way towards describing the disease. Inflammation and demyelination are undoubtedly of major importance in the progression of the disease, but the neurological features of the disease suggest a major contribution of axonal and neuronal impairment and/or degeneration. This contribution is well established in the irreversible paralysis and spasticity of the later stages of disease (Bjartmar and Trapp, 2001; Baker *et al.*, 2000), but the importance of neuronal compromise in the early stages of disease has been largely understated.

2.2.1 Demyelination in the pathogenesis of multiple sclerosis

One of the primary pathological hallmarks of multiple sclerosis is the presence of inflammatory lymphocytes in the central nervous system. This is exemplified by perivascular cuffing and the presence of T-lymphocytes and B-lymphocytes as well as

macrophages and microglia in active, demyelinating lesions (Raine, 1997). In expanding multiple sclerosis lesions, macrophages and activated microglia are found at the interface between normal and demyelinated regions (Cuzner *et al.*, 1988), suggesting they are somehow involved in the process of demyelination. Indeed, the presence of myelin debris in macrophages found in active lesions demonstrates they could well be actively involved, or at least participate in removal of myelin debris from previously damaged axonal tracts.

The stimulus for the destruction of apparently normal myelin in multiple sclerosis patients by the body's own immune system is unknown, but CD4⁺ T cells discovered in inflammatory plaques are known to recognise a number of myelin and non-myelin CNS antigens associated with the pathogenesis of multiple sclerosis (Kerlero de Rosbo *et al.*, 1993). Since T-cells are also occasionally seen in normal brains, there must be other contributory factors, such as autoantibodies or cytokines, involved in immune-mediated damage to myelin.

Autoantibodies against various myelin proteins have been found in the brains of patients with multiple sclerosis (Genain *et al.*, 1999) and indeed, CSF oligoclonal banding is a diagnostic criteria for multiple sclerosis (Ebers, 1984). There are three potential mechanisms of antibody generation in multiple sclerosis: processed antigen on the surface of activated microglia or macrophages are presented directly to invading B-cells at the site of damage in the CNS; CNS antigens can also be presented to B-cells in the lymph nodes following drainage of myelin and oligodendrocyte debris from the cerebrospinal fluid (CSF); or antigenic products of myelin breakdown exit the CNS through a compromised blood-brain barrier into the vasculature where they are recognised by circulating B-cells. Once generated, either in the CNS or in the periphery,

antibodies become expressed on the surface of the myelin sheath or on oligodendrocytes which in turn can lead to damage directly through activation of the complement cascade and cytolysis. The ability of antibodies to exacerbate myelin damage is supported by data showing that antibodies to myelin proteins are able to worsen disease in experimental, animal models of multiple sclerosis and promote demyelination in models otherwise relatively free of myelin loss (Linington *et al.*, 1988).

Other agents of interest are those released from lymphocytes, macrophages and microglia within the multiple sclerosis lesion. Macrophages and activated microglia are capable of producing pro-inflammatory cytokines such as tumour necrosis factor- α (TNF α) and interferon- γ (IFN- γ), generating free radicals (O₂⁻ or NO[•]), releasing excitatory amino acids and activating complement, all of which have the potential to damage myelin, oligodendrocytes, neurons and axons. T-cells can cause damage through release of products including perforins and granzyme, or through interactions with Fas ligand subsequent to binding of CD8⁺ T-cells to class I major-histocompatibility-complex (MHC) presented by resident cells. For the role of potential immunological mediators of damage in multiple sclerosis and experimental autoimmune encephalomyelitis see reviews of De Groot and Woodroffe (2001), Singh *et al.* (2000) and Kieseier *et al.* (2000).

2.2.2 Neuronal degeneration in the pathogenesis of multiple sclerosis

The rapidity of onset of relapse and remission, and the comparative slowness of the processes of demyelination and remyelination, suggests that the physical disability associated with multiple sclerosis could be partly a consequence of neuronal impairment

and/or damage. This idea is supported by examples of primary progressive multiple sclerosis in which there is extensive axonal loss associated with rapid functional decline, but relatively little demyelination (Matthews, 1999). This is also true of some animal models of the disease where demyelination is not extensive yet the animals exhibit a relapsing, remitting profile of paralysis (Pender, 1988).

The first descriptions of axonal degeneration in multiple sclerosis, including the existence of axonal terminal bulbs in association with axonal transection, were made by Charcot (1868). This pathological aspect of multiple sclerosis was subsequently overlooked for over a century in favour of the inflammatory, demyelinating component of the disease. Only in the last decade has attention re-focused on the contribution of axonal loss to the pathogenesis of multiple sclerosis. It has become increasingly well accepted that the extent and location of axonal lesions in the later stages of disease correlates with the severity and nature of disability (Davie *et al.*, 1999; Bjartmar *et al.*, 2000), but there is also a growing body of evidence which suggests that at least part of the axonal loss occurs in acute, active lesions and is a product of acute episodes of inflammation in the relapsing, remitting stages of disease (Ferguson *et al.*, 1997; Evangelou *et al.*, 2000; Bitsch *et al.*, 2000b). The early axonal damage and demyelination in acute lesions is closely associated with inflammatory cells, in particular macrophages, microglia and CD8⁺ T-cells, moreover, there is no longer extensive active axonal degeneration in chronic lesions, instead the axonal atrophy seen in the latter stages is a consequence of the destruction of axons in primary active lesions (Ferguson *et al.*, 1997; Bitsch *et al.*, 2000b). Active chronic lesions represent an intermediate stage where there is very little axonal damage in the centre of the lesion, instead, the ongoing degeneration is found at the border of the lesions in areas containing active macrophages.

Further evidence in support of ongoing axonal injury in multiple sclerosis comes from combined magnetic resonance imaging (MRI), magnetic resonance spectroscopy (MRS) studies. *In vivo*, axonal damage can be monitored and located through the detection of *N*-acetylaspartate (NAA) by MRS in combination with MRI. The dipeptide, NAA, thought to be a marker of axonal integrity (Birken and Oldendorf, 1989), is reduced not only in chronic but also acute lesions (Bjartmar *et al.*, 2000; Davie *et al.*, 1999; Davie *et al.*, 1994; Reddy *et al.*, 2000). The decrease in the latter may be reversed suggesting a degree of recovery in compromised axons (Reddy *et al.*, 2000). Furthermore, in the absence of open demyelination, NAA is reduced in normal appearing white matter (NAWM) in the vicinity of acute and chronic lesions (Lee, *et al.*, 2000; Fu *et al.*, 1998), perhaps reflecting local axonal damage due to soluble inflammatory mediators, further expansion of the demyelinating lesion, or axonal disruption at a site along the tract remote from the changes detected locally. It should be noted that rat oligodendrocytes contain NAA which may contribute to the signal *in vivo* (Bhakoo and Pearce, 2000), although NAA remains unchanged in central pontine myelinolysis where axons remain undamaged following the complete loss of myelin (Davie *et al.*, 1999).

2.3 Current therapies

The majority of current therapies for use in multiple sclerosis are targeted at the suppression of, or the resolution of the inflammatory response in patients. The choice of therapy and regime is dependent on the state of disease in the patient at the time of presentation (see Clegg *et al.*, 2000 for an in depth review of current therapies).

The drugs of choice for acute relapse are adrenocorticotrophic hormone (ACTH) and the corticosteroids. In many patients they are able to reduce the severity and duration of relapses, although they are not disease modifying having no effect on the progression of disease, or on relapse rate (Sharrack *et al.*, 2000). In addition to the anti-inflammatory effects of the steroids, their efficacy is thought to be in part due to restoration of blood-brain barrier integrity and stimulation of T-cell apoptosis (Gold *et al.*, 2001). Steroids are only taken short-term due to the side effects associated with chronic treatment, so once the patient has gone into remission therapy is halted. No efficacy has been demonstrated for any other current treatment on acute relapse, so in patients that fail to respond to corticosteroid therapy, plasma exchange is the only other alternative available. Plasma exchange therapy involves the replacement of the patients blood plasma every other day over a seven day period. A recent clinical trial suggested there was significant clinical improvement in 40 % of patients who were previously unresponsive to corticosteroids (Weinshenker *et al.*, 1999).

The most effective current therapy for relapsing remitting multiple sclerosis (RRMS) is interferon- β (IFN- β) which is manufactured in two different forms, interferon β -1a and -1b. Betaseron, a Schering AG (Berlin) compound, is produced from bacterial cell lines, whereas the Biogen and Ares-Sereno products Avonex and Rebif, respectively, are both generated in mammalian cells. The two products differ in the extent of glycosylation, Avonex and Rebif are both highly glycosylated and are thought to be closer to the natural cytokine. Interferon- β therapy has been shown to reduce the frequency of relapse by around 30 % in relapsing remitting multiple sclerosis (Paty and Li, 1993; The IFN- β Multiple Sclerosis Study Group, 1993, 1995). In addition interferon- β has recently been shown to be effective in the treatment of secondary progressive multiple sclerosis

(SPMS; European Study Group, 1998; Simon *et al.*, 2000). In these studies, Interferon- β treatment was shown to delay time to the progressive stage of disease (European Study Group, 1998) and slow the development of hypointense MRI lesions (indicative of severe CNS damage; Simon *et al.*, 2000), although other clinical studies have failed to corroborate these observations (SPECTRIMS Study Group, 2001). The interferons are thought to act by reducing T-cell proliferation and altering the cytokine profile in the CNS in favour of type 2 helper T-cells (Th2), thereby reducing the number of circulating T-cells and promoting resolution of existing inflammatory lesions (Yong *et al.*, 1998).

Copolymer-1 (Copaxone: Glatiramer acetate) is a Teva Pharmaceuticals compound which is effective in the treatment of relapsing-remitting multiple sclerosis (Johnson *et al.*, 1995). It is a mixture of synthetic polypeptides, which are thought to work by promoting production of Th2 cytokines and competing with myelin peptides at MHC class II molecules so preventing activation of myelin-specific T-cells.

All three of these treatments are approved by the FDA for the treatment of multiple sclerosis, although only Interferon- β is approved for multiple sclerosis therapy in the United Kingdom. A number of other therapies for relapsing remitting multiple sclerosis do exist, but their use is not widespread and the clinical evidence for efficacy is questionable. Intravenous immunoglobulin is used in the treatment of autoimmune diseases and in at least one trial was effective in reducing the frequency of relapse in relapsing remitting multiple sclerosis (Fazekas *et al.*, 1997), although use in multiple sclerosis patients remains uncommon. Azothioprine, cladribine, cyclophosphamide, and methotrexate are all immunosuppressants shown to offer some benefit in multiple sclerosis patients, however, the studies have usually been small, of short duration and the

methodology has been questioned in a number of cases (Clegg *et al.*, 2000). None of these therapies is currently licensed in the UK for the treatment of multiple sclerosis.

Mitoxantrone, from Wyeth Laboratories, is a cytotoxic immunosuppressant with anti-inflammatory actions. It is the only compound other than interferon- β shown to have a beneficial effect in secondary progressive multiple sclerosis (Millefiorini *et al.*, 1997). Mitoxantrone is not licensed in the United Kingdom and its use is limited due to a serious side effect profile.

There are currently no therapies for primary progressive multiple sclerosis (PPMS), although both glatiramer acetate and interferon- β are in phase III trials at present. The lack of efficacy of the current immunomodulatory therapies in the prevention, or slowing of disease progression, even with complete T-cell deletion as in the case of CAMPATH-1H antibody treatment (Paolillo *et al.*, 1999), indicates that certain neuropathological processes, uncoupled from CNS inflammation, may be important in the pathogenesis of multiple sclerosis. The therapies described above rely on modulation of the inflammatory response. Since it is unlikely that CNS inflammation could be fully prevented without severely compromising the peripheral immune system, a pharmacological intervention which addresses the consequences of inflammation in the CNS environment would represent a novel and complementary therapy for the treatment of multiple sclerosis.

2.4 Involvement of glutamate in the pathogenesis of multiple sclerosis

Glutamate is widely implicated in the pathology of many acute and chronic neurological disorders. The role of glutamate in demyelinating disorders is less clearly defined, however, a number of studies have addressed the issue in the context of glutamate in multiple sclerosis. The concentration of glutamate in the CSF of multiple sclerosis patients has been measured in a variety of studies and several investigators, although not all, have reported elevated levels (Stover *et al.*, 1997a; 1997b; Launes *et al.*, 1998; Klivenyi *et al.*, 1997). Memantine, an NMDA antagonist offered symptomatic relief of pendular nystagmus in multiple sclerosis patients (Starck *et al.*, 1997) and a second report claimed a reduction in relapse rate in multiple sclerosis patients treated with amantidine, although in a very small patient cohort (Plaut, 1987). No study to date has examined the role of AMPA receptors in multiple sclerosis. An AMPA-targeted glutamatergic therapy in multiple sclerosis may have two major theoretical advantages over NMDA antagonists, the protection of oligodendrocytes, and prevention of motor neuron degeneration.

2.4.1 Oligodendrocyte protection in multiple sclerosis

The fate of oligodendrocytes in multiple sclerosis lesions is still a matter of contention. In early lesions there is initial recruitment of additional oligodendrocytes from a progenitor cell pool, resulting in an increase in the total number (Brück *et al.*, 1994; Ozawa *et al.*, 1994; Raine *et al.*, 1981), however, there are some notable exceptions in more aggressive acute lesions. The recruitment of oligodendrocytes to acute lesions allows limited remyelination to occur which may manifest itself as shadow plaques

(Lassmann, 1998). In chronic demyelinated lesions the pattern of distribution is very different. At this stage, hardly any oligodendrocytes remain and progenitor cells are no longer recruited to the lesion. What remains is extensive glial scar tissue and demyelination is irrecoverable (Prineas *et al.*, 1993).

The precise mechanism of oligodendrocyte death is not known, although a number of factors have been proposed including tumour necrosis factor- α (TNF α ; Bitsch *et al.*, 2000a), and complement (Scolding *et al.*, 1989). As for glutamate, oligodendrocytes do not express NMDA receptors but are known to express both kainate and AMPA glutamate receptors (Patneau *et al.*, 1994) rendering them vulnerable to glutamate excitotoxicity (Yoshioka *et al.*, 1995; 1996; Matute *et al.*, 1997; McDonald *et al.*, 1998). *In vivo*, kainic acid infusion into the optic tract induces demyelination of the optic nerve and formation of lesions similar to those seen in multiple sclerosis (Matute, 1998).

2.4.2 A role for neuroprotection in multiple sclerosis?

Neuronal and axonal loss are extensive in multiple sclerosis particularly in the later, progressive stages of disease (Losseff and Miller, 1998), but there is also more recent evidence suggesting that axonal disruption occurs in acute lesions much earlier in the disease course (Ferguson *et al.*, 1997; Evangelou *et al.*, 2000; Bitsch *et al.*, 2000b).

Whilst the underlying cause of this damage is again unknown, there is limited evidence for the involvement of glutamate and, in particular, AMPA receptors in the pathology of two other inflammatory CNS diseases, Rasmussen's encephalitis and paraneoplastic neurodegenerative syndrome. In Rasmussen's encephalitis there is widespread perivascular cuffing, gliosis and neuronal and axonal destruction. Paraneoplastic

neurodegenerative syndrome, a disease concomitant with certain cancers, has a predominant pathology related to T-cell infiltration and subsequent neuronal destruction. Both of these diseases are also linked with autoantibodies to AMPA receptors including GluR1, GluR3, GluR4 and GluR5/6 (Rogers *et al.*, 1994; Gähring *et al.*, 1995). Plasma exchange provides significant improvement for Rasmussen's encephalitis patients emphasising the importance of the autoantibodies in the disease pathology (Rogers *et al.*, 1994), and circulating autoantibodies in serum taken from paraneoplastic neurodegenerative syndrome patients are associated with an enhancement in glutamate-elicited currents *in vitro*, indicating the potential role of glutamate receptor activation in the pathogenesis (Gähring *et al.*, 1995).

Glutamate-induced neuronal damage is also implicated in the spinal motor neuron degeneration characteristic of amyotrophic lateral sclerosis (Ludolph *et al.*, 2000; Cleveland and Rothstein, 2001). A number of studies have demonstrated that motor neurons in the spinal cord are more sensitive to AMPA receptor-mediated excitotoxicity than other spinal neurons (Hugon *et al.*, 1998; Ikonomidou *et al.*, 1996) and consequently an imbalance in the glutamate system has been proposed as a key mediator in the pathogenesis of amyotrophic lateral sclerosis (Shaw and Ince, 1997; Ludolph *et al.*, 2000). Since spinal cord lesions are also a prominent feature of multiple sclerosis, it is possible that a disturbance in the glutamatergic system combined with the high sensitivity of spinal motor neurons to glutamate could also contribute to the axonal/neuronal damage described in this disease.

2.5 Experimental autoimmune encephalomyelitis

In order to investigate the pathogenesis of multiple sclerosis *in vivo*, a number of experimental animal models have been developed which reproduce various aspects of the disease. Experimental autoimmune encephalomyelitis (EAE), the main *in vivo* tool for the investigation of multiple sclerosis, was first described in the monkey by Rivers *et al.* (1933). Since then models in guinea pigs, rabbits, pigs and chickens have been established (Waksman, 1959), although latterly, mouse and rat models are extensively used given the convenience of size, availability and characterisation of their immune system.

Experimental autoimmune encephalomyelitis is generated in susceptible strains by immunising animals with either CNS tissue homogenates, or with whole or peptide fragments of CNS myelin proteins. Adoptive or passive transfer experimental autoimmune encephalomyelitis is induced by injection of appropriately sensitised T cells into naïve animals (Gold *et al.*, 2000). The composition of the inflammatory infiltrate and the extent of the pathology are dependent on the immunising antigen. Four main protein or peptide immunogens are used for the induction of experimental autoimmune encephalomyelitis in animals: myelin basic protein (MBP); proteolipid protein (PLP); myelin oligodendrocyte glycoprotein (MOG); and myelin-associated glycoprotein (MAG). The most commonly used protein, MBP, produces an acute experimental autoimmune encephalomyelitis, in Lewis rats, with a single phase of disease and a predominant T-cell and macrophage response. There is some peripheral demyelination in the spinal roots, but little in the CNS (Pender, 1988). PLP does not affect the peripheral nervous system (PNS), but does result in more extensive CNS demyelination than MBP

(Chalk *et al.*, 1994). In mice, the PLP-induced experimental autoimmune encephalomyelitis model has the advantage that the profile of disease is relapsing-remitting (Sobel *et al.*, 1990). MOG peptide produces a more severe model of disease in both rats and mice, particularly when combined with injection of anti-MOG antibody (Linington *et al.*, 1993). The disease profile is hyperacute and characterised by a large antibody response, the presence of neutrophils in addition to the normal inflammatory infiltrate and the model can also result in haemorrhagic oedema. The strong disease induction with MOG is often attributed to expression of the protein on the surface of the myelin sheath, making the epitope more readily exposed to anti-MOG antibodies. More recently, a MOG-induced experimental autoimmune encephalomyelitis model was described in the Dark Agouti (DA)/Brown Norway (BN) rat, which displays a prolonged relapsing remitting profile with accompanying CNS myelin and axonal pathology akin to that seen in multiple sclerosis (Storch *et al.*, 1998). MAG is also expressed at the outer surface of the myelin sheath (Quarles, 1997) and therefore, a similar extent of disease and demyelination might be expected with MAG as with MOG. However, although MAG is able to induce extensive CNS inflammation, there is little demyelination and, indeed, disease induction is very weak (Weerth *et al.*, 1999). If combined with anti-MOG antibody a demyelinating phenotype is expressed. The immunising autoantigen need not be a component of CNS myelin in order to produce an encephalitogenic response. S100 β , an astrocyte-derived calcium binding protein, is also found in peripheral cells such as adipocytes. Animals immunised with this protein develop extensive CNS inflammation including the retina and uvea (Kojima *et al.*, 1997). The changes in the eye are interesting because a similar phenomenon is seen in multiple sclerosis, but not in animals models which use myelin antigens as the immunogen. This indicates that autoantigens possibly expressed in multiple sclerosis could also represent a diverse array

of epitopes. Indeed the different lesion distributions seen in multiple sclerosis may reflect differences in the antigen specificity of encephalitogenic T-cells (Berger *et al.*, 1997).

2.6 Pathogenesis of experimental autoimmune encephalomyelitis

The pathology of experimental autoimmune encephalomyelitis is varied and dependent on the immunogen used in the inoculum. However, the evolution of the inflammatory response contains elements common to all antigens. T-cells are able to cross the blood-brain barrier under normal physiological conditions performing a form of immune surveillance (Flugel *et al.*, 1999; 2000), but if they fail to encounter their specific antigen, they re-enter the vasculature, or die. In experimental autoimmune encephalomyelitis, and as is assumed in multiple sclerosis, antigen specific CD4⁺ T-cells cross into the CNS where they are presented with their specific antigenic epitope by MHC class II-positive antigen presenting cells. This stimulates the production and release of pro-inflammatory cytokines and chemokines into the extracellular milieu prompting a subsequent full scale inflammatory response (reviewed in Cuzner and Smith, 1995). The end result is further recruitment of CD4⁺ T-cells, with a range of antigen specificity, expansion of the T-cell population within the CNS, recruitment of macrophages and antibody infiltration through opening of the blood-brain barrier. In some models it is this antibody response which leads to complement activation and demyelination (Linington *et al.*, 1989).

The composition of the inflammatory infiltrate is highly dependent on the immunising protein. For example, S100- β causes extensive CNS infiltration but no clinical phenotype (Kojima *et al.*, 1997), whereas MBP immunisation causes inflammation which

is associated with an ascending muscle paralysis. Upon closer inspection it is clear that the infiltrate in S100- β is primarily composed of T-cells with very few macrophages. However, in MBP-immunised animals, whilst there are still many T-cells there are also many more macrophages, approximately twice as many macrophages as T-cells (Smith *et al.*, 1996). It could be concluded from this that whilst there can be extensive T-cell infiltration in experimental autoimmune encephalomyelitis, it is the macrophages that are responsible for clinical phenotype. Indeed, depletion of peripheral macrophages using toxin-loaded liposomes, results in a T-cell-dominated lesion without symptoms of paralysis (Huitinga *et al.*, 1990).

The clinical consequence of the directed CNS inflammatory response seen in experimental autoimmune encephalomyelitis is an ascending muscle weakness and paralysis preceded by weight loss. The paralysis, in both multiple sclerosis and experimental autoimmune encephalomyelitis, is attributed to an impairment in neuronal conduction as a consequence of demyelination (Pender, 1987; 1988) and oedema (Simmons *et al.*, 1982; Kerlero de Rosbo *et al.*, 1985).

As with the relapsing, remitting form of multiple sclerosis, in the acute phase of experimental autoimmune encephalomyelitis in animals, paralysis is followed by spontaneous symptomatic recovery. The mechanisms underlying resolution of disease are not fully understood, but in experimental autoimmune encephalomyelitis recovery is thought to represent a change in the cytokine profile and concomitant switch in T-cell population from Th1 to Th2-type which coincides with an increase in endogenous steroid levels at the peak of disease (MacPhee *et al.*, 1989). Apoptosis has also been shown to be an important mechanism in the clearance of T-cells from the CNS and thus, resolution of inflammation (Pender *et al.*, 1991; Schmied *et al.*, 1993).

2.7 Evidence for the glutamatergic system in the pathogenesis of experimental autoimmune encephalomyelitis

Information on the involvement of glutamate in the pathogenesis of multiple sclerosis is limited, although there are a greater number of studies which address the issue in experimental autoimmune encephalomyelitis. Levels of glutamate in whole tissue homogenates from experimental autoimmune encephalomyelitis animals reportedly decrease at the peak of disease with concomitant increases in the glutamate metabolite, glutamine, the NMDA co-agonist, glycine and the neurotoxin quinolinic acid (Honegger *et al.*, 1989; Turecky *et al.*, 1980; Flanagan *et al.*, 1995). These data suggest that, at this time point, there are alterations in glutamate homeostasis which could be attributed to either a decrease in synthesis and release of glutamate and/or increased metabolism. Glutamate is normally removed from the extracellular compartment by uptake into astrocytes where it is converted into glutamine by glutamine synthetase (GS), or deaminated by glutamate dehydrogenase (GDH). In EAE, however, expression of these enzymes is reduced in astrocytes (Hardin-Pouzet *et al.*, 1997), conversely, GS is detectable in oligodendrocytes (Cammer *et al.*, 1990). Utilisation of this oligodendrocyte pathway may help to explain the elevations in glutamine.

As in multiple sclerosis, therapeutic intervention during experimental autoimmune encephalomyelitis has focused on the potential of NMDA antagonists. Both MK-801 and memantine were effective in reducing neurological symptoms in acute rat models of experimental autoimmune encephalomyelitis (Bolton and Paul, 1997; Wallstrom *et al.*, 1996). The efficacy of NMDA antagonism, in both cases, appeared to be independent of effects on lymphocyte proliferation and CNS infiltration.

Whilst there are few studies of the direct involvement of AMPA receptors in the pathogenesis of experimental autoimmune encephalomyelitis or multiple sclerosis, there is a body of evidence concerning AMPA-mediated toxicity to oligodendrocytes and neurons (Matute *et al.*, 1997; Hugon *et al.*, 1989). Moreover, the high density of AMPA receptors in the dorsal horn of the spinal cord and dorsal root ganglia (Tachibana *et al.*, 1994) correlates with the primary sites of the limited demyelination seen in the Lewis rat model of experimental autoimmune encephalomyelitis (Pender, 1988). White matter injury was also the focus of a study by Li and Stys (2000) which found that oligodendrocytes, astrocytes and particularly the myelin sheath were the target of AMPA receptor-mediated excitotoxicity *in vitro*.

In addition to synaptic release from neurons, glutamate has a number of potential sources in CNS inflammatory disease. Resident glial cells are able to produce glutamate and represent an important pathological source from within the CNS (Vesce *et al.*, 1999; Haydon, 2001). In addition, infiltrating leucocytes, prevalent in the CNS during disease, are able to release glutamate when activated (Piani *et al.*, 1991). More recently, inhibitors of *N*-acetylated- α -linked-acidic dipeptidase (NAALADase), an enzyme with a unique involvement in synaptosomal release of glutamate under pathological conditions (Stauch *et al.*, 1989), have been shown to be protective in a large number of models of CNS neurodegeneration (Slusher *et al.*, 1999; Gong *et al.*, 2000; Wozniak *et al.*, 2000; Slusher *et al.*, 2000). NAALADase is able to generate glutamate by hydrolysis of *N*-acetyl-aspartyl-glutamate (NAAG).

2.8 Models of experimental autoimmune encephalomyelitis

The experiments described aimed to establish the effect of a variety of AMPA receptor antagonists in the disease progression of experimental autoimmune encephalomyelitis using three different rodent models. The first, MBP-induced acute active experimental autoimmune encephalomyelitis in Lewis rats, is the simplest model to perform and is particularly useful for investigating the acute phase of disease from T-cell expansion, through CNS infiltration, to production and resolution of clinical symptoms (Flugel *et al.*, 1999, 2001). Also, for the purposes of these studies, in the Lewis rat demyelination is limited which suggests a larger possible role for neuronal and axonal impairment in the evolution of clinical symptoms.

The adoptive transfer experimental autoimmune encephalomyelitis model in Lewis rats is highly reproducible and bypasses the T-cell expansion phase of disease, therefore eliminating the possibility of a pharmacological agent acting at the early stages (Paterson, 1960).

The third *in vivo* model used in these studies was chronic experimental autoimmune encephalomyelitis in Biozzi mice (Baker *et al.*, 1990). This model was chosen because it has a relapsing, remitting secondary phase. There is also extensive demyelination during the course of disease, which is unseen in the acute models, and therefore is more representative of relapsing remitting and chronic progressive multiple sclerosis.

In addition to examining the clinical protection exhibited by AMPA antagonists, the anti-inflammatory effects of the compounds were investigated to differentiate the protective effects attributable to neuronal and oligodendrocyte protection, from any

immunomodulatory actions. Furthermore, ultrastructural analysis was undertaken to establish the pathological changes associated with disease and the effect of the compounds on these changes.

2.9 Materials and methods

2.9.1 Animals

Female adult Lewis rats (200-220 g) were obtained from Charles River, UK and adult male Biozzi mice (ABH, H-2^{dq1}; 20-22 g) from Harlan, UK. All Lewis rats were housed in pairs and Biozzi mice were housed individually under environmentally controlled conditions (6:00 - 18:00; 12 hour light/dark cycle; 24-25 °C) and permitted free access to food and water.

2.9.2 Induction of experimental autoimmune encephalomyelitis in Lewis rats

Adult Lewis rats were lightly anaesthetised with 2 % halothane in 70 % nitrous oxide/30 % oxygen, and injected subcutaneously in the dorsal surface of each hind foot with 50 µl inoculum containing 50 µg purified guinea pig MBP (final concentration of 1 mg/ml; MBP was prepared according to the method of Dunkley and Carnegie (1974)), complete Freund's adjuvant (CFA; Sigma, Dorset, UK) and *Mycobacterium tuberculosis* H37Ra (5.5mg/ml; Difco Laboratories, Surrey, UK). Sham-immunised rats received subcutaneous Freund's complete adjuvant containing *Mycobacterium tuberculosis* alone. Typically, disease onset was between days 9 and 11 post immunisation with peak disease occurring at around day 13 and animals recovering by day 16. The experiments were terminated on day 18 and tissues removed for histological investigation. Neurological deficits were determined daily according to the scale in 2.9.4.

2.9.3 Adoptive transfer experimental autoimmune encephalomyelitis in Lewis rats

Lewis rats were immunised as in section 2.9.2. Ten days after immunisation, rats were culled and spleens removed. The spleens were placed into chilled Earle's balanced salt solution (EBSS; Gibco Ltd., Paisley, UK) and placed on ice. The spleens were then washed twice in EBSS and homogenised through a stainless steel gauze with the plunger of a 5 ml syringe. The cells were then re-suspended in 50 ml EBSS and centrifuged at 1500 g for 10 min at 4 °C. After centrifugation the supernatant was removed and the pellet re-suspended in a further 20 ml EBSS and filtered through two nylon mesh (132 µm and 80 µm) placed one on another. Splenic lymphocytes were cultured at 2×10^6 /ml in RPMI 1640 medium supplemented with 10 % heat inactivated foetal calf serum (First Link UK Ltd), 2 mM glutamine, 100 U/ml penicillin, 100 µg/ml streptomycin (Gibco Ltd., Paisley, UK), 2 µM 2-mercaptoethanol, 1 mg/ml indomethacin (Sigma, Poole, UK) with purified guinea pig MBP at 1 µg/ml for 72 hrs at 37 °C in an atmosphere of 5 % CO₂/95 % O₂. Harvested lymphocytes were finally washed three times in unsupplemented RPMI 1640 and 4×10^7 cells were injected intraperitoneally (i.p.) to naïve Lewis rats. Following transfer, disease onset occurs on day 4, the peak of disease is reached by day 6 and animals recover by day 8. The experiments were terminated on day 10 and tissues collected for evaluation of pathology. Neurological deficits were determined daily according to the scale in 2.9.4.

2.9.4 Neurological assessment

Monitoring of neurological deficits during the course of EAE was performed daily prior to administration of vehicle or drugs to ensure that the motor side effects of therapy with AMPA antagonists, such as sedation or reduction of muscle tone, did not interfere with

disability scores. The following scoring system was used to grade neurological impairment: (0) no detectable changes in muscle tone and motor behaviour; (1) flaccid tail; (2) impairment of righting reflex and/or loss of muscle tone in hindlimbs; (3) complete hindlimb paralysis; (4) paraplegia; and (5) death. In addition intermediate scores were assigned to animals which demonstrated paralysis lying between points on the scale, for example loss of tail tone in just the distal half of the tail scored 0.5. Body weight was monitored daily by means of a Sartorius model U 6100 electronic balance (Sartorius Ltd., Surrey, UK).

2.9.5 Induction of chronic relapsing experimental autoimmune encephalomyelitis

Biozzi mice (20-22 g) were culled by cervical dislocation. Spinal cords were removed by insulflation, homogenised using a Polytron PT3000 (Kinematica AG, Phillips Harris Scientific, London, UK) and freeze dried (Virtis freeze drier; Biopharma Process Systems Ltd, Winchester, UK). To prepare the inoculum, lyophilised spinal cord homogenate was reconstituted in phosphate buffered saline to a final concentration of 6.6 mg/ml. Incomplete Freund's adjuvant (IFA; Difco Laboratories, Surrey, UK) was supplemented with *M. tuberculosis* (H37Ra; Difco Laboratories, Surrey, UK) and *M. butyricum* (8:1; Difco Laboratories, Surrey, UK). Naïve Biozzi mice were lightly anaesthetised with 2 % halothane in 70 % nitrous oxide/30 % oxygen and immunised subcutaneously (s.c.) on day 0 and day 7 in the flank at three sites with 0.3 ml of the emulsion (1 mg spinal cord homogenate, 60 µg of combined *Mycobacterium tuberculosis* and *Mycobacterium butyricum*). In addition, mice were injected (i.p.) with 200 ng of pertussis toxin (*Bordetella pertussis*, Calbiochem; 2 µg/ml in phosphate buffered saline) immediately and 24 hours after immunisation with neuroantigens. Monitoring of neurological deficits

was performed daily before administration of vehicle or drugs. The following scoring system was used to grade neurological impairment: (0) no detectable changes; (1) flaccid tail; (2) impairment of righting reflex and/or loss of muscle tone; (3) complete hindlimb paralysis; (4) paraplegia; and (5) death. In addition intermediate scores were assigned to animals which demonstrated paralysis lying between points on the scale, for example loss of tail tone in just the distal half of the tail scored 0.5. During the observation period mice were housed individually under environmentally controlled conditions (6:00 a.m. to 6:00 p.m.; 12-hr light/dark cycle; 24-25 °C) and permitted free access to food and water. The evaluation of clinical deficits continued up to day 48 when the animals were culled and tissue collected for investigation.

2.9.6 Compounds and dosing regimens

Six different AMPA antagonists were used in these studies. NBQX (2,3-dihydroxy-6-nitro-7-sulfamoylbenzo(f)quinoxaline; gift from Chrissanthy Ikonomidou, Berlin, Germany) and MPQX ([1,2,3,4-tetrahydro-7-morpholinyl-2,3-dioxo-6-(trifluoromethyl)quinoxalin-1-yl]methylphosphonate) are both competitive antagonists, whilst GYKI52466 (1-(4-aminophenyl)-4-methyl-7,8-methylene-dioxy-5H-2,3-benzodiazepine; Sigma, Dorset, UK), GYKI53773 ((-)-1-(4-aminophenyl)-4-methyl-7,8-methylene-dioxy-4,5-dihydro-3-methylcarbamoyl-2,3-benzodiazepine), BIIR561 (5-(2-[N,N-dimethylamino]oxy-phenyl)-3-phenyl-1,2,4-oxadiazol), and CP465022 (3-(2-chlorophenyl)-2-[2-[6-[(diethylamino)methyl]-2-pyridinyl]ethenyl]-6-fluoro-4(3H)-quinazolinone) are all non-competitive antagonists (all AMPA receptor antagonists were a gift from Eisai Co., Japan, unless otherwise stated). In addition to the six antagonists investigated, aniracetam (Tocris Cookson Ltd., Avon, UK) was used in order to assess

the effects of potentiation of AMPA receptor activation. Aniracetam potentiates AMPA receptor activation by reducing receptor desensitisation.

NBQX, MPQX, GYKI52466, GYKI53773, BIIR561, CP465022 and vehicle were administered in a volume of 0.5 ml/100 g of body weight i.p.. The vehicles for drug administration were different for each AMPA antagonist. NBQX was dissolved in 10 M NaOH, made up to the correct volume with water. The pH was then titrated back to 7.0 with dropwise additions of concentrated HCl (12 M). MPQX is highly soluble in water, but the pH did need correcting with NaOH. The other compounds GYKI52466, GYKI53773, BIIR561, CP465022 and aniracetam were all prepared as a suspension in 5 % Cremophor in PBS. Doses were selected to ensure optimal plasma concentrations for the duration of disease (personal communication, Prof. Lechoslaw Turski, Solvay Pharmaceuticals, Weesp, Netherlands).

2.9.6.1 Actively-induced acute experimental autoimmune encephalomyelitis

In the active-induction experimental autoimmune encephalomyelitis model, NBQX at 3, 10 and 30 mg/kg i.p. and MPQX at 2.5, 5 and 10 mg/kg i.p. were given twice daily for 7 days starting 10 days post immunisation (dpi). GYKI52466, GYKI53773, BIIR561 and aniracetam were given using the same treatment protocol, but only a single dose of 30 mg/kg i.p. twice daily was tested. CP465022 was examined at a single dose of 10 mg/kg i.p. twice daily. These doses were selected to assure that relevant concentrations were achieved in the brain for AMPA/kainate receptors antagonism (Sheardown *et al.*, 1990; Turski *et al.*, 1998; Tarnawa and Vizi, 1998).

2.9.6.2 Adoptive transfer acute experimental autoimmune encephalomyelitis

NBQX alone was used in the adoptive transfer acute experimental autoimmune encephalomyelitis. The compound was prepared as in 2.9.6 and rats were given either NBQX at 30 mg/kg i.p. or vehicle twice daily starting on day 4 post transfer. Rats were dosed for seven days.

2.9.6.3 Chronic experimental autoimmune encephalomyelitis in Biozzi mice

Chronic NBQX treatment is associated with nephrotoxicity, due to compound precipitation in renal tubules. In order to avoid problems in this chronic model, two different dosing schedules were chosen to cover the different phases of disease. The first schedule was designed to investigate the disease modifying potential of NBQX on the acute phase of disease and subsequent disease progression. NBQX was prepared in the same vehicle as described in 2.9.6 and mice received either vehicle or NBQX, administered at a dose of 30 mg/kg i.p., twice daily from days 10-16 post immunisation. The second regimen evaluated the efficacy of AMPA antagonists on the chronic phase of disease. In order to avoid nephrotoxicity and allow for a longer period of therapeutic coverage in the chronic phase, NBQX or vehicle were given once daily between days 26 and 42 post immunisation. NBQX was administered at a dose of 30 mg/kg i.p..

2.9.7 Quantification of neuroinflammation

Rats were culled at the peak of disease (day 12 or 13) by concussion and cervical dislocation. The brainstems were then removed and immediately frozen on dry ice. Frozen sections of rat brainstem (AP -7.0 to -15.0; V -8.60) (Paxinos and Watson, 1998),

10µm thick, were cut on a Bright cryostat and fixed in 100 % ethanol. Sections were then stained with hematoxylin for 4 min and washed for 10 min in running water before mounting under DPX. All sections were assessed by light microscopy for the presence of perivascular cuffs. The following scoring system was used to grade histopathological changes induced by inflammation: (0) no detectable changes; (1) perivascular inflammation of up to three cell layers; (2) perivascular inflammation of more than three cell layers; and (3) parenchymal cell infiltrates. The histopathological score was calculated by adding all scores for lesions detected in a given section and the mean of 2 sections was taken for statistical analysis.

2.9.8 Evaluation of immunosuppression in a T-cell proliferation assay *in vitro*

Splenic lymphocytes from Lewis rats were prepared as in 2.9.3 and after the final wash, incubated in RPMI 1640 modified medium at a concentration of 1×10^6 /ml with concanavalin A (1 µg/ml; Sigma, Dorset, UK) and increasing concentrations of AMPA antagonists or dexamethasone. Ninety six hours after the addition of the stimulating mitogen, 1 µCi of ^3H -thymidine (Amersham International plc, Buckinghamshire, UK) was added for a further 6 hrs, then the cells were harvested (Semat International Ltd., Hertfordshire, UK) onto filter mats (Camo, Suffolk, UK), air dried, 2.5 ml of scintillant added (Beckman Instruments UK Ltd., Buckinghamshire, UK) and incorporated radioactivity determined (Beckman™ LS6000IC scintillation counter). NBQX, MPQX, GYKI52466, GYKI53773, CP465022 and BIIR561 were tested at concentrations of 0.01, 1, 10 and 100 µM, while dexamethasone, used here as a positive control, was tested in concentrations of 0.001, 0.01, 0.1 and 1 µM. Lymphoproliferation in response to the lectins, phytohaemagglutinin or concanavalin A, requires the engagement of the T-

lymphocyte receptor and the synthesis of the T-lymphocyte growth factor interleukin-2. Agents that inhibit lymphoproliferation such as dexamethasone exhibit immunosuppressive action.

2.9.9 Quantification of neuronal density in the spinal cord

To provide an estimate for possible neuronal loss in the spinal cord at the time of peak disease symptoms (13-16 d.p.i.), numerical densities (N_V) of neurons in the ventral and dorsal horns, and in the intermediate zone of the lumbar cord were determined using the stereologic disector method (Cruz-Orive and Weibel, 1990; Ikonomidou *et al.*, 1999). An unbiased counting frame (0.1 mm x 0.1 mm; disector height 0.015 mm) and a high-aperture objective (x100) were used for the sampling (Ikonomidou *et al.*, 1999) to evaluate neuronal density in toluidine blue sections (preparation of toluidine blue sections described in 2.9.11). Normal neurons were identified by the presence of the typical nuclei with clear nucleoplasm and distinct nucleolus surrounded by cytoplasm. An arbitrary horizontal line connecting the lateral ends of the spinal cord and crossing the ventral edge of the central commissure was considered a junction between intermediate zone and ventral horns (Fig. 2.9.9). An arbitrary parallel horizontal line crossing the dorsal edge of the central commissure was considered a junction between intermediate zone and dorsal horns (Fig. 2.9.9).

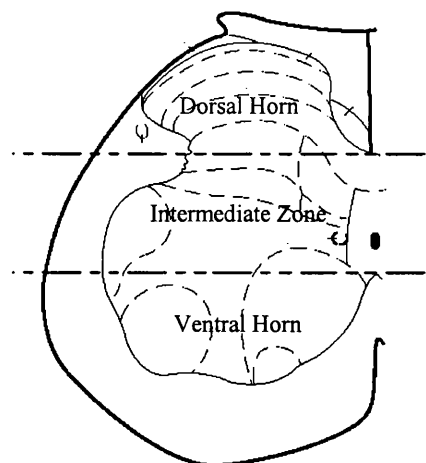


Figure 2.9.9 Schematic of lumbar spinal cord depicting the areas defined as ventral, intermediate and dorsal for neuronal density estimations. Reproduced from Paxinos and Watson, 1998.

The gray matter of the ventral horns contains motor neurons controlling function of the limbs and trunk, and interneurons. The intermediate zone contains sensory neurons projecting towards the cerebellum, preganglionic autonomic neurons and interneurons. The dorsal horns contain sensory projection neurons connecting supraspinal centres.

2.9.10 Light microscopy

Rats were deeply anaesthetised with sodium pentobarbitone (100 mg/kg i.p. Sagatal™; Rhône Mérieux Ltd., Essex, UK) and perfused through the left ventricle with a fixative containing 4 % paraformaldehyde (Sigma, Dorset, UK) and 0.5 % glutaraldehyde (Sigma, Dorset, UK) in phosphate buffered saline (Sigma, Dorset, UK). Blocks of lumbar spinal cord were then embedded in paraffin and coronal sections of the lumbar spinal cord were cut at 10-15 μm thick on a sledge microtome and mounted on gelatin-coated glass slides. The sections, once dried, were then de-paraffinised in xylene and rehydrated through graded ethanols before staining with Harris's hematoxylin (Sigma, Dorset, UK) for 2 min, rinsing in tap water, differentiating in 70 % ethanol containing 1 % HCl, washing in tap water again for 5 min and counterstaining with eosin (Sigma, Dorset, UK) for up to 1 min. Finally sections were dehydrated through graded ethanols, cleared in Histo-Clear™

(Agar Scientific, Essex, UK) and coverslips mounted with DPX mounting medium (Fisons Scientific Equipment, Loughborough, UK).

2.9.11 Electron microscopy

Rats were anaesthetised and perfused as above (2.9.10). For electron microscopy the tissue was sectioned through the lumbar spinal cord into 200 μm blocks using an Oxford vibratome (Agar Scientific, Essex, UK) and collected in 0.1 M sodium phosphate buffer (pH 7.4). Sections were then osmicated for 40 min in 1 % osmium tetroxide (Agar Scientific, Essex, UK) in 0.1 M phosphate buffer, washed in the phosphate buffer for 5 min, before changing to two washes of 10 min each in 0.1 M sodium acetate followed by staining for 15 min in 2 % uranyl acetate in 0.1 M sodium acetate (Agar Scientific, Essex, UK) at 4°C. The sections were then washed again in 0.1 M sodium acetate and switched to distilled water. Next, the sections were dehydrated in graded ethanol, cleared in four changes of propylene oxide at 10 min each and changed for 50 % propylene oxide/50 % araldite resin for 45 min. The araldite resin is composed of 10 g dodecenyl succinic anhydride (DDSA), 10 g Araldite (CY212) and 0.8 g plasticizer (dibutyl pathalate) which are heated and mixed. When mixed, 0.4 ml benzyldimethylamine (BDMA) is stirred into the resin (all resin reagents are available from Agar Scientific, Essex, UK). The blocks were then soaked in fresh araldite for 24 hours on a rotator and finally embedded in araldite resin between Melinex™ (Dupont Teijin Films, Cleveland, UK) sheets and baked at 60 °C overnight. Semithin (1 μm) coronal sections were cut with adjacent thin (80 nm) sections using a glass knife on a Reichert Ultracut E ultramicrotome (Leica UK Ltd., Bucks, UK). Semithin sections were stained with toluidine blue (Agar Scientific, Essex, UK) for 40 sec and rinsed with distilled water for

light microscopy, whilst thin sections were mounted on 200 μm electron microscope copper grids (Agar Scientific, Essex, UK), counterstained with lead citrate (Agar Scientific, Essex, UK) and examined in a JEOL 1010 transmission electron microscope.

2.9.12 Immunohistochemistry

Rats were culled at the peak of disease by concussion and cervical dislocation and the spinal cords removed by insulflation and rapidly frozen on dry ice. Coronal sections were cut through the lumbar spinal cord at 15 μm on a Bright cryostat (Bright Instrument Company Ltd., Cambridgeshire, UK) and thaw mounted on gelatin-coated slides. The sections were air dried and stored at $-20\text{ }^{\circ}\text{C}$ until staining. The following mouse monoclonal antibodies were used to examine resident and infiltrating cells in the spinal cord: OX34 (1:500, Serotec, Oxford, UK) specific for CD2 on T-lymphocytes; OX33 (1:100, Serotec, Oxford, UK) specific for CD45RA on B-lymphocytes; Clone 10/78 (1:100, Serotec, Oxford, UK) specific for CD161 on NK-lymphocytes (1:100, Serotec, Oxford, UK); ED1 (1:500, Serotec, Oxford, UK) which recognises a lysosomal membrane-related antigen on rat macrophages/microglia; OX-42 (1:3000, Serotec, Oxford, UK) which binds the complement receptor 3 on microglia/macrophages; and 5.2E4 (1:1000, Institute of Neurology, London, UK) for GFAP staining of astrocytes. For staining, spinal cord sections were fixed in ethanol for 1 min at room temperature, washed for 5 min in two changes of phosphate-buffered saline (PBS) and incubated in 2.5 % normal serum for 30 min at room temperature. Sections were incubated with the primary antibody for 1 hour, and washed twice in PBS before adding a biotinylated rat-absorbed anti-mouse IgG (1:200, Vector, Peterborough, UK). The sections were washed again in PBS and peroxidase labelled avidin-biotin complex (ABC, Vector,

Peterborough, UK) added to the sections for 45 min. Peroxidase activity was detected in 3,3'-diaminobenzidine (Sigma, Dorset, UK) solution in phosphate buffered saline containing 0.01 % hydrogen peroxide (Sigma, Dorset, UK). Rinsed sections were counterstained in Harris's hematoxylin (Sigma, Dorset, UK) for 30-60 sec, washed in running water, dehydrated in graded alcohols, cleared in Histo-Clear™ (Agar Scientific, Essex, UK) and mounted on glass slides under DPX mounting medium (Fisons Scientific Equipment, Loughborough, UK). Sections with no primary antibody were included into each staining run as controls.

2.9.13 Statistics

Data for peak disease and cumulative disease scores in all three *in vivo* models were analysed by Mann-Whitney U-test. Onset, duration and percent weight loss analysed by Student's t-test. The data for the adoptive transfer model were analysed by χ^2 test and the efficacy of NBQX in the Biozzi model was analysed by repeated measures analysis of variance (ANOVA) as was the dose dependency of NBQX and MPQX in acute EAE. All statistics were performed using Statview statistical software (Abacus concepts Inc., Berkeley, California).

2.10 Results

2.10.1 The effects of AMPA modulation on the progression of experimental autoimmune encephalomyelitis in the Lewis rat

In MBP-immunised Lewis rats, encephalitogenic MBP-specific T-cells are generated in the periphery during the pre-clinical phase, approximately 0-8 d.p.i.. Subsequently, these T-cells migrate to the brain and spinal cord and initiate the cascade of CNS inflammation (Flugel *et al.*, 1999, 2000). The clinical symptoms in vehicle treated animals typically start to develop between 9 and 12 days post immunisation (d.p.i.) and reach a peak disease of about score 3.0 (complete hindlimb paralysis) around day 12 or 13 d.p.i.. By day 16 d.p.i. the animals have fully recovered from disease and the experiments are terminated on day 18 d.p.i.. Fig. 2.10.1.1b shows the typical disease profile of onset and recovery seen with this model. Weight loss precedes the onset of disease. Control animals begin to lose weight from around day 9 d.p.i. and there is typically a 15-20 % weight loss over the course of disease compared with the pre-disease peak (the maximum weight prior to disease onset was used for the determination of percent weight change). The profile of weight loss is shown in Fig. 2.10.1.1c.

2.10.1.1 NBQX in acute Lewis rat experimental autoimmune encephalomyelitis

Disease onset occurred in 100 % of vehicle, 3 and 10 mg/kg NBQX treated animals and in 21/30 of 30 mg/kg NBQX animals (Table 2.10.1.1). 3 and 10 mg/kg NBQX did not effect any of the disease parameters investigated (Table 2.10.1.1 and Fig. 2.10.1.1), but twice daily treatment with NBQX (30 mg/kg i.p.) significantly reduced duration of disease, peak disease score, cumulative score and weight loss (Table 2.10.1.1 and Fig.

2.10.1.1). These changes represent a significant improvement in motor function with NBQX treatment. A mean score of 3.2, as seen in the vehicle treated group, represents complete hindlimb and tail paralysis with additional weakness of the forelimbs, whereas the NBQX treated group scored a mean of 1.8. These animals on average would only have exhibited tail paralysis and a slightly unsteady gait. These data also show the steep dose response curve typically seen with AMPA antagonists (Ikonomidou and Turski, 1997; Turski *et al.*, 1998).

Treatment	Incidence (%)	^a Onset /d.p.i.	Duration /days	Peak Disease Score	^b Cumulative Disease Score	^c Weight Loss %
Vehicle	40/40 (100)	11.1 (9-14)	4.6 (3-6)	3.1 (1.0-4.0)	11.1 (5.25-18.5)	21 (11-25)
NBQX (3)	10/10 (100)	11.1 (9-12)	4.2 (2-5)	3.2 (0.5-5.0)	11.0 (0.75-12.75)	20 (10-25)
NBQX (10)	10/10 (100)	11.0 (10-11)	4.2 (1-6)	3.2 (0.5-5.0)	11.5 (0.5-18.25)	22 (6-27)
NBQX (30)	21/30 (70)	11.0 (10-12)	3.1 (0-6)††	1.8 (0-3.5)††	5.9 (0-14.75)††	17 (5-25)††

Table 2.10.1.1 Parameters of disease activity during experimental autoimmune encephalomyelitis in Lewis rats. ††p<0.001 vs. vehicle by Mann-Whitney U-test or Student's t-test for non-parametric and parametric data, respectively. a; n=21 for NBQX. b; calculated by summation of individual daily disease scores. c; weight on cessation of the experiment as a percentage of the maximum weight before disease onset. Values represent mean and range.

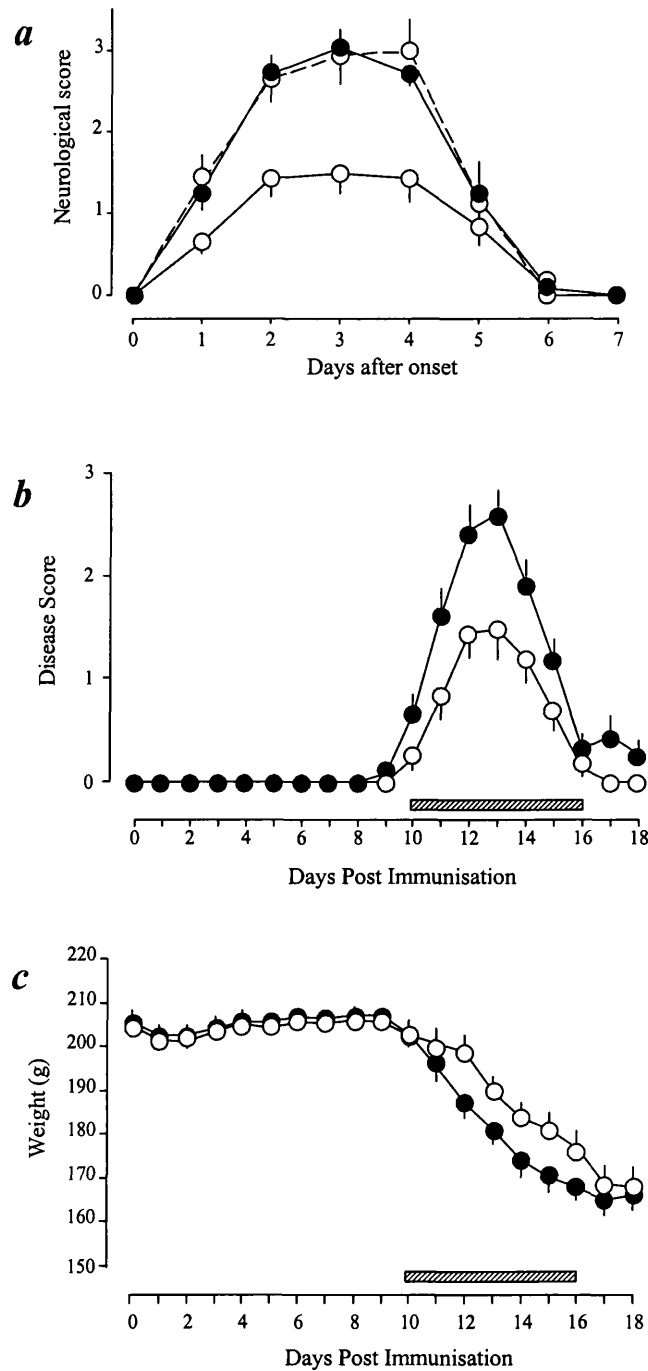


Figure 2.10.1.1 The effect of NBQX on motor disability induced by experimental autoimmune encephalomyelitis in Lewis rats. NBQX (○) or vehicle (●) were administered twice daily i.p. for 7 days starting on day 10 (hatched bar in *b* and *c*). *a* shows the dose response relationship synchronised to days post disease onset with Vehicle (n=40) or NBQX at 3 mg/kg (dashed line; n=10) and 30 mg/kg (solid line; n=16). *b* shows data for NBQX at 30 mg/kg (○) and vehicle (●) as days post immunisation. *c* gives the change in weight following immunisation for the data shown in *b*. Data represent mean ± s.e.m..

2.10.1.2 MPQX in acute Lewis rat experimental autoimmune encephalomyelitis

MPQX caused a dose-dependent reduction in disease disability compared with vehicle treated animals ($F(3, 42)=13.40$, $p<0.001$ by ANOVA). Only 63 % of high dose MPQX animals showed signs of disease compared with 100 % of vehicle animals (Table 2.10.1.2). 2.5 mg/kg MPQX had no effect on any of the disease parameters in this study and although 5 mg/kg MPQX appears to reduce disease (Fig. 2.10.1.2), this did not quite reach statistical significance (Table 2.10.1.2 and Fig. 2.10.1.2). However, twice daily treatment with MPQX at 10 mg/kg i.p. did significantly delay disease onset and reduce duration of disease, peak disease score and cumulative score (Table 2.10.1.2 and Fig. 2.10.1.2). The degree of protection was such that the highest dose animals only scored a mean of 1.2 (floppy tail) compared to complete hindlimb paralysis with partial forelimb involvement (mean score 3.2) in vehicle animals.

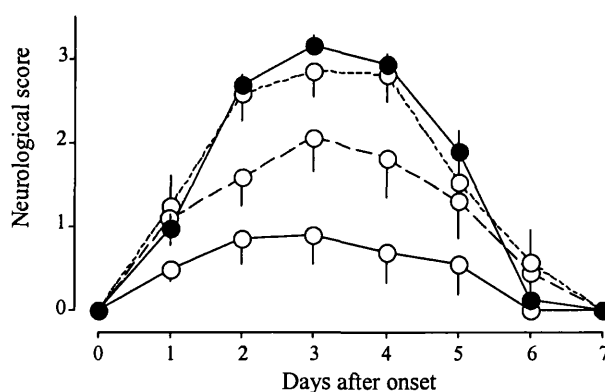


Figure 2.10.1.2 Dose-dependent effect of MPQX on motor disability induced by experimental autoimmune encephalomyelitis in Lewis rats. MPQX (○) at 2.5 mg/kg (dotted line; $n=10$), 5 mg/kg (dashed line; $n=10$) and 10 mg/kg (solid line; $n=16$). or vehicle (●; $n=26$) were administered twice daily i.p. for 7 days starting on day 10. Data represent mean \pm s.e.m..

Treatment	Incidence (%)	^a Onset /d.p.i.	Duration /days	Peak Disease Score	^b Cumulative Disease Score	^c Weight Loss /%
Vehicle	26/26 (100)	11.2 (10-13)	4.8 (4-6)	3.2 (2.5-5.0)	11.0 (8.0-13.75)	21 (15-28)
MPQX (2.5)	10/10 (100)	10.8 (9-14)	5.2 (3-6)	3.0 (0.5-3.75)	11.6 (1.25-19.75)	22 (14-30)
MPQX (5)	10/10 (100)	11.2 (10-13)	4.7 (3-6)	2.3 (0.5-3.75)	8.4 (1.5-16.5)	20 (8-27)
MPQX (10)	10/16 (63)	11.7 (10-14)*	1.7 (0-5)††	1.2 (0-3.0)††	3.2 (0-11.5)††	22 (12-30)

Table 2.10.1.2 Parameters of disease activity during experimental autoimmune encephalomyelitis in Lewis rats. * $p < 0.05$ and †† $p < 0.001$ vs. vehicle by Mann-Whitney U-test or Student's t-test for non-parametric and parametric data, respectively. a; $n=10$ for MPQX (10mg/kg). b; calculated by summation of individual daily disease scores. c; weight on cessation of the experiment as a percentage of the maximum weight before disease onset. Values represent mean and range.

2.10.1.3 GYKI52466 in acute Lewis rat experimental autoimmune encephalomyelitis

Following immunisation with MBP, disease onset occurred in 14/15 vehicle and 15/16 GYKI52466 treated animals (Table 2.10.1.3). Twice daily treatment with GYKI52466 (30 mg/kg i.p.) did not delay onset or effect the duration of disease, but there was a significant reduction in both peak disease score and cumulative disease score (Fig. 2.10.1.3 and Table 2.10.1.3).

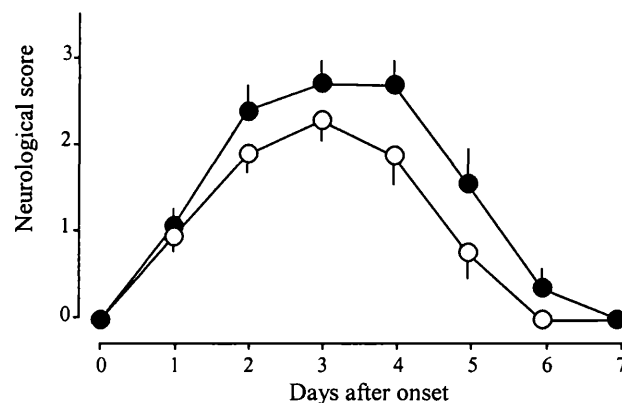


Figure 2.10.1.3 The effect of GYKI52466 on motor disability induced by experimental autoimmune encephalomyelitis in Lewis rats. Vehicle (●; $n=15$) or GYKI52466 (○; $n=16$; 30 mg/kg) were administered twice daily by i.p. administration for 7 days starting on day 10. Data represent mean \pm s.e.m..

Treatment	Incidence (%)	^a Onset /d.p.i.	Duration /days	Peak Disease Score	^b Cumulative Disease Score	^c Weight Loss /%
Vehicle	14/15 (93)	11.4 (10-16)	4.3 (0-6)	2.8 (0-3.5)	10.9 (0-14.75)	20 (7-26)
GYKI52466	15/16 (94)	11.6 (10-13)	4.0 (0-6)	2.4 (0-3.0)†	8.0 (0-13.75)†	20 (8-26)

Table 2.10.1.3 Parameters of disease activity during experimental autoimmune encephalomyelitis in Lewis rats. † $p < 0.01$ vs. vehicle by Mann-Whitney U-test. a; $n=14$ for vehicle and $n=15$ for GYKI52466. b; calculated by summation of individual daily disease scores. c; weight on cessation of the experiment as a percentage of the maximum weight before disease onset. Values represent mean and range.

2.10.1.4 GYKI53773 in acute Lewis rat experimental autoimmune encephalomyelitis

GYKI53773 was highly effective at suppressing disease in experimental autoimmune encephalomyelitis animals. Only 6/10 GYKI53773 treated animals developed disease following immunisation with MBP compared with 8/9 vehicle animals (Table 2.10.1.4) and although twice daily treatment with GYKI53773 (30 mg/kg i.p.) did not delay onset, there was a significant reduction in the duration of disease, peak disease score and cumulative disease score (Fig. 2.10.1.4 and Table 2.10.1.4). The mean peak score in drug treated animals was only 0.9, a score which corresponds to moderate impairment of tail function.

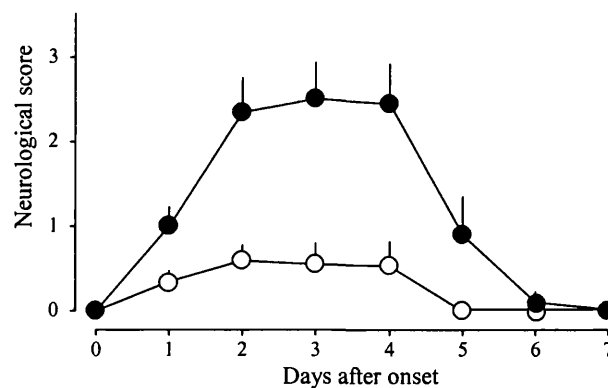


Figure 2.10.1.4 The effect of GYKI53773 on motor disability induced by experimental autoimmune encephalomyelitis in Lewis rats. Vehicle (●; $n=9$) or GYKI53773 (○; $n=10$; 30 mg/kg) were administered twice daily by i.p. administration for 7 days starting on day 10. Data represent mean \pm s.e.m..

Treatment	Incidence (%)	^a Onset /d.p.i.	Duration /days	Peak Disease Score	^b Cumulative Disease Score	^c Weight Loss /%
Vehicle	8/9 (89)	11.9 (10-16)	3.8 (0-5)	2.6 (0-3.5)	9.5 (0-14.75)	19 (7-26)
GYKI53773	6/10 (60)	12.7 (11-14)	1.9 (0-5)*	0.9 (0-2.25)†	2.1 (0-6.0)†	16 (11-20)

Table 2.10.1.4 Parameters of disease activity during experimental autoimmune encephalomyelitis in Lewis rats. * $p < 0.05$ and † $p < 0.01$ vs. vehicle by Mann-Whitney U-test or Student's t-test for non-parametric and parametric data, respectively. a; $n=8$ for vehicle and $n=6$ for GYKI53773. b; calculated by summation of individual daily disease scores. c; weight on cessation of the experiment as a percentage of the maximum weight before disease onset. Values represent mean and range.

2.10.1.5 BIIR561 in acute Lewis rat experimental autoimmune encephalomyelitis

The effects of BIIR 561 were less pronounced than for the other antagonists studied, although the protection did reach statistical significance for duration of disease, peak score, cumulative score and weight loss (Fig. 2.10.1.5 and Table 2.10.1.5).

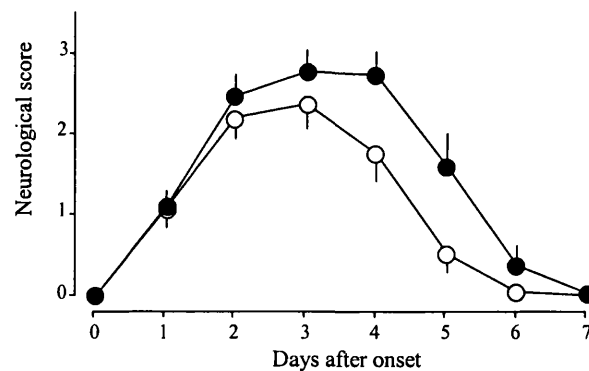


Figure 2.10.1.5 The effect of BIIR561 on motor disability induced by experimental autoimmune encephalomyelitis in Lewis rats. Vehicle (●; $n=15$) or BIIR561 (○; $n=16$; 30 mg/kg) were administered twice daily by i.p. administration for 7 days starting on day 10. Data represent mean \pm s.e.m..

Treatment	Incidence (%)	^a Onset /d.p.i.	Duration /days	Peak Disease Score	^b Cumulative Disease Score	^c Weight Loss /%
Vehicle	14/15 (93)	11.4 (10-16)	4.3 (0-6)	3.5 (0-3.5)	10.9 (0-14.75)	20 (7-26)
BIIR561	16/16 (100)	12.4 (11-19)	3.9 (1-5)††	2.6 (0.5-3.25)*	7.8 (0.5-11.5)†	17 (5-23)*

Table 2.10.1.5 Parameters of disease activity during experimental autoimmune encephalomyelitis in Lewis rats. * $p < 0.05$ † $p < 0.01$ and †† $p < 0.001$ vs. vehicle by Mann-Whitney U-test or Student's t-test for non-parametric and parametric data, respectively. a; $n=15$ for vehicle, $n=16$ for BIIR561. b; calculated by summation of individual daily disease scores. c; weight on cessation of the experiment as a percentage of the maximum weight before disease onset. Values represent mean and range.

2.10.1.6 CP465022 in acute Lewis rat experimental autoimmune encephalomyelitis

Twice daily treatment with CP465022 at 10 mg/kg i.p. resulted in a significant reduction in duration of disease, peak score and cumulative disease score (Fig. 2.10.1.6 and Table 2.10.1.6). This protection was particularly impressive given that the disease was more severe in this experiment than usual and the dose was lower than for the other compounds investigated. Vehicle animals averaged a peak disease score of 3.5 (complete hindlimb paralysis and partial forelimb paralysis). The CP465022 treated animals displayed average symptoms of tail paralysis and an unsteady gait only (score 2.0).

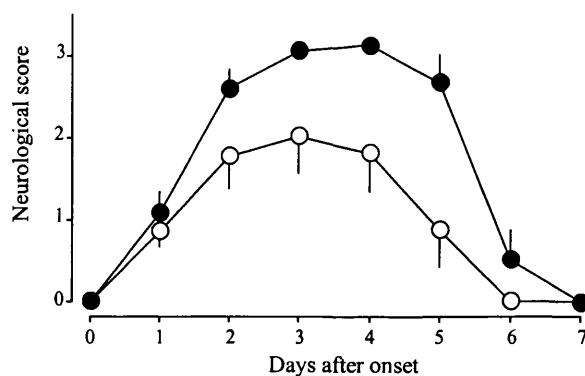


Figure 2.10.1.6 The effect of CP465022 on motor disability induced by experimental autoimmune encephalomyelitis in Lewis rats. Vehicle (●; $n=9$) or CP465022 (○; $n=9$; 10 mg/kg) were administered twice daily by i.p. administration for 7 days starting on day 10. Data represent mean \pm s.e.m..

Treatment	Incidence (%)	^a Onset /d.p.i.	Duration /days	Peak Disease Score	^b Cumulative Disease Score	^c Weight Loss /%
Vehicle	9/9 (100)	10.6 (10-16)	5.1 (4-6)	3.5 (3.0-3.5)	12.8 (11.75-14.75)	23 (18-26)
CP465022	8/9 (89)	13.4 (11-17)†	3.4 (0-5)*	2.0 (0-3.0)†	7.2 (0-13.5)†	20 (10-28)

Table 2.10.1.6 Parameters of disease activity during experimental autoimmune encephalomyelitis in Lewis rats. * $p < 0.05$ and † $p < 0.01$ vs. vehicle by Mann-Whitney U-test or Student's t-test for non-parametric and parametric data, respectively. a; $n=9$ for CP465022. b; calculated by summation of individual daily disease scores. c; weight on cessation of the experiment as a percentage of the maximum weight before disease onset. Values represent mean and range.

2.10.1.7 Aniracetam in acute Lewis rat experimental autoimmune encephalomyelitis

Aniracetam prevents AMPA receptor desensitisation and, therefore, prolongs receptor activation. Thus, this compound was used to investigate the effect of potentiation of AMPA receptor function in the context of experimental autoimmune encephalomyelitis. There were no differences in the peak or cumulative disease scores following aniracetam treatment, relative to vehicle animals, although the severity of disease was near maximal in this study and further exacerbation would probably have resulted in mortality. However, the onset of disease was significantly earlier than in the vehicle group (Table 2.10.1.7) and the duration of disease was extended, but just failed to reach significance ($p=0.053$; Fig. 2.10.1.7).

Treatment	Incidence (%)	^a Onset /d.p.i.	Duration /days	Peak Disease Score	^b Cumulative Disease Score	^c Weight Loss /%
Vehicle	10/10 (100)	11.7 (11-13)	3.9 (3-5)	2.9 (1.0-3.5)	8.5 (3.25-12.25)	17 (13-22)
Aniracetam	9/10 (90)	11.0 (10-12)*	4.7 (0-7)	3.0 (0-3.5)	11.2 (0-16.25)	16 (5-21)

Table 2.10.1.7 Parameters of disease activity during experimental autoimmune encephalomyelitis in Lewis rats. * $p < 0.05$ vs. vehicle by Student's t-test. a; $n=9$ for aniracetam. b; calculated by summation of individual daily disease scores. c; weight on cessation of the experiment as a percentage of the maximum weight before disease onset. Values represent mean and range.

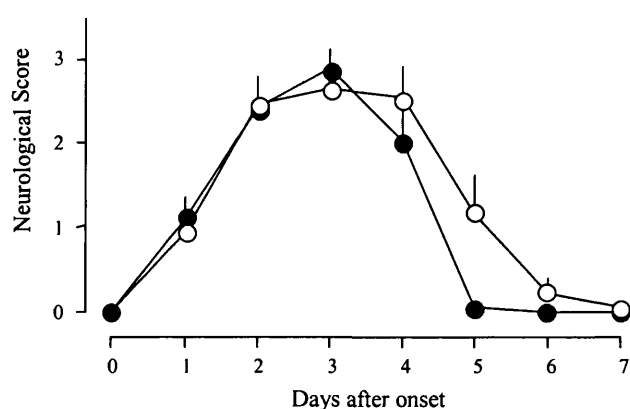


Figure 2.10.1.7 The effect of aniracetam on motor disability induced by experimental autoimmune encephalomyelitis in Lewis rats. Vehicle (●; $n=10$) or aniracetam (○; $n=10$; 30 mg/kg) were administered twice daily by i.p. administration for 7 days starting on day 10. Data represent mean \pm s.e.m..

2.10.1.8 NBQX in Lewis rat adoptive transfer experimental autoimmune encephalomyelitis

The disease profile in the adoptive transfer model is much more synchronous than in the active model of experimental autoimmune encephalomyelitis. Disease onset usually occurs on day 4 post transfer of MBP-sensitised T-cells, with peak disease two days later. The disease is not as severe as the active model, peak disease normally lying between score 2.0 and 3.0. The animals fully recover by day 8. In this particular experiment the disease was very mild. Seven of eight vehicle rats showed symptoms ranging from flaccid tail to hindlimb weakness compared with only one of eight rats, receiving NBQX

30 mg/kg i.p. twice daily, which only showed mild changes in tail tone (Fig. 2.10.1.8). None of the NBQX-treated animals exhibited any motor disability. The disease incidence was significantly lower in the NBQX group compared with vehicle by χ^2 test ($p < 0.05$). Since only one NBQX animal developed disease onset and duration could not be statistically analysed. However, NBQX significantly reduced peak and cumulative disease score compared with vehicle rats (Table 2.10.1.8).

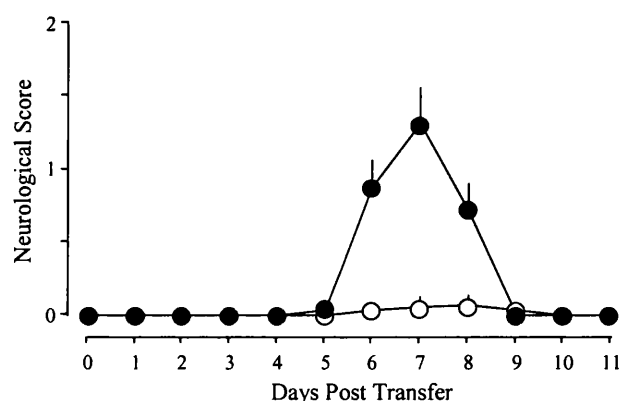


Figure 2.10.1.8 The effect of NBQX on motor disability induced by adoptive transfer experimental autoimmune encephalomyelitis in Lewis rats. Vehicle (●; n=8) or NBQX (○; n=8; 30 mg/kg) were administered twice daily by i.p. administration for 7 days starting on day 4 post transfer. Data represent mean \pm s.e.m..

Treatment	Incidence (%)	^a Onset /d.p.i.	Duration /days	Peak Disease Score	^b Cumulative Disease Score
Vehicle	7/8 (88)	5.9 (0-6)	2.7 (0-4)	1.2 (0-2.0)	2.8 (0-5.0)
NBQX	1/8 (13)*	6.0 (0-6)	0.6 (0-4)	0.1 (0-0.5)††	0.2 (0-1.5)††

Table 2.10.1.8 Parameters of disease activity during adoptive transfer experimental autoimmune encephalomyelitis in Lewis rats. * $p < 0.05$ vs. vehicle by χ^2 -test. †† $p < 0.001$ vs. vehicle by Mann-Whitney U-test. a; n=7 for vehicle and n=1 for NBQX. b; calculated by summation of individual daily disease scores. Values represent mean and range.

2.10.2 AMPA antagonism ameliorates chronic Biozzi mouse experimental autoimmune encephalomyelitis

The Biozzi mouse model of experimental autoimmune encephalomyelitis has a relapsing, remitting secondary phase of disease with extensive demyelination in the latter stages. In these experiments, disease onset occurred at around day 12 post immunisation and the acute phase peaked around 16 d.p.i. in control animals. The primary phase resolved around 20 d.p.i. and the mice then progressed into a secondary phase of relapsing progressive disease. The relapsing progressive stage continued over the next few weeks and the experiments were terminated on day 48 d.p.i..

2.10.2.1 Acute phase treatment with NBQX and long term outcome in chronic mouse experimental autoimmune encephalomyelitis

Treatment with 30 mg/kg NBQX between 10 and 16 days post immunisation protects experimental autoimmune encephalomyelitis animals during the acute phase of disease from days 10 to 25 post immunisation (Fig. 2.10.2.1a and Table 2.10.2.1). There was a significant reduction in cumulative score over this period, but no change in any of the other parameters examined (Table 2.10.2.1). More importantly there was a significant protection which extended over the entire course of the experiment. When examining neurological outcome over the disease course from 10 to 42 days post immunisation there was a significant reduction in disease score in the NBQX group, as determined by repeated measures analysis of variance ($F_{10-48}(1,38)=9.21, p<0.001$).

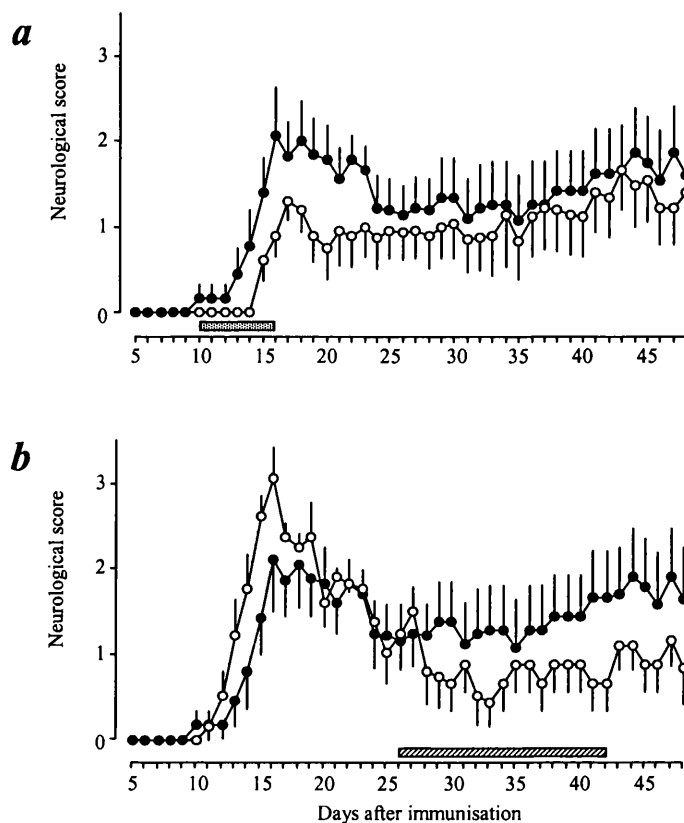


Figure 2.10.2.1 The effect of NBQX on motor disability induced by experimental autoimmune encephalomyelitis in Biozzi mice. In **a**, NBQX (○; n=10) or vehicle (●; n=10) were administered twice daily i.p. for 7 days starting on day 10 post immunisation (hatched bar in **a**). Panel **b** shows the data for NBQX (○; n=10) at 30 mg/kg and vehicle (●; n=10) with once daily administration i.p. from days 26 to 42 post immunisation (hatched bar). Data represent mean \pm s.e.m..

Treatment	Incidence (%)	^a Onset /d.p.i.	Peak Disease Score	^b Cumulative Disease Score	^c Weight Loss /%
Vehicle	9/10 (90)	14.6 (10-17)	2.6 (0-5.0)	18.4 (0-27.30)	26 (14-37)
NBQX	9/10 (90)	15.8 (15-17)	1.8 (0-3.0)	10.4 (0-20.50)*	32 (20-38)

Table 2.10.2.1 Parameters of disease activity during experimental autoimmune encephalomyelitis in Biozzi mice between 10-25 days post immunisation (d.p.i.). Mice were treated twice daily i.p. with 30 mg/kg NBQX or vehicle from 10-16 d.p.i.. * $p < 0.05$ vs. vehicle by Mann-Whitney U-test. a; n=9 for vehicle and NBQX. b; calculated by summation of individual daily disease scores. c; weight on day 25 of the experiment as a percentage of the maximum weight before disease onset. Data analysed are those presented in Fig. 2.10.2.1a. Values represent mean and range.

2.10.2.2 NBQX treatment during the secondary phase of disease in chronic mouse experimental autoimmune encephalomyelitis

When treatment with NBQX at 30 mg/kg was delayed until after the primary phase of disease, the disease curves began to separate (Fig. 2.10.2.1b). In this experiment the treatment period was extended, so NBQX treatment was limited to once per day to avoid the potential renal toxicity described previously. By the end of the experiment, the vehicle animals had a mean disease score of 1.66 which corresponds to complete tail paralysis and impaired righting reflex. This can be compared with a mean score of 0.82 in the NBQX group which relates to only a partial tail paralysis. When analysed by repeated measures analysis of variance there is a significant reduction in disease score in NBQX-treated animals between 26 and 48 days post immunisation ($F_{28-48}(1,20)=2.76$, $p<0.05$). The effect of NBQX on relapse rate during the chronic phase could not be determined as the vehicle group had a more severe progressive disease and entered remission infrequently.

2.10.3 AMPA antagonism and perivascular inflammation in Lewis rat experimental autoimmune encephalomyelitis

Twice daily administration of NBQX, 30 mg/kg significantly reduced the cumulative disease score from 11.06 ± 0.48 with vehicle to 5.9 ± 0.98 in NBQX animals (Table 2.10.1.1). If the effects of the AMPA antagonists were due to an anti-inflammatory action, a reduction in the CNS inflammatory pathology might be expected. However, analysis of perivascular cuffs in brainstems taken from NBQX and vehicle treated animals at the peak of disease showed that NBQX did not cause a significant reduction in CNS inflammation (Table 2.10.3). Inflammation was extensive in both vehicle and drug treated animals.

Treatment	Number	Histopathological Score Mean \pm s.e.m.
Vehicle	n=18	166.9 \pm 23.3
NBQX (30mg/kg)	n=17	118.5 \pm 15.0

Table 2.10.3 Quantification of CNS inflammation in experimental autoimmune encephalomyelitis Lewis rats. Vehicle vs. NBQX not significant by Mann-Whitney U-test. Data represent mean \pm s.e.m..

2.10.4 The effects of AMPA antagonism on *in vitro* T-cell proliferation

In order to determine whether the therapeutic effect of the AMPA antagonists in experimental autoimmune encephalomyelitis could be attributed to peripheral immunosuppression, the effect of the antagonists against mitogen-stimulated, *in vitro* T-cell proliferation was examined. The competitive and non-competitive AMPA antagonists, over a concentration range of 0.1-100 μ M, exhibited differing effects in the *in vitro* stimulation assay. NBQX and MPQX (both competitive antagonists) had no effect on lymphoproliferation (Fig. 2.10.4.1), whilst the non-competitive 2,3-benzodiazepines, GYKI52466 and GYKI53773, inhibited proliferation at 100 μ M (Fig. 2.10.4.1). BIIR561 and CP465022 were even more potent, causing inhibition at 10 μ M (Fig. 2.10.4.2). Dexamethasone was used as a control and inhibited lymphoproliferation in a dose dependent manner with an IC_{50} of 0.5 μ M (Fig. 2.10.4.2). The inhibition by the AMPA antagonists showed a very steep dose response with an “all or nothing effect” over a ten fold change in concentration.

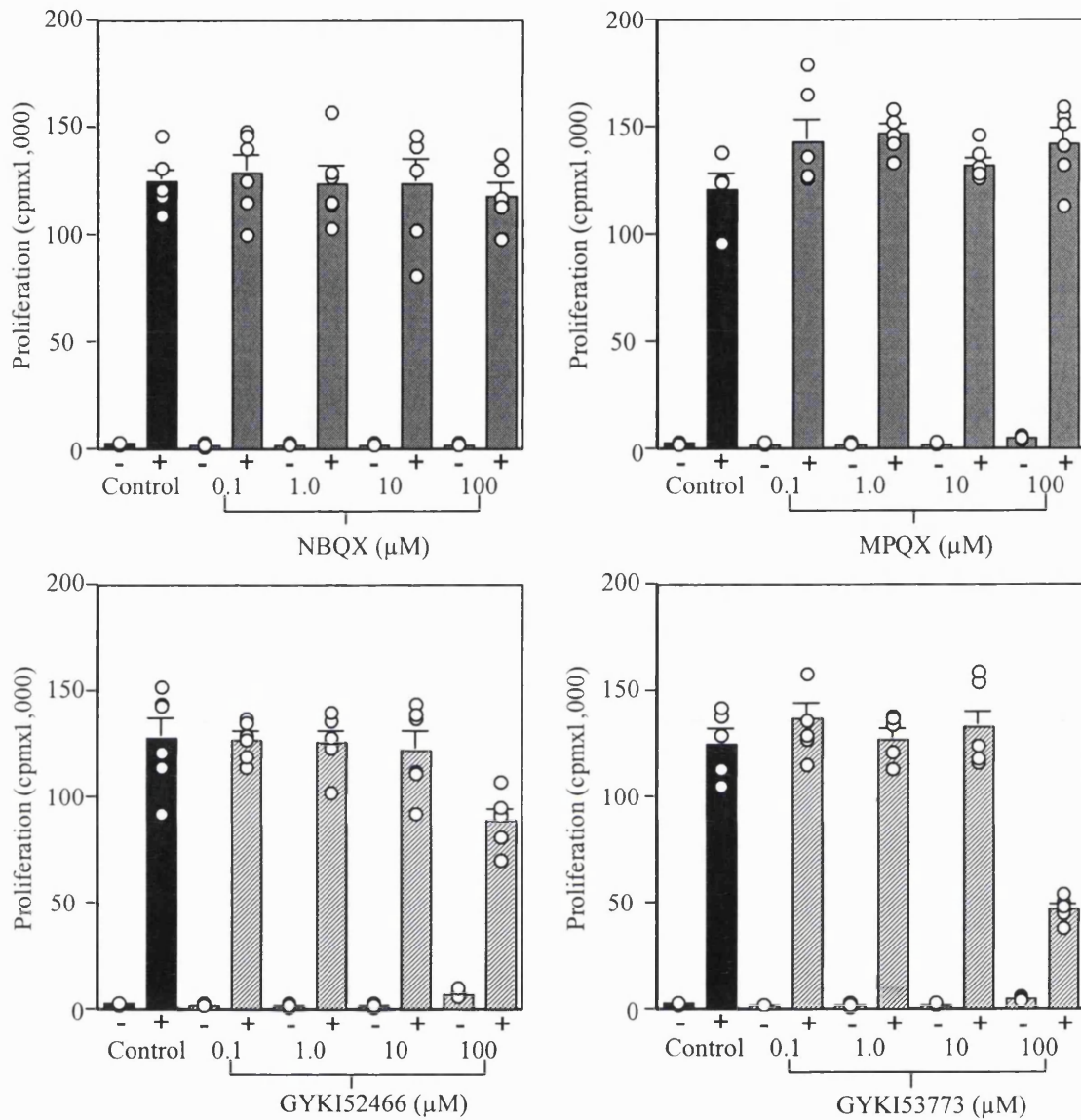


Figure 2.10.4.1 Dose response relationship for AMPA antagonists against mitogen-induced *in vitro* T-cell proliferation. Cultures containing non-competitive AMPA antagonists, NBQX and MPQX (grey bars) and competitive AMPA antagonists, GYKI52466 and GYKI53773 (hatched bars) were compared over a concentration range of 0.1 to 100 μM with untreated control cultures (black bars). + indicates mitogen-stimulated and - indicates unstimulated cultures. x axis indicates the extent of proliferation in counts per minute (cpm). Open circles represent individual values for each well. n=5 wells per sample. Bars represent mean ± s.e.m..

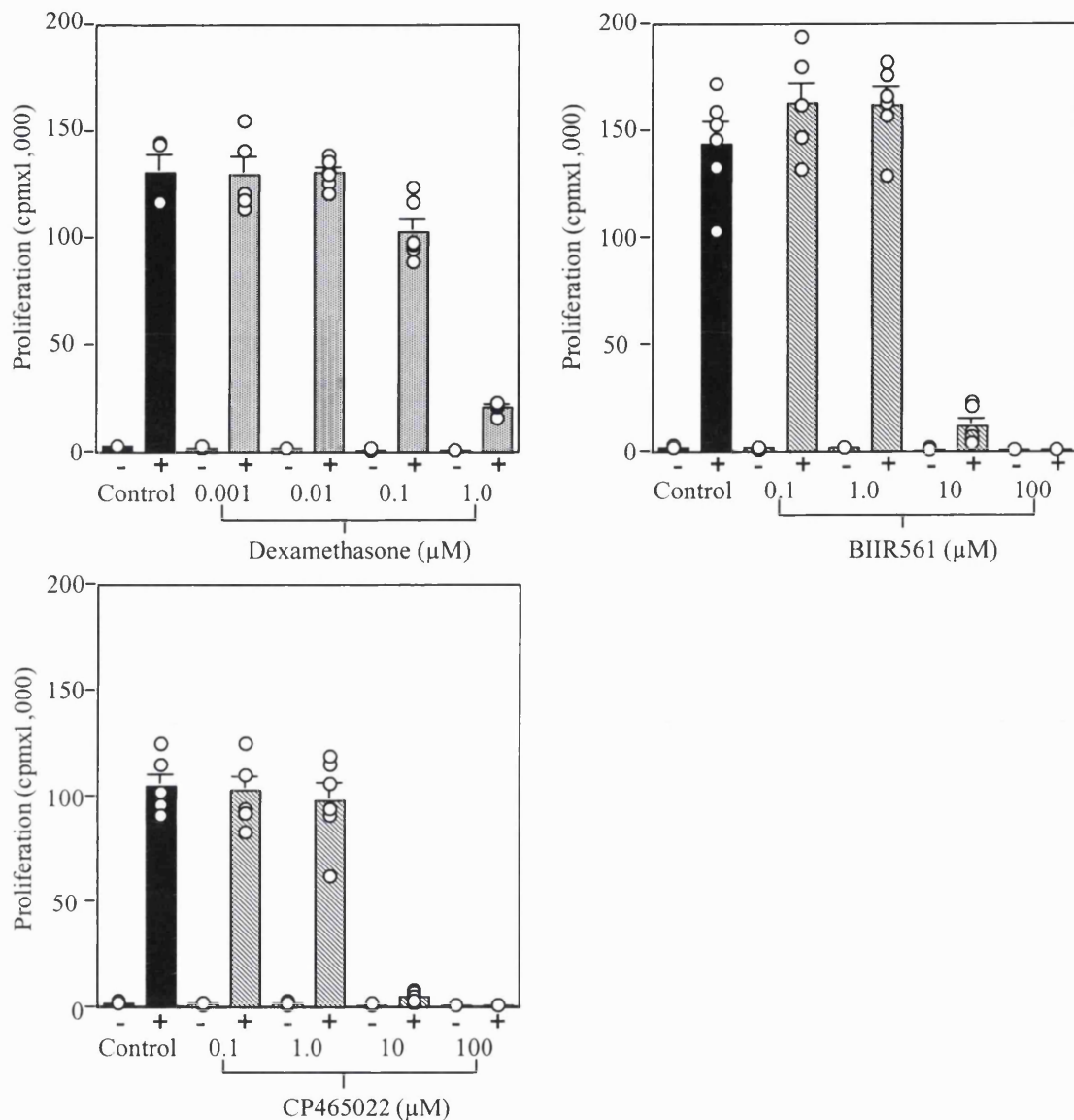


Figure 2.10.4.2 Dose response relationship for AMPA antagonists against mitogen-induced *in vitro* T-cell proliferation. Cultures containing the competitive AMPA antagonists, BIIR561 and CP465022 (hatched bars; 0.1 to 100 μ M) and the corticosteroid dexamethasone (grey bars; 0.001 to 1.0 μ M) were compared with untreated control cultures (black bars). + indicates mitogen-stimulated and - indicates unstimulated cultures. x axis indicates the extent of proliferation in counts per minute (cpm). Open circles represent individual values for each well. n=5 wells per sample. Bars represent mean \pm s.e.m..

2.10.5 Morphological analysis of lumbar spinal cord from Lewis rats with acute experimental autoimmune encephalomyelitis.

Lumbar spinal cord was chosen for histopathological analysis because the α -motor neurons in the ventral horn of this region are responsible for primary motor control of the back legs, and hindlimb paralysis is the predominant clinical feature of experimental autoimmune encephalomyelitis. Analysis of sections from lumbar spinal cord showed extensive perivascular lesions throughout the white and gray matter. Whilst the myelin sheath appeared to be largely unaltered during the disease course, there were signs of ongoing myelin breakdown. A small number of activated macrophages seen in the white matter, were found to contain spirals of myelin debris (Fig. 2.10.5.1), suggesting that, although not extensive, there is an element of demyelination in this model.

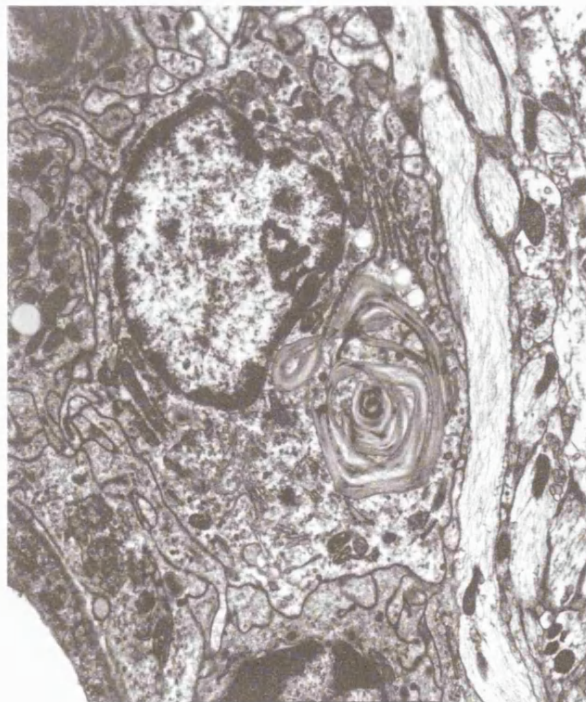


Figure 2.10.5.1 Electron micrograph of myelin debris contained within a macrophage. Section taken from the ventral horn of the lumbar spinal cord in a Lewis rat with experimental autoimmune encephalomyelitis at the peak of disease. Magnification: x8000.

Since AMPA antagonists have been shown to protect against experimental autoimmune encephalomyelitis in the absence of any effect on the inflammatory response, the motor neurons of the ventral horn were studied for any unusual pathology. A number of neurons during the early stages of disease displayed satellitosis of oligodendrocytes, a protective reaction in response to neuronal stress (Fig. 2.10.5.2; Ludwin, 1979; 1984).



Figure 2.10.5.2 Electron micrograph of perineuronal satellitosis of oligodendrocytes in the ventral horn of a Lewis rat spinal cord. Taken from a peak score animal with experimental autoimmune encephalomyelitis. Magnification: x2500.

However, the most striking observation was the apparent involvement of inflammatory cells in motor neuron degeneration in the ventral horns (Fig. 2.10.5.3). By analysing several hundred fields from experimental autoimmune encephalomyelitis animals at different stages of disease, the following composite was prepared to demonstrate the series of events observed at the peak of disease. Lymphocytes initially approached motor

neurons in the ventral horn, attached to their membranes (Fig. 2.10.5.3a) and were subsequently internalised (Fig. 2.10.5.3b). It was not possible to determine whether the lymphocyte entered the neuron, or the neuron engulfed the lymphocyte, although from the insert in 2.10.5.3a processes from the neuron are evident which may ultimately surround the lymphocyte. Indeed, lymphocytes integrated within neurons appeared morphologically normal and were surrounded by a membrane forming vacuolar structure rather than being wholly within the cytosol, suggesting that the neuron had surrounded the lymphocyte (Fig. 2.10.5.3b).

Once internalised, nuclear chromatin in lymphocytes formed clumps attached to the nuclear membrane. This was followed by disintegration of the nuclear membranes, mixing of the lymphocyte nucleoplasm and cytoplasm and the formation of apoptotic bodies. At the later stages of lymphocyte breakdown within intraneuronal vacuoles, cell masses and the apoptotic bodies were transformed into amorphous debris (Fig. 2.10.5.3c). As the process of sequestration of lymphocytes into motor neurons continued, the neuronal cytoplasm became overwhelmed while the nucleus remained intact (Fig. 2.10.5.3c). This process culminated in the decomposition of the motor neuron leaving a large circular vacuole filled with apoptotic lymphocytes and amorphous cellular debris (Fig. 2.10.5.3d). These neuronal vacuoles were clearly visible under normal light microscopy in the ventral horn of semithin sections (Fig. 2.10.5.4). The vacuoles were not preserved with other means of tissue preparation. Analysis of the outer membranes of cells filled with lymphocytes and lymphocyte debris revealed that synaptic densities and presynaptic endings were preserved (Fig.2.10.5.3b,c,d; insets) confirming their neuronal origin.

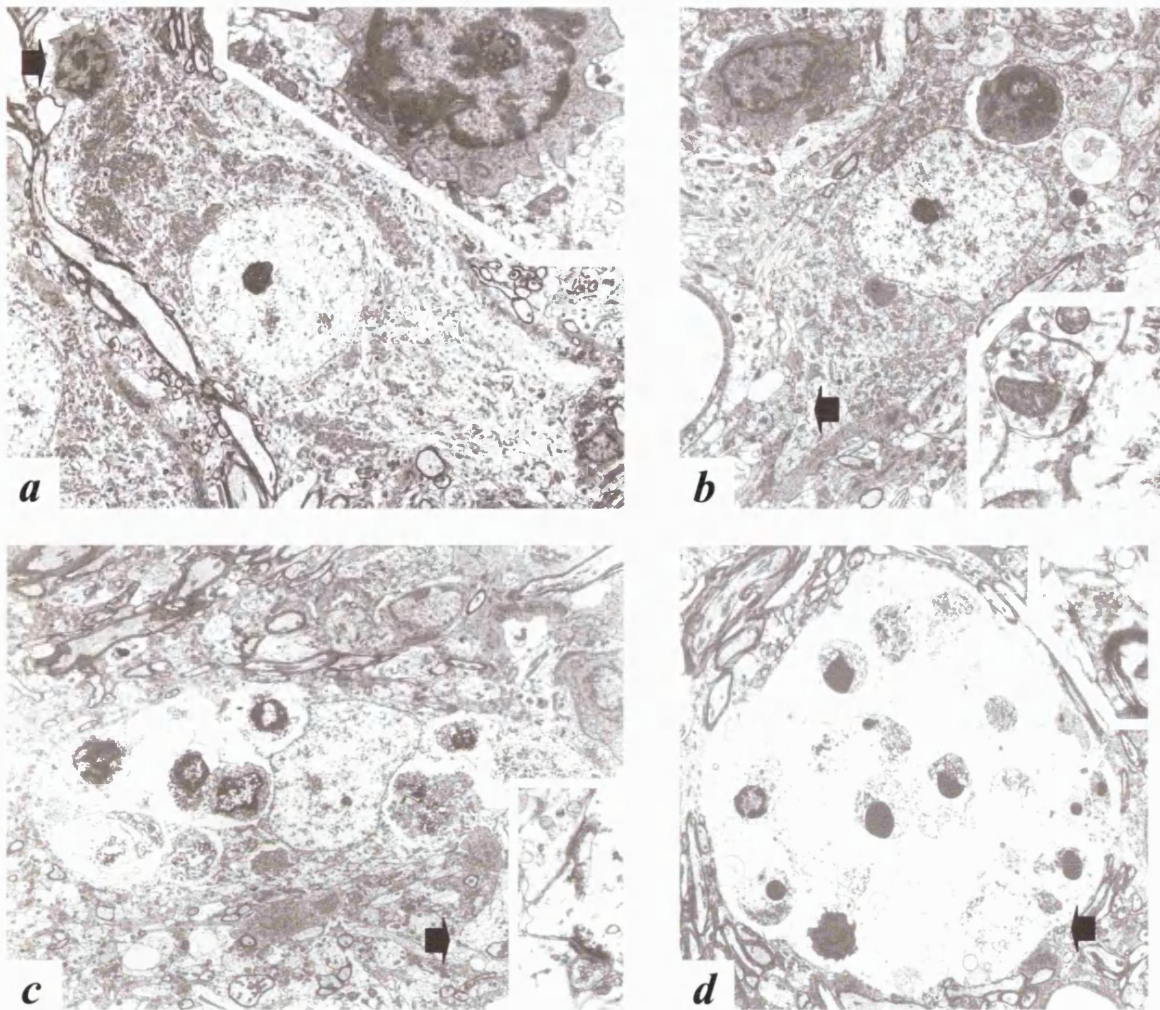


Figure 2.10.5.3 Electron micrographs depicting different stages of degeneration of motor neurons associated with lymphocyte entry (*a-d*). In *a*, the arrow indicates a lymphocyte, shown magnified in the inset, is attached to the membrane of the motor neuron. In *b*, a lymphocyte which has invaded the motor neuron, is entirely engulfed by its cytoplasmic membrane and is beginning to undergo apoptosis. The host motor neuron appears intact. In *c*, several lymphocytes have entered the motor neuron, are filling up its cytoplasm and are captured in different stages of apoptosis. In *d*, a decomposed motor neuron forms a vacuole filled with lymphocytes and amorphous cellular debris. The presence of synaptic densities on the cytoplasmic membranes, indicated with arrows and shown magnified in the insets in *b*, *c*, and *d* identifies the cells as neurons. Photomicrographs were taken from the ventral horn of the lumbar spinal cord of Lewis rats following immunisation with MBP, at the peak of the disease course. Magnifications: *a* x1500; inset *a* x6000; *b* x3000; inset *b* x25000; *c* x2000; inset *c* x30000; *d* x1500; inset *d* x20000.

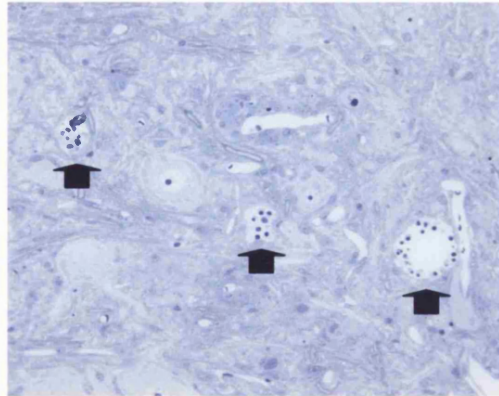


Figure 2.10.5.4 Neuronal vacuoles (arrows) in the lumbar spinal cord ventral horn of a peak score experimental autoimmune encephalomyelitis Lewis rat. The large vacuoles containing lymphocytic debris and apoptotic bodies are clearly visible under light microscopy. Semithin section stained with toluidene blue. Magnification: x40.

The appearance in the spinal cord of neuronal vacuoles containing lymphocytes undergoing apoptosis appeared to correlate with the clinical stage of disease. In animals with early scores of 1, or 2 there were no large vacuoles seen in the ventral horn of the lumbar region. These only appeared at the peak of disease and then only transiently. In animals which had recently recovered, no such vacuoles were seen. At the earlier stages of disease, although large neuronal vacuoles were not seen, a number of examples of apoptotic bodies and cellular debris within axons and/or dendrites distant from the cell body were found (Fig. 2.10.5.5).

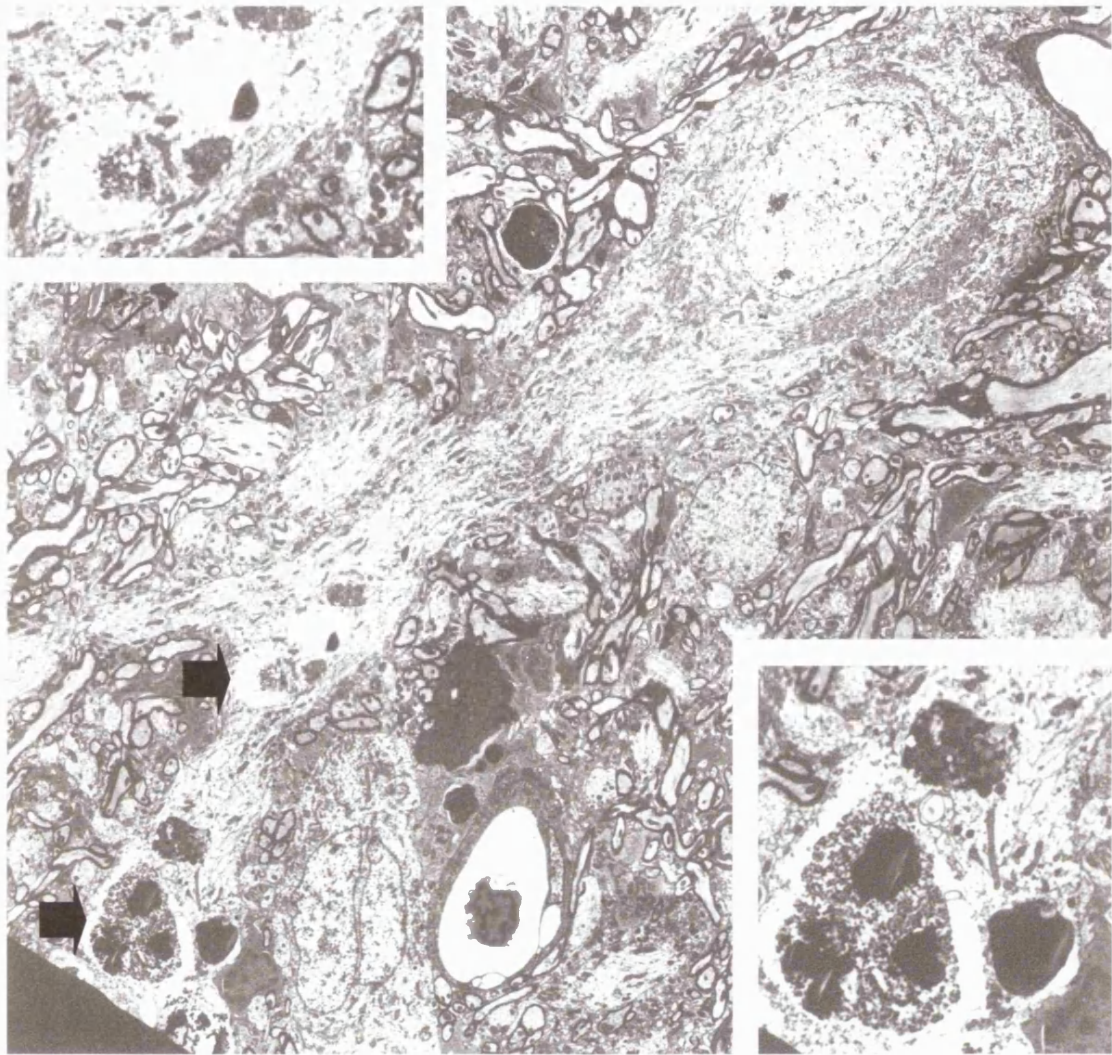


Figure 2.10.5.5 Electron micrograph depicting the invasion and subsequent death of lymphocytes in an axon of a ventral horn motor neuron. The arrows indicate lymphocytic debris within the cytosol of the axon, shown magnified in insets. Magnification: x1500; insets x3000.

Additional evidence of axonal disruption is indicated by the presence of chromatolytic neurons in the ventral horn. The neuronal body of the neuron swells in response to damage or transection of the axon. This appears as an opaque region of the cell body on hematoxylin and eosin or cresyl violet stained sections (Fig. 2.10.5.6).

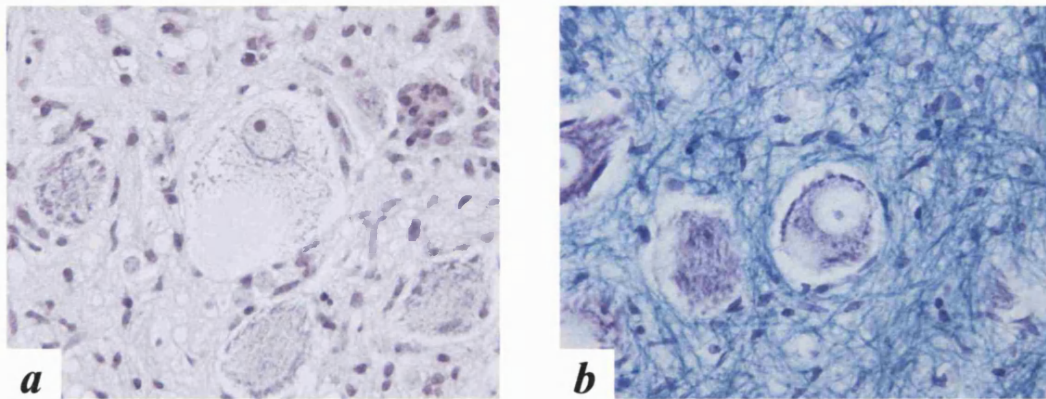


Figure 2.10.5.6 Chromatolysis and neuronal swelling in the ventral horn of the lumbar spinal cord from experimental autoimmune encephalomyelitis Lewis rats. Panel *a* is a hematoxylin and eosin stained section and *b* shows a cresyl violet/luxol fast blue stained neuron from an adjacent section. The chromatolytic neurons appear rounded with an eccentric nuclei, loss of Nissl bodies from the centre of the cell and deposition at the periphery. Other neurons appear swollen with normal Nissl body distribution. Magnification: x40.

In order to make sure that non-neuronal cells were not involved in the interaction with lymphocytes and to determine the identity the cell type entering motor neurons, a series of immunohistochemical studies on lumbar spinal cord tissue were performed. Light microscopical examination of these sections revealed that T-lymphocytes but not macrophages or microglia were invading motor neurons (Fig. 2.10.5.7). These studies also revealed that astrocytes were not involved in the sequestration of lymphocytes. In Fig. 2.10.5.7a, an OX34-positive cell can be seen inside a motor neuron (arrow). OX34 is specific for CD2 on T-lymphocytes. Fig. 2.10.5.7b shows cells stained positive for ED1, which recognises a lysosomal membrane-related antigen on macrophages/microglia, throughout the parenchyma and in perineuronal clusters outside motor neurons, but these cells did not show a propensity to invade them. In 2.10.5.7c, GFAP-positive cells (astrocytes) represent a distinct population from those involved in interactions with lymphocytes and are not seen to invade motor neurons themselves. Similarly, OX33- (specific for CD45RA on B-lymphocytes) or clone 10/78-positive

(specific for CD161 on NK-lymphocytes) cells were found throughout the parenchyma, although to a much lesser extent, and were not involved in the invasion of motor neurons.

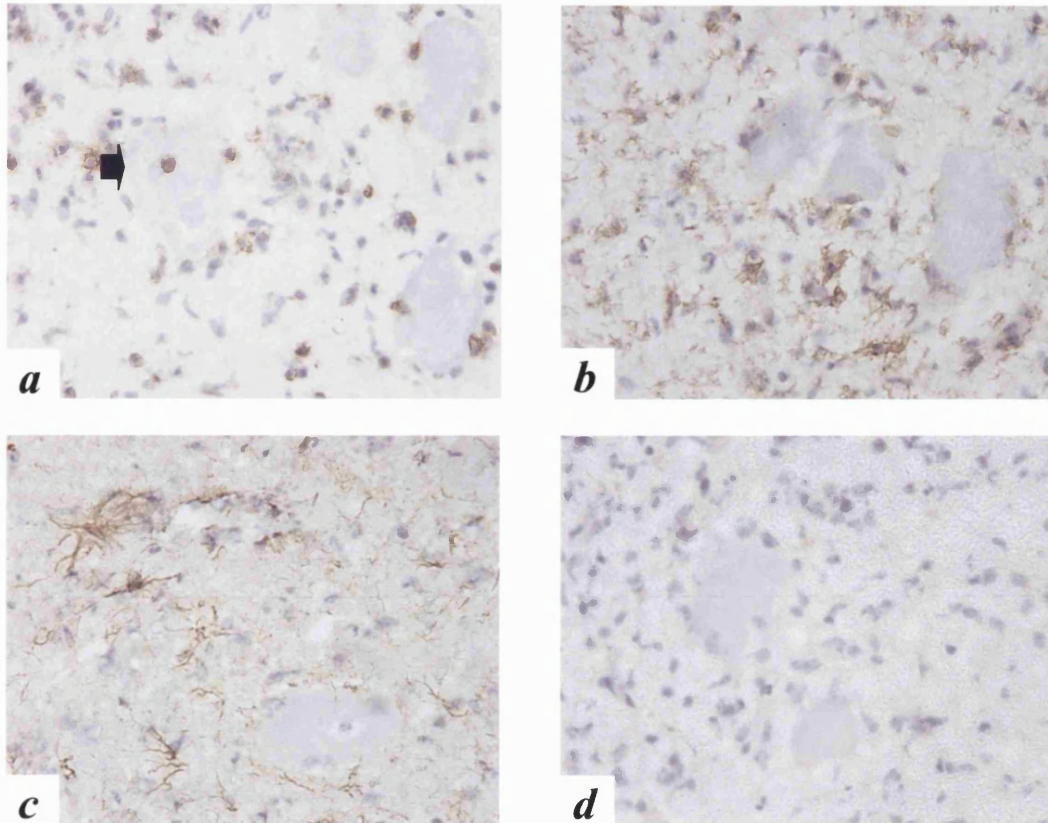


Figure 2.10.5.7 Immunohistochemistry depicting the invasion of ventral horn motor neurons in the lumbar spinal cord by T-lymphocytes, but not macrophage/microglia, or astrocytes. Positive staining appears as a brown diaminobenzidine precipitate. Panel *a* shows an OX34-positive T-cell apparently inside an ventral horn motor neuron (arrow). In *b*, ED1 staining for macrophages/microglia demonstrates their presence in proximity to, but not inside motor neurons. *c* shows the distribution of GFAP, astroglial staining. The stain is distinct from both neuronal bodies and invading inflammatory cells. Panel *d* is a control section with no primary antibody. It shows a low background stain but no specific staining of any of the important cellular elements. Original magnification: x40. All sections are counterstained with hematoxylin.

In addition to the lymphocyte-mediated damage to neurons, evidence of early excitotoxic injury was also found. A number of ventral horn motor neurons were seen with swollen cell bodies, but normal Nissl bodies (Fig. 2.10.5.6 and Fig. 2.10.5.8) and swollen

mitochondria (Fig. 2.10.5.8). Both are indicative of glutamate-mediated excitotoxicity (Olney, 1971; Stewart *et al.*, 1991).

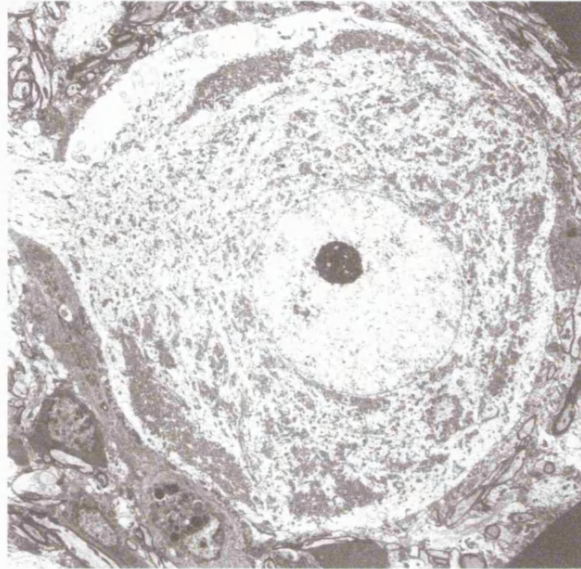


Figure 2.10.5.8 Electron micrograph of a ventral horn motor neuron from the lumbar spinal cord of a Lewis rat with experimental autoimmune encephalomyelitis. The cell body is swollen and rounded with swollen mitochondria, indicative of glutamate-mediated excitotoxicity. Magnification: x1200.

2.10.6 Change in neuronal density in the lumbar spinal cord of Lewis rats with experimental autoimmune encephalomyelitis

The histopathological data show that the neurons in the spinal cord of experimental autoimmune encephalomyelitis animals are under considerable stress as a result of CNS inflammation. It was, therefore, important to determine whether this inflamed environment could lead to neuronal destruction, which could then account for the paralysis. Measurement of neuronal densities throughout the lumbar spinal cord revealed that there was indeed a reduction in neuronal density in the ventral horn of diseased animals (Table 2.10.6). There was a significant reduction in neuronal density of 30 % in experimental autoimmune encephalomyelitis animals compared with sham animals and

NBQX significantly protected against this loss (Table 2.10.6). There were no significant changes in either the dorsal horn, or the intermediate zone.

Treatment	n	Neuronal density					
		Ventral horn, N _v ; mean/mm ³ ± SEM		Intermediate zone, N _v ; mean/mm ³ ± SEM		Dorsal horns, N _v ; mean/mm ³ ± SEM	
			%		%		%
Sham + Vehicle	7	11,746 ± 408	100	38,952 ± 820	100	77,747 ± 1,353	100
EAE + Vehicle	8	8,264 ± 386†	70	36,934 ± 2,056	95	72,098 ± 2,701	93
EAE + NBQX	8	10,250 ± 715*	87	39,040 ± 1,685	100	76,983 ± 2,661	99

Table 2.10.6 Neuronal density in the lumbar spinal cord of rats subjected to experimental autoimmune encephalomyelitis and the effect of NBQX at 30 mg/kg i.p. on cell loss in the ventral horns. To estimate neuronal loss, numerical densities (N_vs) were determined by means of a stereological disector in ventral and dorsal horns, and in the intermediate zone between 13 to 16 days after immunisation. n; number of animals per group. %, represents the change in neuronal density expressed as a percent of sham immunised animals. The difference between sham-immunised and immunised vehicle treated or NBQX treated rats was analysed statistically by means of Student's t-test. *p<0.05 vs. immunised vehicle-treated rats; †p<0.001 vs. sham-immunised vehicle-treated rats.

2.10.7 Demyelination in the lumbar spinal cord of Biozzi mice with experimental autoimmune encephalomyelitis

Demyelination is clearly visible in the spinal cords of Biozzi mice. Figure 2.10.7 shows two toluidine blue sections taken from the primary phase of disease (Fig. 2.10.7a) and from day 28 post immunisation (Fig. 2.10.7b). During the primary phase of paralysis there is clearly little demyelination, but by the end of the study the demyelination is extensive, is associated with a lack of complete recovery between relapses and in some cases, irreversible spasticity.

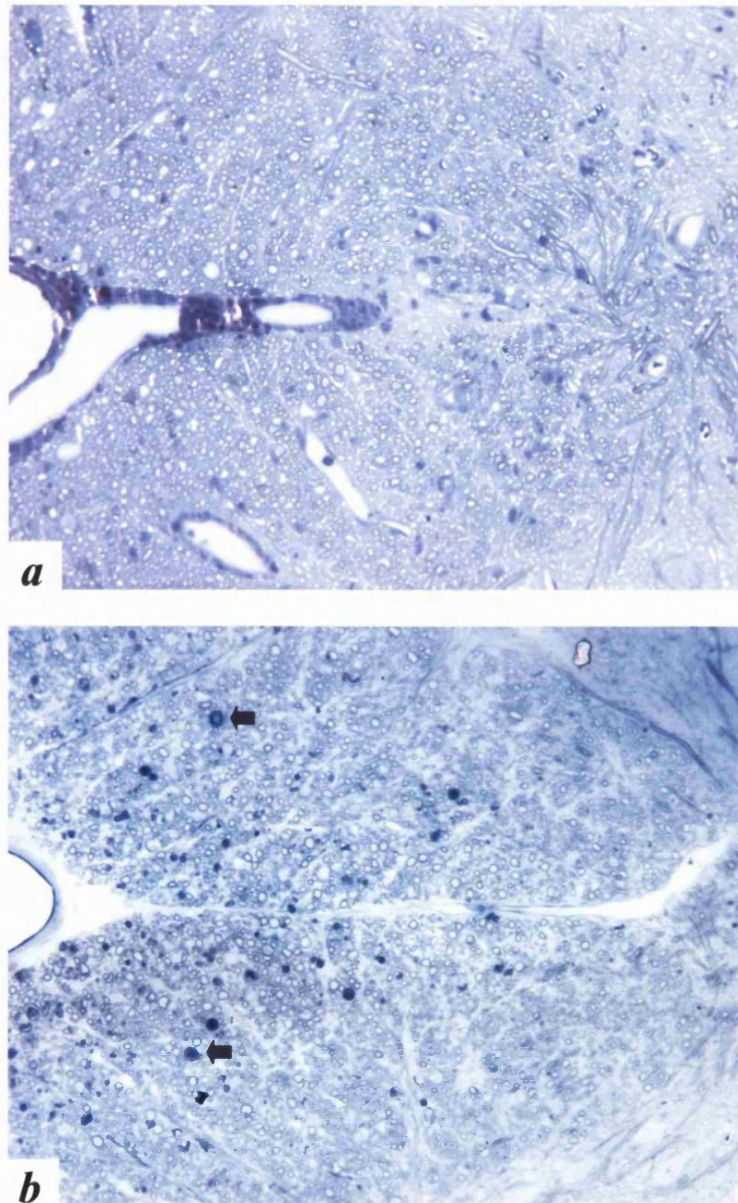


Figure 2.10.7 Tolidine blue sections taken from the lumbar spinal cord, ventral commissure of Biozzi mice with experimental autoimmune encephalomyelitis. Panel *a* shows an animal taken during the primary phase of paralysis. Note the absence of extensive demyelination in the white matter. In *b*, an animal taken at the end of the study shows widespread demyelination in the white matter with deposition of myelin debris (arrows). Magnification: x20.

2.11 Discussion

2.11.1 AMPA receptor antagonist *in vivo* efficacy

The pharmacological studies presented in chapter 2.10 suggest that AMPA glutamate receptors are involved in the development of neurological deficits in experimental autoimmune encephalomyelitis in rodents. The administration of a number of structurally diverse, competitive and non-competitive AMPA receptor antagonists was able to protect Lewis rats against serious paralysis in acute experimental autoimmune encephalomyelitis. In most cases, the neurological deficit was reduced, on average, from complete hindlimb paralysis in vehicle groups to unsteady gait and in the case of two of the compounds, GYKI53773 and MPQX, a loss of tail tone only. Moreover, aniracetam, which potentiates AMPA receptor activation by preventing desensitisation, had a tendency to worsen disease in rats, as might be anticipated if glutamate acting via AMPA receptors was a key pathological mediator in disease development. NBQX was also protective in two other rodent models of experimental autoimmune encephalomyelitis, the adoptive transfer model and a chronic model in Biozzi mice. By using two different dosing criteria, the latter study also indicated that the AMPA antagonist was effective in protecting against both the acute and chronic relapsing phases of the disease. Moreover, acute short term therapy during the initial stage of disease leads to sustained benefit well into the progressive phase.

A comparison of the effective doses of the compounds used in the experimental autoimmune encephalomyelitis experiments revealed a rank order of potency similar to the IC₅₀ values for the antagonists generated in an *in vitro* AMPA receptor assay (Table

2.11.1). MPQX and CP465022 both have IC_{50} values of less than 1 μ M and had a corresponding minimum effective dose of 10 mg/kg i.p. compared with 30 mg/kg for the remaining antagonists. The least potent *in vitro* were also the least efficacious *in vivo* (GYKI52466 and BIIR561). This correlation supports the notion that the *in vivo* efficacy of the various compounds in the EAE models was a direct consequence of AMPA receptor antagonism.

Compounds		IC_{50} at AMPA receptors; μ M	Minimum ED in Lewis rat EAE; mg/kg i.p.
CP465022	Non-competitive	0.1	10
MPQX	Competitive	0.2	10
NBQX	Competitive	1.0	30
GYKI53773	Non-competitive	3.0	30
BIIR561	Non-competitive	6.5	30
GYKI52466	Non-competitive	9.0	30

Table 2.11.1 IC_{50} values at AMPA receptors compared with the corresponding minimum effective dose (ED) in Lewis rat experimental autoimmune encephalomyelitis for the AMPA antagonists used in these studies. IC_{50} values shown are taken from studies comparing the antagonists in the same AMPA-induced Ca^{++} influx assay in cortical neurons (unpublished data).

The beneficial clinical effects of the AMPA antagonists in experimental autoimmune encephalomyelitis might be attributed to their intervention at any number of stages of disease. Immunosuppressive, anti-inflammatory, neuroprotective or oligodendroglial protective agents are all potentially beneficial in experimental autoimmune encephalomyelitis and multiple sclerosis. However, whilst there is a paucity of literature to suggest that AMPA receptor antagonists are able to modify lymphoproliferation or inflammation, studies of AMPA receptor channel composition and expression in the CNS show that ventral horn motor neurons (Petralia *et al.*, 1997) and mature oligodendrocytes (Matute, 1998) both express AMPA channels lacking the GluR2

subunit. This suggests that an imbalance in the glutamatergic system could lead to oligodendrocyte and/or neuronal cell death via AMPA receptor-mediated Ca^{++} toxicity. Indeed, AMPA receptor agonists do cause focal gray and white matter lesions when administered directly into the spinal cord (Kwak and Nakamura, 1995; Magnuson *et al.*, 1999), or optic nerve (Matute, 1998). Given these observations, the efficacy of AMPA antagonists in experimental autoimmune encephalomyelitis could be due to protection of neurons and oligodendrocytes against AMPA receptor-induced toxicity.

The present studies also support this hypothesis by eliminating the possibility of an immunomodulatory mode of action for these antagonists. The treatment regime employed in the active induction experimental autoimmune encephalomyelitis model (i.e. from day 10 post immunisation, just prior to disease onset, to day 16) bypasses the immune expansion phase of the encephalitogenic T-cell population, suggesting the compounds were not acting at this level. Furthermore, the compounds were effective in adoptive transfer experimental autoimmune encephalomyelitis wherein the induction phase is avoided altogether, suggesting that it is the effector stage of disease that is modified by the AMPA antagonists.

Additional evidence is provided by the general lack of protection against weight loss by the AMPA receptor antagonists. The loss of weight prior to onset of neurological symptoms is generally thought to arise as the consequence of cytokine production (Pollak *et al.*, 2000). Since the AMPA receptor antagonists did not effect weight loss, it would suggest that they were not affecting the generation of cachexic agents (eg. $\text{TNF-}\alpha$) in the periphery or their actions in the CNS.

2.11.2 Immunosuppressive and anti-inflammatory profiles of AMPA receptor antagonists

Confirmation that immunosuppression was not responsible for protection was obtained by assessing the effect of the antagonists on T-cell proliferation *in vitro*. The competitive antagonists NBQX and MPQX had no effect on lymphoproliferation up to 100 μM and the non-competitive antagonists only displayed immunosuppressive properties at the higher non-pharmacological concentrations (10-100 μM). Typical plasma concentrations expected after i.p. administration of the compounds used in these studies are in the region of 1-3 μM (unpublished pharmacokinetic observations by Eisai Co. Ltd., Japan) well below the concentration at which antiproliferative effects were observed with BIIR561 and CP465022 (10 μM). In support of the current findings, Pitt *et al.*, 2000 reported no effect of NBQX on MBP-induced T-cell proliferation *in vitro*, suggesting that it is unlikely that the antagonists were suppressing the induction of MBP-sensitised T-cells in the periphery. Furthermore, the abrogation of neurological deficits in experimental autoimmune encephalomyelitis by the NMDA receptor antagonist, memantine, was also independent of lymphoproliferative effects (Wallström *et al.*, 1996) implying that, as a class of neuroprotective agents, glutamate antagonists do not impact on immune function. This can be contrasted with certain Ca^{++} channel antagonists, the efficacy of which in experimental allergic neuritis is related to antiproliferative effects (Mix *et al.*, 1992).

The synthetic glucocorticoid, dexamethasone, exhibited potent inhibitory effects in the *in vitro* proliferation assay, in line with the known immunosuppressive and anti-inflammatory action of this compound. Indeed, the severity of experimental autoimmune encephalomyelitis is decreased by either administration of exogenous glucocorticoids (Mason *et al.*, 1990; Bolton *et al.*, 1997), or exacerbated through the removal of the endogenous rodent glucocorticoid, corticosterone, following adrenalectomy (MacPhee *et*

al., 1989). In each instance, a concomitant decrease (Mason *et al.*, 1990; Bolton *et al.*, 1997) or increase (MacPhee *et al.*, 1989) in CNS inflammation accompanies the change in experimental autoimmune encephalomyelitis disease profile. Given that i.c.v. infusion of the AMPA antagonist, DNQX, elevates plasma corticosterone levels (Tokarev and Jezova 1997) and the short term consequences of compound administration elicit motor disturbances which might activate a stress response, it is conceivable that the ameliorating effects of the compounds in experimental autoimmune encephalomyelitis were related to increases in circulating steroids. Whilst plasma steroid concentration was not determined in the present studies, if the antagonists were to induce a stress-related corticosterone response, then a concomitant reduction in CNS lymphocyte infiltration might be expected. However, the extent of CNS perivascular inflammation, as determined by the histopathological score in brainstem samples taken from vehicle- and NBQX-treated animals at the peak of disease, was unaffected by the AMPA receptor antagonists. These data suggests that even if there was an induction of steroid release following NBQX administration, it was insufficient to prevent lymphocyte passage into the CNS. In addition, where other investigators describe the ameliorating effects of glutamate receptor antagonists, including NBQX, MK-801 and memantine in experimental autoimmune encephalomyelitis, these were largely independent of changes in CNS inflammation (Wallström *et al.*, 1996; Bolton and Paul, 1996). Bolton and Paul (1996) were able to take these observations a step further and demonstrate that the protection against neurological deficit in experimental autoimmune encephalomyelitis with low dose MK-801 was associated with a reduction in BBB permeability independent of any changes in perivascular lesion formation, suggesting that modulation of BBB permeability is not necessarily coupled to a modification in CNS inflammation.

Since AMPA receptor antagonists do not appear to modify the inflammatory response, their efficacy must be the result of protection of CNS components against the consequences of lymphocyte invasion. Immune-mediated demyelination, as a consequence of oligodendrocyte cell death or axon stripping, and damage to neurons or axons can both result in the paralysis which is the primary clinical feature of experimental autoimmune encephalomyelitis.

2.11.3 Oligodendrocyte protection in Lewis rat acute experimental autoimmune encephalomyelitis

Oligodendrocytes are exquisitely sensitive to AMPA receptor-mediated death both *in vitro* (Matute *et al.*, 1997) and *in vivo* (Matute, 1998; Magnuson *et al.*, 1999). However, protection of oligodendrocytes is unlikely to be the primary mechanism of efficacy of AMPA receptor antagonists in the acute rat experimental autoimmune encephalomyelitis models, since demyelination is limited. The majority of myelin sheaths appeared normal by ultrastructural examination, although there was evidence that myelin breakdown was ongoing (Fig. 2.10.5.1) and limited demyelination has been previously described in the dorsal root entry and exit zones (Pender, 1988). Combined with the observed neuronal and axonal pathology, this does raise the question as to whether, at least in this model of MBP-induced experimental autoimmune encephalomyelitis, demyelination is a prerequisite for axonal damage and motor impairment, or if direct inflammatory-mediated damage to axons is more important. In support of the latter, Ahmed *et al.* (2001), using MBP-induced experimental autoimmune encephalomyelitis in rats, recently reported axonal damage which was independent of myelin loss.

2.11.4 Neuronal and axonal pathology in the Lewis rat model of acute experimental autoimmune encephalomyelitis

Immunohistochemical and ultrastructural analysis in rats revealed a major contribution to disease from neuronal and axonal damage. There were several signs of neuronal and axonal stress in the ventral horns of the spinal cord lumbar region. Satellitosis of oligodendrocytes around ventral horn neurons, indicative of neuronal stress (Ludwin, 1979; 1984), was a common observation and a number of neurons were found with a swollen cytoplasm and enlarged mitochondria under electron microscopy. These latter characteristics are classical features of early glutamate-mediated excitotoxicity in neurons (Stewart *et al.*, 1991). In addition, chromatolytic neurons were readily detectable in the ventral horn, indicating that axonal damage was occurring during experimental autoimmune encephalomyelitis. Chromatolysis can be seen when the axoplasm retracts into the neuronal cell body following axonal damage, or transection (Kreutzberg *et al.*, 1997). This suggests that axonal compromise and damage can occur in experimental autoimmune encephalomyelitis in the absence of frank demyelination, a phenomenon reported in early multiple sclerosis lesions (Ferguson *et al.*, 1997). Whilst the present study did not directly quantify measures of axonal damage following AMPA receptor antagonist treatment, NBQX, has been shown to reduce the appearance of SMI32 staining, a measure of axonal damage, in the early stages of experimental autoimmune encephalomyelitis (Pitt *et al.*, 2000). Goldberg *et al.* have also reported similar protection of axons using AMPA antagonists during simulated white matter ischaemia *in vitro* (Tekkok and Goldberg, 2001.).

An intriguing histological observation in the spinal cords of rodents subjected to experimental autoimmune encephalomyelitis animals was that of lymphocyte-mediated

damage to motor neurons. The phenomenon of emperipolesis, where one cell enters another and emerges again with no harm to either the host or invading cell is described (Humble *et al.*, 1956) and indeed T-cell invasion of motor neurons has been described *in vitro* (Hughes *et al.*, 1968), again with no harm to either lymphocyte or neuron. However, in the case of experimental autoimmune encephalomyelitis, T-cells were unable to survive within the environment of the motor neuron, possibly because of survival factor deprivation, since the dying cells displayed the typical morphological features of apoptosis associated with growth factor withdrawal (Wyllie *et al.*, 1981). In these studies, it was not possible to determine if the process of entry involved phagocytosis by the motor neuron, or invasion by the lymphocyte, although neurons did appear to envelope T-lymphocytes in some instances and the lymphocytes contained within neurons were located within vesicles. T-cells were also observed entering axons in close proximity to the cell body. However, phagocytosis is not a process normally associated with neurons. The situation in experimental autoimmune encephalomyelitis appears to share features of both phagocytosis and emperipolesis.

The reason why T-cells and neurons interact in this manner is unclear. Parallels can be drawn between the mechanisms of neuronal and/or axonal damage in experimental autoimmune encephalomyelitis and the tumour-associated paraneoplastic syndromes or Rasmussen's encephalitis, where inflammatory T-cells also form perivascular cuffs and parenchymal infiltrates linked with neuronal damage and axonal loss (He *et al.*, 1998; Scaravilli *et al.*, 1999). Of interest to the present studies in experimental autoimmune encephalomyelitis, is the existence of autoantibodies to the glutamate receptor subunits and other neuronal markers in both paraneoplastic disorders and Rasmussen's encephalitis (Rogers *et al.*, 1994; Gahring *et al.*, 1995). As in experimental autoimmune

encephalomyelitis, the presence of circulating CNS autoantibodies is thought to contribute to the ensuing inflammatory response, particularly in the case of paraneoplastic syndromes (Dalmau *et al.*, 1999). This may imply that in experimental autoimmune encephalomyelitis and multiple sclerosis, in addition to the secondary axonal damage resulting from demyelination, the neuronal damage could be the result of a primary autoimmune response.

Alternatively, the propensity of T-cells to attack neurons could be an experimental anomaly resulting from an impure MBP preparation. If the inoculum were to contain trace levels of neuronal antigen, then an expansion of T-cells against neuronal elements might ensue and an immune response against neurons could be established. This neuronal antigen-specific attack is unlikely to be the case, since the phenomenon of T-cell infiltration of neurons can also be observed *in vitro* with T-cells stimulated by ovalbumin (Hughes *et al.*, 1968).

The most likely reason for this unusual T-cell activity could be altered MHC class I expression on neurons. Most neuronal populations express little, or no MHC class I under homeostatic conditions. Interestingly, one population of neurons which do have an unusually high basal level of MHC class I expression are the brainstem motor neurons (Linda *et al.*, 1999).

Under pathological conditions which impair neuronal excitability, surface expression of MHC class I has been shown to increase (Neumann *et al.*, 1995). Furthermore, exposure of electrically silent neurons to pro-inflammatory cytokines, such as IFN- γ , results in an additional elevation of MHC class I expression (Neumann *et al.*, 1995). Expression is also increased following other forms of neuronal stress, such as seizure activity following

application of the AMPA/kainate receptor agonist, kainic acid (Corriveau *et al.*, 1998). Any rise in MHC class I expression would leave “sick” neurons susceptible to recognition by parenchymal cytotoxic CD8⁺ T-cells. Certainly, in Rasmussen’s encephalitis, CD8⁺ T-cells are implicated in the T-cell-mediated destruction of neurons (Lassmann and Bauer, 2001; Bauer *et al.*, 2001) and in experimental autoimmune encephalomyelitis, adoptive transfer of MOG-specific CD8⁺ T-cells has been shown to produce a more severe and destructive disease, than active-induction with MOG protein alone (Sun *et al.*, 2001). In addition, antigen-specific CD8⁺ T-cells cause neurite transection and spheroid formation following MHC class I induction on neurites in culture (Medana *et al.*, 2001), indicating the neurotoxic potential of antigen-specific CD8⁺ T-cells. One of the best pieces of evidence for a connection between MHC class I expression and T-cell-mediated neuronal compromise, or death in animal models of multiple sclerosis, comes from experiments carried out in MHC class I-deficient and MHC class II-deficient SJL/J mice (Rivera-Quinones *et al.*, 1998). Rivera-Quinones *et al.* demonstrated that in a Theiler’s mouse encephalomyelitis virus model, whilst both groups of mice showed a similar extent of demyelinated lesions, only the class II-deficient mice developed neurophysiological deficits. The MHC class I-deficient mice were not only functionally normal, but appeared to have relative preservation of axons, suggesting the possible importance of MHC class I receptor complex expression in the pathogenesis of neurological deficit. These data combined with the lack of MHC class II expression on neurons would make it unlikely that CD4⁺ T-cells were directly involved in the death of neurons.

The reduction in neuronal density in the lumbar ventral horns of experimental autoimmune encephalomyelitis animals confirmed the neuropathological consequences

of CNS inflammation and the prevention of neuronal loss by NBQX highlighted the importance of AMPA receptor activation in this process. Quantification of the neuronal loss revealed a 30% reduction in neuronal density within the ventral horns of the lumbar spinal cord. Since these are density measurements, they are sensitive to changes in sample volume, for example following oedema. Spinal cord oedema is a known consequence of experimental autoimmune encephalomyelitis (Adams *et al.*, 1989) and glutamate receptors on blood brain barrier endothelial cells can alter permeability (Koenig *et al.*, 1992), therefore, the reversal of the decrease in neuronal density seen with the AMPA antagonist, might simply reflect a drug-related reduction in oedema. However, if oedema was responsible for the reduction in neuronal density, it might be anticipated that changes would occur throughout the intermediate and dorsal regions of the spinal cord and not just the ventral horns. This was clearly not the case.

The loss of spinal motor neurons might be expected to produce a permanent physical deficit. However, it is known from diseases such as ALS that a degree of neuronal redundancy exists within the spinal cord and there can be quite extensive neuronal loss before the onset of clinical symptoms (Bradley, 1998). This idea also extends to diseases such as Parkinson's disease where individuals can survive an 80% loss of dopaminergic neurons in the substantia nigra before motor symptoms become manifest (Lloyd, 1977). In experimental autoimmune encephalomyelitis and multiple sclerosis a similar situation may be envisaged. Thus, during an episode of inflammation a large number of neurons/axons may be compromised, resulting in motor dysfunction. Upon resolution of the inflammation, the majority of neurons/axons recover with a subset, insufficient to result in permanent disability, dying. Repeated inflammatory insults might result in progressive neuronal/axonal compromise and death, until a threshold is reached beyond

which functional recovery from relapse is not 100 %. In multiple sclerosis, this process may contribute to the temporal change of relapsing remitting multiple sclerosis to secondary progressive disease (Trapp *et al.*, 1999).

The data presented here heavily implicate glutamate-mediated neuronal/axonal toxicity in the development of experimental autoimmune encephalomyelitis. Whilst glutamate levels were not determined in the experiments described, several reports from other investigators indicate there may be a potential imbalance in the glutamatergic system in experimental autoimmune encephalomyelitis and possibly multiple sclerosis. $\text{TNF}\alpha$, expression of which increases in the CNS during the course of experimental autoimmune encephalomyelitis (Villaroya *et al.*, 1996.) and in multiple sclerosis lesions (Brosnan *et al.*, 1988.), inhibits glutamate uptake by astrocytes (Fine *et al.*, 1996.). Glutamate transport into astrocytes is further compromised by a decrease in the expression of the glutamate transporters, GLT and GLAST, in spinal cord (Werner *et al.*, 2001.), whilst glutamate metabolism in spinal cord astrocytes is decreased following dramatic reductions in the glutamate-degrading enzymes, GDH and GS (Hardin-Pouzet *et al.*, 1997). Taken together the current findings suggest a toxic increase in glutamate may occur in the extracellular compartment of the spinal cord. Decreased uptake, or increased release, could also account for the decrease in tissue glutamate described during experimental autoimmune encephalomyelitis (Honegger *et al.*, 1989). We are currently carrying out further studies in our laboratories to look at changes in the expression of glutamate transporters and enzymes of synthesis or metabolism of glutamate.

T-cells and macrophages/microglia represent an important potential source of additional glutamate from outside the CNS, in experimental autoimmune encephalomyelitis and multiple sclerosis. T-cells have been discussed earlier in this section in the context of

neuronal damage in experimental autoimmune encephalomyelitis, but glutamate derived from activated microglia and macrophages can also contribute directly (Piani *et al.*, 1991.), or indirectly (Bezzi *et al.*, 2001) to neuronal death. Moreover, microglia themselves express functional AMPA receptors, activation of which can lead to TNF α release (Noda *et al.*, 2000) which itself is potentially harmful (Taupin *et al.*, 1997). However, the absolute levels of glutamate need not be the crucial determinant of glutamate toxicity. Alterations in AMPA channel configuration can change the glutamate sensitivity of neurons bearing AMPA receptor ion channels. An absence of the GluR2 subunit increases the permeability of AMPA receptor to divalent cations increasing the potential for intracellular calcium-mediated toxicity in neurons unable to process excess calcium. Spinal motor neurons are particularly sensitive in this respect (Williams *et al.*, 1997; Ince *et al.*, 1993). Prevention of AMPA receptor desensitisation could also put extra glutamatergic stress on cells, as is suggested by the slight exacerbation of disease with the AMPA receptor potentiating compound aniracetam (Section 2.10.1.7).

More recently, Hermann *et al.* (2001) presented a study on the effect of co-injection of kainic acid and TNF α into the spinal cord following laminectomy. When injected individually at a low dose, both kainic acid and TNF α produced a slight focal increase in c-fos, but no damage to axons or glial cells. However, when combined they produce an expanding spinal cord lesion, similar to that seen in contusion injury, with extensive neuronal and glial damage and induction of c-fos. The damage was prevented by CNQX indicating the involvement of AMPA receptors activation. These data imply that in experimental autoimmune encephalomyelitis, even physiological levels of glutamate could cause spinal cord toxicity in the presence of TNF α released from inflammatory

cells. Furthermore, as stated earlier, AMPA receptors activation has been reported to promote release of TNF α from microglia *in vitro* (Noda *et al.*, 2000) and TNF α is known to exacerbate experimental autoimmune encephalomyelitis (Taupin *et al.*, 1997).

There are at least two mechanisms by which TNF- α can exacerbate glutamate-induced damage in the CNS. Firstly, TNF- α is able to potentiate extracellular glutamate levels directly by inhibiting glutamate uptake into astrocytes (Fine *et al.*, 1996). The second mechanism involves the recently identified phenomenon of calcium-dependent glutamate release from astrocytes. (Parpura *et al.*, 1994; Araque *et al.*, 1999). In an elaborate scheme, proposed by Bezzi *et al.* (2001), the chemokine, stromal-derived factor-1 (SDF-1) activates the G protein-coupled receptor CXCR4 on astrocytes to elevate intracellular calcium, which in turn stimulates extracellular signal-related kinases (ERKs) to activate a metalloproteinase-dependent TNF- α release (TNF- α is also released from microglia by SDF-1 activation of CXCR4 receptors). Extracellular TNF- α then acts on tumour necrosis factor receptor 1 (TNFR1) on the surface of the astrocytes to stimulate prostaglandin E₂ (PGE₂) production via inducible cyclooxygenase 2 (COX-2). Finally, PGE₂ mobilises intracellular calcium possibly through activation of its receptor, EP1/3, causing glutamate release. This direct link between chemokine activity, TNF- α production and glutamate release has great potential relevance in the aetiology of neuronal and oligodendrocyte death in experimental autoimmune encephalomyelitis and multiple sclerosis. Moreover, the pathway is greatly potentiated in the presence of activated microglia (Bezzi *et al.* 2001). Certain aspects of this pathway were independently corroborated by Han *et al.* (2001).

2.11.5 NBQX in Biozzi mouse experimental autoimmune encephalomyelitis

In the mouse models of experimental autoimmune encephalomyelitis both demyelination and axonal damage become more extensive as the disease progresses (Baker *et al.*, 1990). Pitt *et al.* have recently described oligodendrocyte loss in an acute experimental autoimmune encephalomyelitis model in SJL mice, which was prevented by NBQX treatment (Pitt *et al.*, 2000). Although demyelination was not quantified, this mechanism could contribute to the efficacy of the AMPA antagonists during the secondary phase of disease in the Biozzi mouse study described here. Toluidine blue sections taken from Biozzi mice during the acute and chronic phases of disease, 28 and 48 days post immunisation respectively, show that demyelination is initially limited, but becomes extensive by the end of the experiment (Fig. 2.10.7). Indeed, in the terminal stage of disease the animals no longer make a full recovery between relapses and occasionally show hindlimb spasticity indicative of motor neuron dysfunction. Therefore, it is likely that in the acute phase of disease, direct neuronal and axonal impairment are important, but in the later progressive stage, demyelination becomes more prevalent and contributes to the further loss of motor function and lack of recovery.

2.11.6 Conclusions.

Glutamate is a key pathogenic molecule in neurodegenerative diseases, but in multiple sclerosis, traditionally described as an inflammatory disease, the role of this excitatory amino acid has not been fully elucidated. These studies represent the first description of AMPA-mediated glutamate toxicity in the pathogenesis of experimental autoimmune encephalomyelitis and highlight a potentially important involvement of inflammatory neuronal loss in the acute pathology.

These observations open up a new area of therapeutic potential in multiple sclerosis. Neuroprotectants have not previously been investigated within the context of multiple sclerosis. Traditionally regarded as an inflammatory disorder, therapies have always been targeted towards immunosuppression, or anti-inflammation. Recently, in parallel to these studies, data have been presented which point to the potential of other classes of neuroprotectants of possible benefit in multiple sclerosis. Lassmann and colleagues recently showed an increase in N-type calcium channel expression on axons and axonal spheroids of actively demyelinating regions in both multiple sclerosis and experimental autoimmune encephalomyelitis tissue (Kornek *et al.*, 2001). These data suggest that calcium influx through N-type calcium channels may contribute to axonal pathology, therefore, antagonists of these channels could be protective in multiple sclerosis.

The role of the other two main classes of cation channels, Na⁺ and K⁺, has still not been investigated in terms of neuroprotection. Recently, data were presented by Beeton *et al.* suggesting that K⁺ channel antagonists may be of some benefit in multiple sclerosis (Beeton *et al.*, 2001). They showed that the selective Kv1.1/Kv1.3 K⁺ channel inhibitor, kaliotoxin, protected against the appearance of neurological symptoms in experimental

autoimmune encephalomyelitis, when administered from the time of disease onset. The mechanism of protection was attributed to suppression of T-cell activation. Other groups have shown that K^+ channel expression in oligodendrocytes may be crucial for remyelination following episodes of inflammatory damage in multiple sclerosis (Neusch *et al.*, 2001; Shrager and Novakovic, 1995). This also offers a potential therapeutic opportunity for ion channel modulation.

Na^+ channel modulators also represent an unexplored area in the context of neuronal and axonal protection. It is known that Na^+ channel expression is markedly increased on denuded axons in multiple sclerosis and that this is thought to represent an attempt at restoring functional conductivity (reviewed in Waxman and Ritchie, 1993). However, it has also been suggested that the increased Na^+ channel activity can ultimately be detrimental to axonal survival, since Na^+ -mediated depolarisation of axons can lead to potential degeneration by activation of axonal calcium channels. This concept has been investigated in the context of ischaemic white matter injury (Brown *et al.*, 2001).

Finally, the most exciting implication for this research is that, since AMPA receptor antagonists are effective through modifying the CNS consequences of the inflammatory response in experimental autoimmune encephalomyelitis, there is an obvious potential benefit of combined efficacy with the immunosuppressive and anti-inflammatory therapies currently in clinical use. Also, given the neuroprotective and oligodendrocytes-protective nature of this class of compounds, they should also offer some benefit in slowing disease progression resulting from axonal and oligodendrocyte death, an area of multiple sclerosis treatment which currently has few therapeutic options.

CHAPTER 3 - AMPA and Chronic Neurodegeneration

3.1 Glutamate and neurodegeneration

Glutamate has long been implicated in the pathogenesis of acute neurodegenerative diseases such as stroke (Benveniste *et al.*, 1984; Choi and Rothman, 1990), traumatic brain injury (Faden *et al.*, 1989), spinal cord injury (Faden and Simon, 1988) and during seizure activity in epilepsy (Hayashi, 1954; Croucher *et al.*, 1982). All these disorders are associated with excessive release of glutamate and damage to neurons and glia via activation of ionotropic glutamate receptors. More recently, glutamate receptor activation has been implicated in the neurodegeneration seen in many chronic neurological disorders (amyotrophic lateral sclerosis, Plaitakis, 1990; Leigh and Meldrum, 1996; Parkinson's disease, Turski *et al.*, 1991; Huntington's disease, Coyle and Schwarcz, 1976; DiFiglia, 1991; Alzheimer's disease, Maragos *et al.*, 1987; Greenamyre and Young, 1989; Beal, 1995; multiple sclerosis, Bolton and Paul, 1997; Smith *et al.*, 2000; Pitt *et al.*, 2000). In all of these disorders, cell loss is protracted rather than rapid as seen with acute excitotoxicity. This delayed time course of neuronal death in chronic diseases is thought to be related to perturbations in the glutamatergic system which render neurons sensitive to chronic exposure of either physiological levels of glutamate, or slightly elevated extracellular glutamate. Subtle elevations in glutamate concentrations can arise from an imbalance in the generation and/or removal of glutamate. In amyotrophic lateral sclerosis, the expression of the glial excitatory amino acid transporter 2 (EAAT-2) is reduced in the spinal cord and motor cortex (Rothstein *et al.*, 1995; Fray *et al.*, 1998), as is the equivalent transporter, GLT-1, in transgenic mice

bearing the G85R human Cu⁺⁺/Zn⁺⁺ superoxide dismutase (SOD1) mutation (Bruijn *et al.*, 1997).

Opinions in the literature concerning the fate of cells following glutamate exposure are varied. Some studies suggest death is entirely necrotic, others wholly apoptotic, others still, describe it as a combination of the two (Bonfoco *et al.*, 1995; Charriaut-Marlangue *et al.*, 1996; Portera-Cailliau *et al.*, 1997; Pang and Geddes, 1997). It is tempting to suggest that acute glutamate exposure leads to necrosis, whilst a chronic exposure results in apoptosis. The true situation more likely reflects a continuum between necrosis and apoptosis dependent on the severity of the insult and the underlying energy availability (Ankarcrona *et al.*, 1995; Leist *et al.*, 1997), with the common critical molecular event being the influx of Ca⁺⁺ (Choi, 1988), the intracellular concentration of which is an important determinant of cell fate.

The concept of a glutamate exposure threshold is prevalent in hypoxia and ischaemia. Bonfoco and colleagues (Bonfoco *et al.*, 1995; Nicotera *et al.*, 1997) reported in cultured cortical neurons that intense excitotoxic insults produced necrosis, whilst a milder insult resulted in apoptotic changes. The dependence of commitment to necrotic or programmed cell death on the intensity of insult and energy availability, is highlighted in focal ischaemia. Neurons at the core of the ischaemic lesion have a compromised blood supply and die by necrosis, whilst those in the penumbral region, at the edge of the lesion, are exposed to the excitotoxic insult, but benefit from collateral blood flow and undergo programmed cell death (Li *et al.*, 1995). It is inappropriate to describe this type of neuronal cell death as apoptotic, since it does not share all of the critical features that define this specific form of cell death (Kerr *et al.*, 1972; van Lookeren Campagne and

Gill, 1996; Table 3.5). In global ischaemia, delayed neuronal death, as seen in the hippocampus, exhibits many features of programmed cell death, such as DNA fragmentation and a requirement for new protein synthesis (Goto *et al.*, 1990) and is thought to arise from alterations in glutamate receptor expression which leave the neurons more sensitive to glutamate (Pellegrini-Giampietro *et al.*, 1992). This “slow excitotoxicity” which requires changes in gene expression may be particularly relevant to many of the chronic neurological disorders mentioned above.

3.2 AMPA and neurodegeneration

AMPA receptor activation is particularly important when considering excitotoxicity in relation to chronic low level exposure to glutamate. Low glutamate concentrations are unlikely to result in NMDA receptor activation, as membrane depolarisation is a prerequisite for the relief of the resting Mg^{++} block, therefore, AMPA receptors and metabotropic glutamate receptors (Nicoletti *et al.*, 1996) are more likely to account for the toxicity of glutamate in these circumstances. AMPA receptor toxicity, specifically, has been implicated in the pathogenesis of late onset neurodegeneration in stroke (Turski *et al.*, 1998) and traumatic brain injury (Ikonomidou and Turski, 1996), in delayed neuronal cell death in the hippocampus following global ischaemia (Pellegrini-Giampietro *et al.*, 1992), hippocampal injury in epilepsy (Rogawski and Donevan, 1999), Alzheimer’s disease (Beal, 1995) and motor neuron degeneration in amyotrophic lateral sclerosis (Shaw and Ince, 1997). Other diseases which appear to involve AMPA receptor activation, include those where autoantibodies to AMPA receptors have been detected (Rasmussen’s encephalitis, Rogers *et al.*, 1994; olivopontocerebellar degeneration, Gähring *et al.*, 1997; paraneoplastic neurodegenerative syndrome, Gähring

et al., 1995). Amyotrophic lateral sclerosis is probably the disease in which the connection between chronic AMPA receptor activation and neuronal loss has been most clearly established (Shaw and Ince, 1997).

3.3 Mechanism of AMPA receptor pathogenesis

In many neurodegenerative diseases it is the larger neurons, such as motor neurons, pyramidal neurons and Purkinje cells, which seem predisposed to AMPA receptor-mediated excitotoxicity. One reason is that these cells have a higher metabolic rate in order to maintain extensive axonal systems, and are therefore more sensitive to excitatory signals (Shaw, 1998). In addition, some of these neurons are ill equipped to deal with the intracellular Ca^{++} changes arising from the activation of ionotropic glutamate receptors. For example, motor neurons which are sensitive to damage in disorders such as amyotrophic lateral sclerosis, do not express the calcium binding proteins parvalbumin and calbindin D28K (Ince *et al.*, 1993). Research into AMPA receptor regulation has revealed three major potential mechanisms of AMPA receptor-mediated toxicity: an increase in the number and density of cell surface receptors; the extent of editing of the glutamate receptor; and regulation of the level of expression of the GluR2 subunit.

3.3.1 Increase in AMPA receptor density

Motor neurons are known to have a high density of glutamate receptors, both NMDA (Shaw *et al.*, 1991) and AMPA (Williams *et al.*, 1996), which makes them more sensitive than other types of neuron to elevations in extracellular glutamate. Vandenberghe *et al.* (2000) demonstrated that not only did ventral horn motor neurons have an increased

AMPA receptor current density compared with dorsal horn neurons, but pharmacological reduction of the current density in ventral horn motor neurons to the same level as in dorsal horn neurons eliminated the selective motor neuron vulnerability to AMPA, emphasising the importance of AMPA receptor density for neuronal survival.

3.3.2 Q/R editing in the GluR2 subunit

The most critical factor in determining AMPA receptor-mediated excitotoxicity is the regulation of Ca^{++} permeability. As mentioned in 1.1.1.2i, Q/R site editing in the M2 domain of the GluR2 AMPA receptor determines the calcium permeability of AMPA receptors containing this subunit. To investigate the consequences of Q/R editing *in vivo*, Brusa *et al.* (1995) created a transgenic mouse expressing unedited, calcium permeable GluR2 subunits, GluR2(Q). These mice showed a manifold increase in AMPA receptor-mediated calcium permeability and displayed seizures and neurodegeneration which culminated in death at the age of 3 weeks (Brusa *et al.*, 1995). The phenotype was reversed when the under edited transcripts were replaced with the correct transcript (Higuchi *et al.*, 2000). Moreover, subtle changes in the expression of calcium permeability of AMPA channels by altering the extent of Q/R site editing, or the introduction of an asparagine residue at the Q/R site resulted in a non-lethal mutation which produced mild to severe neurological dysfunction (Feldmeyer *et al.*, 1999). The asparagine residue-containing mutant, GluR2(N), expressed GluR2 AMPA channels that have a low level of Ca^{++} permeability. These animals developed normally, but revealed late onset degeneration in selective regions, beginning at around 1 year of age. Ultrastructural investigation at this time showed neuronal loss in areas corresponding with the neurological deficits and changes in intracellular constituents consistent with

excitotoxicity (Kuner *et al.*; manuscript in preparation). The changes in this animal highlight the potential damage of subtle long term defects in GluR2 function.

GluR2 subunits can also be modulated by switching between flip and flop variants (1.1.1.2i) which alters the rate of receptor desensitisation. Following global ischaemia there is a switch from flop to flip variants in the GluR2 receptor, which changes the Ca^{++} permeability of the AMPA channel by potentiating channel opening (Pollard *et al.*, 1993).

3.3.3 Absence of GluR2 expression within the AMPA receptor channel complex

The regulation of Ca^{++} permeability by the expression of GluR2 has been described earlier in this thesis (1.1.1.2ii). GluR2 subunit expression is highly conserved throughout the CNS (Bettler and Mulle, 1995) although certain neurons contain AMPA channels which do not express GluR2 and are permeable to Ca^{++} . Since Ca^{++} permeability is an important determinant of excitotoxicity, these neurons are more vulnerable to excitotoxic insults. Most principal excitatory neurons, such as hippocampal, neocortical pyramidal cells and dentate gyrus cells exhibit low Ca^{++} permeability and a high relative GluR2 expression (Bochet *et al.*, 1994; Jonas *et al.*, 1994; Geiger *et al.*, 1995), but there are a few small populations of neurons in the CNS that appear to lack the GluR2 subunit. These include a sub-populations of neurons in the cerebellum, certain interneurons and spinal motor neurons (Petralia *et al.*, 1997; Williams *et al.*, 1997; Bochet *et al.*, 1994; Jonas *et al.*, 1994; Geiger *et al.*, 1995) and, indeed, some of these neurons have been shown to be susceptible to non-NMDA agonist excitotoxicity (Brorson *et al.*, 1995; Hugon *et al.*, 1989; Ikonomidou *et al.*, 1996).

3.4 The *spa/spa* rat

The nature of excitotoxic death within the adult brain was investigated in the Han/Wistar *spa/spa* rat. This rat has several advantages over the GluR2 transgenic mice as a model of AMPA toxicity. The GluR2(Q) mouse has extensive hippocampal degeneration, but the mutation means that the animals die by three weeks of age (Brusa *et al.*, 1995). The relatively rapid time course of death suggests a sub-chronic neurodegeneration and, as seizure activity is so dominant in the phenotype, acute excitotoxic degeneration could account for a portion of the injury, interspersed with the more prolonged neuronal death. Furthermore, the brain is still relatively immature at 3 weeks, so it is not possible to say with any certainty that any apoptotic cell death seen is of mature, adult neurons. Neuronal cell death during development is well defined as apoptotic (Bittigau *et al.*, 1999) and could, therefore, cloud any interpretation.

The GluR2(N) mouse has more subtle changes in AMPA channel conductivity, which leads to early observable neurological deficit in mutants (Feldmeyer *et al.*, 1999), but degeneration is not discernible until the mice are one year old and then progresses over the next year, until death (Kuner *et al.*, manuscript in preparation). This allows monitoring of long term phenotypic changes, but means that experiments are long and it is difficult to obtain animals in large enough numbers for statistical analysis.

The *spa/spa* strain of Han/Wistar rats, first described by Pittermann *et al.* (1976), is characterised by progressive degeneration of upper and lower motor neurons leading to the development of spasticity (*spa*) and follows an autosomal recessive inheritance pattern of unknown genetic location. *spa/spa* rats are indistinguishable from littermate controls up to 30 days of age. At this time homozygous *spa* rats start to develop motor

anomalies such as head and forelimb tremors followed by an increase in muscle tone. Between P40 and P50, hindlimb dragging becomes evident and is seen in 100 % of animals by P70. This progresses rapidly over the next 10 days and remains severe up to P80. The final phase of the syndrome occurs around P70-P74, when 75 % of *spa/spa* rats lose their righting reflex, develop bulbar palsy and die between P70 and P80. Neurodegeneration has been described in three main cell populations, the cerebellar Purkinje cells, hippocampal CA3 pyramidal cells and spinal motor neurons (Wagemann *et al.*, 1991; Müller *et al.*, 1998) coincident with the onset of neurological dysfunction. At 4 weeks when head tremors first appear, Purkinje cell loss in the cerebellum is already present (Müller *et al.*, 1998). The development of spasticity is associated with changes in neurotransmitter activity in the entopeduncular nucleus (Turski *et al.*, 1990) and motor dysfunction with concomitant spinal cord α -motor neuron degeneration (Müller *et al.*, 1998). Neurodegeneration is always accompanied by extensive gliosis (Wagemann *et al.*, 1995).

3.4.1 Involvement of AMPA in the pathophysiology

The first description of the involvement of the glutamatergic system in the *spa/spa* rat showed that NMDA antagonists could reverse muscle spasticity by their actions in the CNS (Turski *et al.*, 1985). Later, two reports by Cohen *et al.* showed altered glutamate receptor function in the cerebellum and a reduced expression of GluR2 subunits in cerebellar Purkinje cells prior to the onset of disease in the *spa/spa* mutant, suggesting that the neurons which are involved in the pathology are predisposed to glutamate excitotoxicity (Cohen *et al.*, 1991; Margulies *et al.*, 1993). Moreover, in AMPA binding studies in hippocampal CA3 neurons, there was a selective loss of AMPA channel-

containing neurons with age (Müller *et al.*, 1998). Subsequently, a number of pharmacological studies have demonstrated the efficacy of ionotropic glutamate receptor antagonists against neurodegeneration and functional decline in these rats (Müller *et al.*, 1998; Nisim *et al.*, 1999; Brunson *et al.*, 2001), although protection with NMDA receptor antagonists was limited (Brunson *et al.*, 2001).

3.5 Mechanism of cell death

In order to assess the type of neuronal cell death in the *spa/spa* rat CNS, it is first necessary to define the differences between the two major classes of cell death, apoptosis and necrosis. The key elements defining necrotic and apoptotic cell death are highlighted in Table 3.5. Early descriptions by Kerr *et al.* (1972), distinguished the two types of cell death on a morphological basis, with the major changes occurring in the cell architecture and nuclear morphology. Necrotic cells are associated with rapid cellular, mitochondrial and nuclear swelling and ultimately rupture of the cell membrane, whilst apoptotic cells undergo a more protracted condensation, with folding of the cell membrane but maintenance of membrane integrity. The distinctive nuclear changes include early breakdown of the nuclear membrane and non-specific deoxyribonucleic acid (DNA) degeneration in necrotic cells. In apoptotic cells, the deconstruction of the nucleus is more ordered. Nuclear morphology is maintained for much longer before mixing of nucleoplasm and cytoplasm. Prior to the final nuclear breakdown, chromatin condenses and becomes marginated along the inner surface of the nuclear membrane (Kerr *et al.*, 1972).

Criterion	Apoptosis	Necrotic cell death
Morphological		
Cell Volume	Condensation	Swelling
Nucleus	Chromatin condensation Chromatin margination	Rupturing of nuclear membrane
Cytoplasmic organelles	No changes	Mitochondrial swelling Endoplasmic reticulum swelling
Cytoplasmic membrane	Remains intact Membrane blebbing at later stages	Membrane failure
Cell fate	Apoptotic body formation Cleared by phagocytosis No inflammation	Catastrophic membrane failure and cell rupture Extensive inflammatory response
Pattern of death	Individual cells affected	Expanding foci of multiple cells affected
Biochemical		
Metabolic	ATP required	Loss of membrane potential and osmotic damage
Intracellular calcium	Low rise in calcium promotes apoptosis	High calcium promotes necrosis
DNA fragmentation	Inter-nucleosomal cleavage	Non-specific
Phagocytic markers	Surface expression of phagocytic “flags” – phosphatidylserine, lectins, etc	Non-specific
Execution pathways	Two defined cascades involved. Both culminate in caspase-3 activation	Non specific activation of Ca ⁺⁺ -activated proteases
Kinetics	Slow – several hours to days	Rapid – minutes to hours

Table 3.5 Comparison of the main morphological and biochemical criteria identifying apoptotic and necrotic cell death. Adapted from Sperandio *et al.* (2000) and Bredesen (1995).

The second major feature which sets apoptosis and necrosis apart is in the way the dying cell is removed. In apoptosis the process of cell death is highly regulated with one of two currently known cascades initiated to systematically dismantle the cell to form apoptotic bodies (Hengartner, 2000; Kerr *et al.*, 1972). Early in the process a number of ligands are expressed on the cell surface which trigger phagocytosis by neighbouring glial cells

(Henson *et al.*, 2001). The result is the controlled removal of the cell with no inflammatory response. Necrotic cell death is in general an altogether more destructive process. Death is triggered by a loss of membrane potential, as a consequence of depolarisation and energy failure (Majno and Joris, 1995). This results in osmotic swelling and rupture of nuclear, organelle and plasma membranes, and concludes with release of pro-inflammatory stimuli into the extracellular space provoking an inflammatory response to remove the cellular debris (Majno and Joris, 1995).

It is on these current strict morphological and biochemical criteria that apoptotic and necrotic cell death are defined. Yet it is increasingly clear that not all cell death can be categorised into these two classes, particularly programmed cell death of adult neuronal populations. Certain recently described forms of cell death do not satisfy all the criteria of apoptotic cell death (Turmaine *et al.*, 2000; Sperandio *et al.*, 2000). Sperandio *et al.* (2000) call this death “paraptosis”, suggesting it is related to apoptosis, but with a number of important distinctions, such as the lack of chromatin margination, or apoptotic body formation and more importantly the late swelling of mitochondria and lack of internucleosomal DNA cleavage, or caspase-3 activity. In addition, it is important to distinguish apoptosis from autophagic cell death. Schwiechel and Merker (1973) and Clarke (1990) characterised three types of programmed cell death in development. Type I is apoptotic; Type II, autophagy, is characterised by the prominent early formation of autophagic, lysosomal vacuoles. In apoptosis, autophagic vacuoles are not involved in the early stages of degradation, but are involved later during the removal of apoptotic bodies. In type III cell death, the cell is degraded into fragments without the involvement of lysosomes. Autophagy and apoptosis share many common characteristics, including cell condensation. One particularly important feature by which to distinguish between

the two types is the fate of the cytoskeleton. In apoptosis, the cytoskeletal elements are broken down early in the death process, whereas, in autophagic cell death, the intermediate and microfilaments are largely preserved until late in the process (Bursch *et al.*, 2000), possibly because the cytoskeleton is important in the processing of phagocytic vesicles.

3.6 Neuronal death in *spa/spa* rat

Neuronal cell death in *spa/spa* rat develops slowly starting between 4 and 6 weeks and continuing until the animal's death between 8 and 10 weeks. Over this period approximately 50 % of neurons are lost in each of the regions involved (Müller *et al.*, 1998). The protracted cell death of selective neuronal populations over a period of weeks lead one group to propose that the neurons in *spa/spa* animals die by apoptosis (Pikula *et al.*, 1998). This conclusion was based purely on the kinetics of cell death and TdT (terminal deoxynucleotidyl transferase)-mediated dUTP (d-uridine triphosphate) nick end labelling (TUNEL) of cerebellar Purkinje cells. In apoptosis, DNA is cleaved between nucleosomes to form the agarose gel ladders of nucleosomal DNA fragments which have become one of the hallmarks of this mode of cell death (Wyllie, 1980). It is the 3'-OH terminal residues of the fragmented DNA, which appear early in the process, that the TUNEL technique labels. The problem is that whilst DNA strand breaks are present and labelled, positive staining does not mean that the DNA breaks appeared as the result of internucleosomal cleavage, thus, the appearance of an exposed 3'-OH terminus in DNA is not unique to programmed cell death. This means that the TUNEL technique can potentially detect any situation where DNA is nicked to expose a 3'-OH terminal (van

Lookeren-Campagne and Gill, 1996), even certain forms of necrotic cell death, and can not be relied on as a sole indicator of apoptotic cell death.

The current studies were undertaken to define the morphological and biochemical changes which accompany neuronal death in the *spa/spa* rat. To specifically address the role of apoptosis in this process, electron microscopy was utilised, whilst biochemical markers of the apoptotic process were also assessed to determine whether the cell death involved met the current criteria for apoptosis.

3.7 Materials and methods

3.7.1 Animals

Male and female Han-Wistar *spa/spa* rats aged 4, or 8 weeks were obtained from Harlan, Holland. All animals were housed under environmentally controlled conditions (12 hour light dark cycle) and permitted free access to food and water. In 8 week old animals when spastic symptoms began to appear and animals were unable to feed from overhead hoppers, food and water were provided in the cage. *spa/spa* animals were identifiable from around 3 weeks of age when head and forelimb tremors began to appear. At this stage the animals were separated into *spa/spa* and heterozygous- plus homozygous-recessive littermate controls (phenotypically-normal littermates).

3.7.2 Light microscopy

Rats were anaesthetised with an overdose of sodium pentobarbitone (100 mg/kg i.p. Sagatal™; Rhône Mérieux Ltd., Essex, UK) and perfused through the left ventricle with a fixative containing 4 % paraformaldehyde (Sigma, Dorset, UK) and 0.5 % glutaraldehyde (Sigma, Dorset, UK) in phosphate buffered saline (Sigma, Dorset, UK). Blocks of brain and spinal cord were then embedded in paraffin wax and coronal sections throughout the brain and lumbar spinal cord were cut at 10 µm thick on a sledge microtome and mounted on gelatin-coated glass slides. The sections, once dried, were then de-paraffinised in xylene and rehydrated through graded ethanols. Two different empirical stains were used to investigate the neuronal pathology. For hematoxylin and eosin staining sections were first stained in Harris's hematoxylin (Sigma, Dorset, UK) for

2 min, then rinsed in tap water, differentiated in 70 % ethanol containing 1 % HCl, washed in tap water again for 5 min and counterstained with eosin (Sigma, Dorset, UK) for up to 1 min. The sections were then dehydrated through graded ethanols, cleared in Histo-Clear™ (Agar Scientific, Essex, UK) and mounted in DPX mounting medium (Fisons Scientific Equipment, Loughborough, UK). Silver staining was carried out at the University College Hospital Histology Department according to the Glees and Marsland modification of the Bielchowsky method (Glees and Marsland, 1954).

3.7.3 Electron microscopy

Rats were culled and perfused as above (3.7.2). For electron microscopy the tissue was sectioned through the lumbar spinal cord into 200 µm blocks using an Oxford vibratome (Agar Scientific, Essex, UK) and collected in 0.1 M sodium phosphate buffer (pH 7.4). Sections were then osmicated for 40 min in 1 % osmium tetroxide (Agar Scientific, Essex, UK) in 0.1 M phosphate buffer, washed in the phosphate buffer for 5 min, before changing to two washes of 10 min each in 0.1 M sodium acetate followed by staining for 15 min in 2 % uranyl acetate in sodium acetate (Agar Scientific, Essex, UK) at 4°C. The sections were then washed again in sodium acetate and switched to distilled water. Next, the sections were dehydrated in graded ethanol, cleared in four changes of propylene oxide at 10 min each and changed for 50 % propylene oxide/50 % araldite resin for 45 min. The araldite resin is composed of 10 g dodecenyl succinic anhydride (DDSA), 10 g Araldite (CY212) and 0.8 g plasticizer (dibutyl pathalate) which are heated and mixed. When mixed, 0.4 ml benzyldimethylamine (BDMA) is stirred into the resin (all resin reagents are available from Agar Scientific, Essex, UK). The blocks were then soaked in fresh araldite for 24 hours on a rotator and finally embedded in araldite resin between

Melinex™ (Dupont Teijin Films, Cleveland, UK) sheets and baked at 60 °C overnight. Semithin (1 µm) coronal sections were cut with adjacent thin (80 nm) sections using a glass knife on a Reichert Ultracut ultramicrotome (Leica UK Ltd., Bucks, UK). Semithin sections were stained with toluidine blue (Agar Scientific, Essex, UK) for 40 sec and rinsed with distilled water for light microscopy, whilst thin sections were mounted on 200 µm electron microscope copper grids (Agar Scientific, Essex, UK), counterstained with lead citrate (Agar Scientific, Essex, UK) and examined in a JEOL 1010 transmission electron microscope.

3.7.4 Sample preparation for caspase activity assay and nucleosome ELISA

Rats were anaesthetised with an overdose of sodium pentobarbitone (100 mg/kg i.p. Sagatal™; Rhône Mérieux Ltd., Essex, UK) and the brains removed. The brains were then placed on a petri dish containing a block of ice to keep them cool and dissected into cingulate, retrosplenial, frontal, parietal and occipital cortex, hippocampus, striatum, thalamus, substantia nigra, hypothalamic nucleus, tectum, cerebellum, pons and olfactory bulbs. The spinal cord was also removed for analysis. All samples were placed in 1.5 ml Eppendorf™ microfuge tubes and frozen in liquid nitrogen. For the homogenisation protocol, all steps were carried out on ice. The samples were thawed and 100 µl of homogenisation buffer (incubation buffer from Boehringer Mannheim's Cell Death Detection ELISA, Boehringer Mannheim UK Ltd., East Sussex, UK) was added to the microfuge tubes and the samples gently homogenised using a Treff pellet mixer (Scotlab, Lanarkshire, UK) until all large pieces of tissue had disappeared (approximately 1 min). The suspension was made up to 20 volumes with homogenisation buffer and mixed, then incubated at room temperature for 30 min and centrifuged (5 min, 4 °C, 13,500 g;

Haraeus Biofuge Fresco, Jencons Scientific Ltd., Bedfordshire, UK). The supernatant was then collected and stored at $-80\text{ }^{\circ}\text{C}$ until assayed.

3.7.5 Nucleosome enzyme-linked immunosorbent assay (ELISA)

A cell death detection ELISA (Roche Diagnostics Ltd, East Sussex, UK) was used to measure internucleosomal cleavage of DNA in rat brain extracts. The procedure was carried out according to the manufacturers specification. Briefly, 96 well plates were coated with an anti-histone antibody. The plates were then exposed to the rat brain supernatant as prepared in 3.7.4, followed by the secondary antibody, a peroxidase-conjugated anti-DNA antibody which recognises single and double stranded DNA. The ELISA was developed in the presence of hydrogen peroxide with the chromagen ABTS (2,2'-azino-di-[3-ethylbenzthiazoline sulfonate(6)]) as the substrate. Absorbance was measured at 405 nm using a Dynatech MR7000 spectrophotometer (Dynatech Laboratories, Sussex, UK)

3.7.6 Caspase-3 activity assay

Caspase-3 activity was determined according to a fluorescence assay developed in our laboratories (Bittgau *et al.*, 1999). 20 μl of the supernatant, as prepared in 3.7.4, was diluted with 160 μl reaction buffer (50 mM HEPES (N-[2-hydroxyethyl]piperazine-N'-[2-ethanesulfonic acid]), pH 7.5, 1 % sucrose, 0.1 % CHAPS (3-[(3-cholamidopropyl)-dimethylamminio]-1-propanesulfonate) and 5 mM dithiothreitol (all from Sigma, Dorset, UK)), and incubated at $37\text{ }^{\circ}\text{C}$ for 2 hours with 10 μl of the fluorogenic tetrapeptide substrate DEVD-AMC (Asp-Glu-Val-Asp-aminomethylcoumarin; Bachem UK Ltd.,

Essex, UK; 1 mM). Free AMC accumulation, which resulted from cleavage of the aspartate-AMC bond, was measured using a Perkin Elmer luminescence spectrophotometer at 380 nm extinction and 460 nm emission wave lengths. Specific activity was defined as the difference between total activity in the presence and absence of 10 μ l of the caspase-3 inhibitor Ac-DEVD-CHO (acetyl-Asp-Glu-Val-Asp-aldehyde; 20 μ M).

3.7.7 TdT-mediated dUTP nick end labelling (TUNEL)

TUNEL staining was carried out in wax-embedded sections prepared as in 3.7.2 using an *in situ* cell death detection kit (Roche Diagnostics Ltd, East Sussex, UK). The procedures were carried out according to the manufacturers specifications. Sections were de-paraffinised and rehydrated as in 3.7.2 and treated with 20 μ g/ml proteinase K (Sigma, Dorset, UK) in phosphate-buffered saline (PBS; pH 7.4; Sigma, Dorset, UK). The sections were quenched and permeabilised before adding the TUNEL reaction mixture containing fluorescein-conjugated dUTP and the terminal deoxynucleotidyl transferase enzyme. The reaction was visualised using a peroxidase-conjugated anti-fluorescein antibody and peroxidase activity was detected in 3,3'-diaminobenzidine (Sigma, Dorset, UK) solution in phosphate buffered saline containing 0.01 % hydrogen peroxide (Sigma, Dorset, UK). Rinsed sections were counterstained in Harris's hematoxylin (Sigma, Dorset, UK) for 30-60 sec, washed in running water, dehydrated in graded alcohols, cleared in Histo-Clear™ (Agar Scientific, Essex, UK) and mounted on glass slides under DPX mounting medium (Fisons Scientific Equipment, Loughborough, UK). Some sections were pre-treated with 1 mg/ml DNAaseI (Sigma, Dorset, UK) after the permeabilisation step in order to provide a positive control for DNA cleavage. In

addition, negative controls were included in each run with PBS in place of the TUNEL reaction mixture.

3.7.8 Statistics

Data from the DNA nucleosome ELISA and the Caspase-3 activity assay did not exhibit a Gaussian distribution and were, therefore, analysed by Mann-Whitney U-test. All statistics were performed using Statview statistical software (Abacus concepts Inc., Berkeley, California).

3.8 Results

3.8.1 Verification of the cell death detection ELISA and caspase-3 activity assay sensitivity

The nucleosome ELISA was originally developed for the detection of DNA cleavage *in vitro* and although the assay has been used successfully for the detection of nucleosome production *in vivo* in rat pups (Bittigau *et al.*, 1999), it has not been used with adult CNS tissue. Therefore, the olfactory bulb was included in the current studies to provide a positive control from a CNS region with known apoptotic neuronal cell death, the result of turnover of olfactory neurons derived from neuroepithelial cells (Deckner *et al.*, 1997; Hayward and Morgan, 1995). Caspase-3 activity was also measured in the olfactory bulb to assess the relationship between programmed cell death as indicated by specific DNA cleavage and executor caspase activity.

There were strong signals for both DNA breakdown and caspase-3 activity in the olfactory bulb compared with those signals obtained from the other brain regions (Fig. 3.8.1). This confirmed that the nucleosome assay was, indeed, able to detect DNA breakdown products *ex vivo* and that caspase-3 activity was also associated with degeneration. Additionally, DNA cleavage and caspase-3 activity in the olfactory bulb were significantly higher in the *spa/spa* rat compared with control littermates. Whilst this was unexpected, it may explain part of the behavioural phenotype of the mutant. Under observation, *spa/spa* rats appear to spend more time “sniffing” around their environment than their phenotypically-normal littermates, possibly due to a loss in sensitivity of the olfactory system as a result of increased cell death.

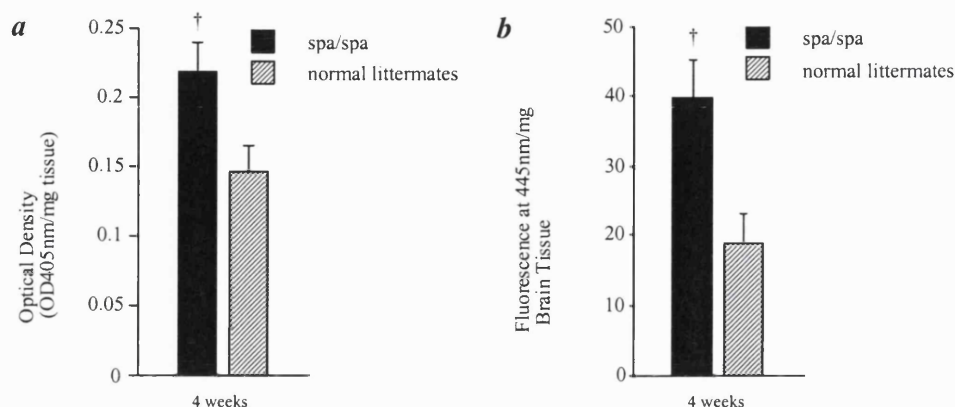


Figure 3.8.1 Change in DNA degradation and caspase-3 activity in the olfactory bulbs of *spa/spa* rats and age-matched littermates at 4 weeks. Panel *a*. shows DNA cleavage in *spa/spa* rats (solid bars) versus phenotypically normal littermates (hatched bars) as measured by production of DNA-histone complexes arising from internucleosomal DNA cleavage. Panel *b*. shows caspase-3 activity in the same samples described in *a*. † $p < 0.01$ vs. vehicle by Mann-Whitney U-test. Bars depict mean \pm s.e.m.. $n = 11$ per group.

3.8.2 Regional distribution of DNA damage in *spa/spa* rats at 4 weeks

The ELISA for nucleosome/DNA complex detection was used in order to quantify the extent of specific DNA cleavage in a number of regions of brain and spinal cord from *spa/spa* rats and littermate controls (Fig. 3.8.2.1 and Fig. 3.8.2.2). From this analysis, four regions shared a significant change in nucleosome cleavage. Of the sub-cortical regions, the striatum was the only region to show a significant increase in nucleosome cleavage (Fig. 3.8.2.1a). In the cortex, there was a general trend suggesting that nucleosome cleavage was elevated in the rostral cortex relative to frontal areas (Fig. 3.8.2.1b). Although the occipital cortex was the only area to reach statistical significance, the retrosplenial and parietal cortices also demonstrated a trend towards significance (Fig. 3.8.2.1b). In the hindbrain and spinal cord, the cerebellum showed a trend towards significance in the *spa/spa* rats (Fig. 3.8.2.2), a region of known cell loss

(Wagemann *et al.*, 1991). Both the pons and the spinal cord had significantly higher signals in the *spa/spa* group (Fig. 3.8.2.2).

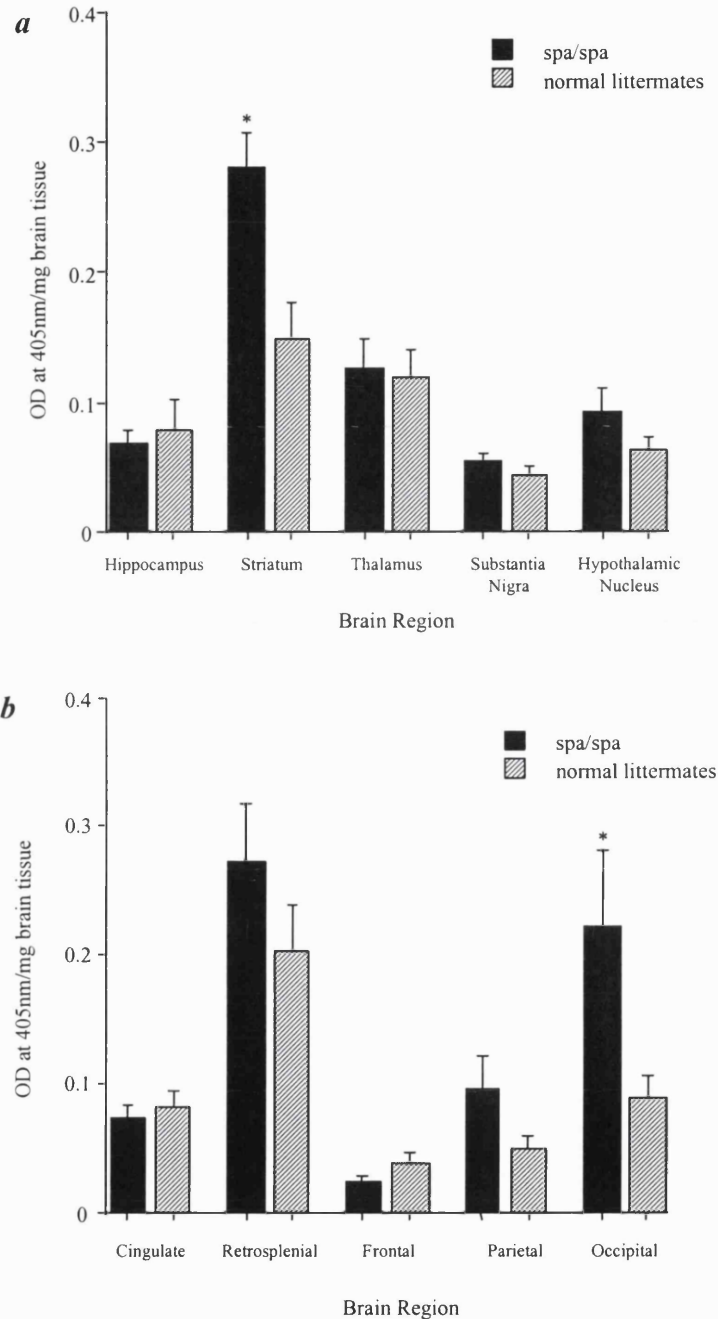


Figure 3.8.2.1 Increased DNA degradation in discrete brain regions of *spa/spa* rats at 4 weeks of age. Panel *a*. shows the sub-cortical distribution of DNA cleavage in *spa/spa* rats (solid bars) versus phenotypically normal littermates (hatched bars) as measured by production of DNA-histone complexes arising from internucleosomal DNA cleavage. Panel *b*. shows the distribution of DNA cleavage for cortical regions. * $p < 0.05$ vs. vehicle by Mann-Whitney U-test. Bars depict mean \pm s.e.m., $n = 5$ animals per group except for cingulate cortex ($n = 4$).

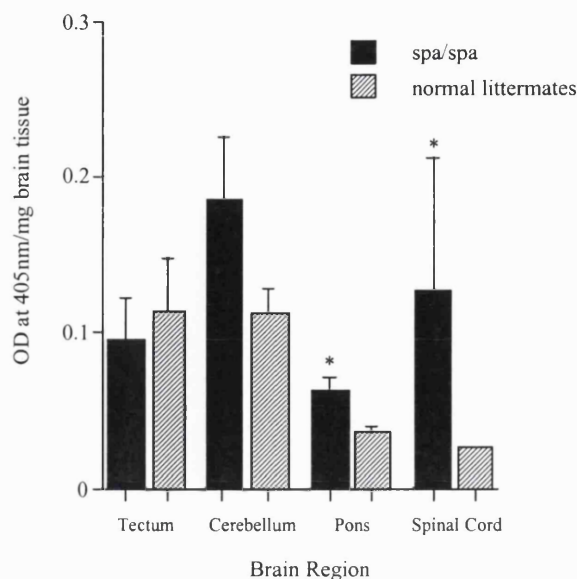


Figure 3.8.2.2 Increased DNA degradation in the hindbrain and spinal cord of *spa/spa* rats at 4 weeks of age. The data show the distribution of DNA cleavage in *spa/spa* rats (solid bars) versus phenotypically normal littermates (hatched bars) as measured by production of DNA-histone complexes arising from internucleosomal DNA cleavage. * $p < 0.05$ vs. vehicle by Mann-Whitney U-test. Bars depict mean \pm s.e.m.. $n = 5$ animals per group.

3.8.3 Regional distribution of caspase-3 activity in 4 week old *spa/spa* rats

Caspase-3 activity was measured as an increase in fluorescence following specific cleavage of the fluorogenic substrate Ac-DEVD-AMC. The detectable levels of caspase-3 activity were very low in all brain regions. The only region to show a significant increase in the *spa/spa* versus littermate controls was the cerebellum (Fig. 3.8.3.2). Despite the lack of statistical significance, several other brain regions, which demonstrated an increase in nucleosome cleavage, also showed a trend towards an increase in caspase-3 activity (Fig. 3.8.3.1 and Fig. 3.8.3.2).

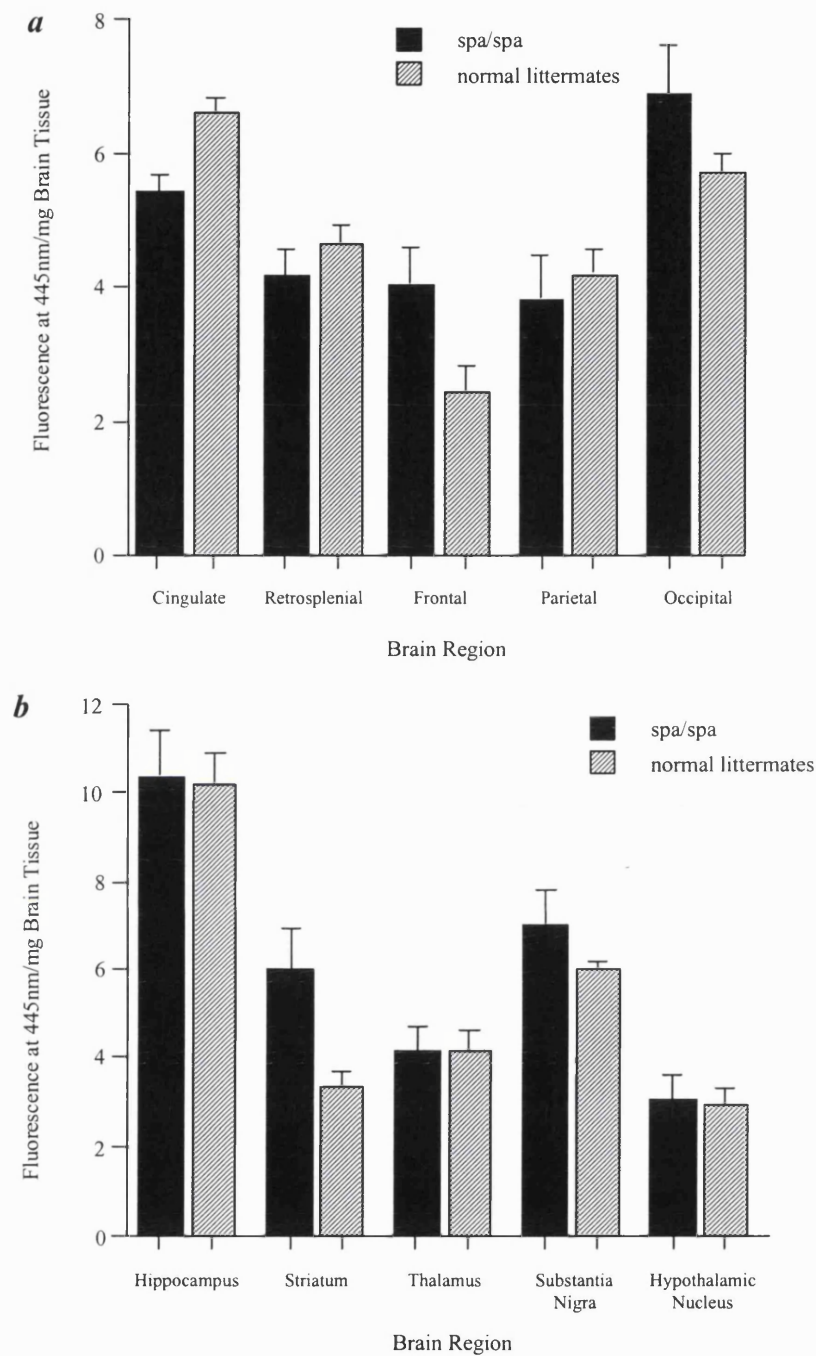


Figure 3.8.3.1 Caspase-3 activity in discrete brain regions of 4 week old *spa/spa* rats. Panel *a*. shows the cortical distribution of caspase-3 activity in *spa/spa* rats (solid bars) versus phenotypically normal littermates (hatched bars) as measured by specific cleavage of the fluorogenic caspase-3 substrate, Ac-DEVD-AMC. Panel *b*. shows the distribution of caspase-3 cleavage activity for sub-cortical regions. Bars depict mean \pm s.e.m.. $n=5$ animals per group except for cingulate cortex ($n=4$).

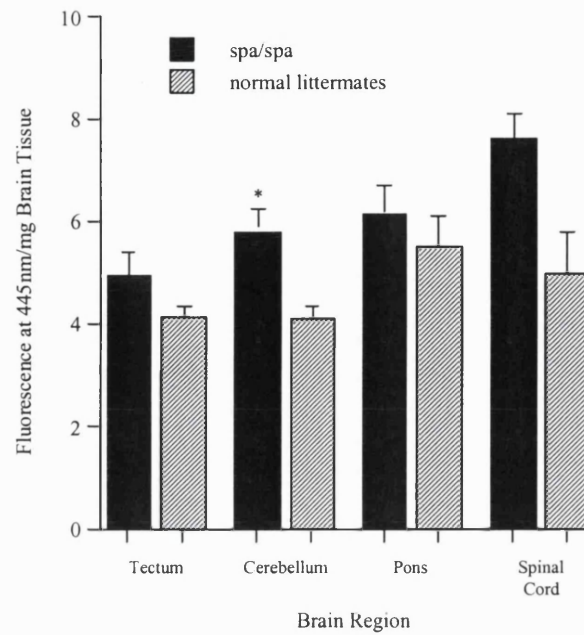


Figure 3.8.3.2 Caspase-3 activity in the hindbrain and spinal cord of 4 week old *spa/spa* rats. The data show the distribution of caspase-3 activity in *spa/spa* rats (solid bars) versus phenotypically normal littermates (hatched bars) as measured by specific cleavage of the fluorogenic caspase-3 substrate, Ac-DEVD-AMC. * $p < 0.05$ vs. vehicle by Mann-Whitney U-test. Bars depict mean \pm s.e.m.. $n = 5$ animals per group.

3.8.4 Comparison of DNA cleavage in selected brain regions at 4 and 8 weeks in *spa/spa* rats

In order to investigate the progression of neurodegeneration in the *spa/spa* rat, DNA degradation was compared between 4 and 8 weeks in those regions in which neurodegeneration has already been documented, the cerebellum, spinal cord and hippocampus (Wagemann *et al.*, 1991; Müller *et al.*, 1998). Two of these regions also demonstrated an increase in DNA cleavage at 4 weeks (cerebellum, spinal cord). The remaining region, the hippocampus, is a region known to undergo neurodegeneration from around six weeks of age (Wagemann *et al.*, 1991).

The changes between 4 and 8 weeks were varied. In the cerebellum, nucleosome cleavage was close to achieving statistical significance at 4 weeks. By 8 weeks, the difference between *spa/spa* and control littermates was now statistically significant (Fig. 3.8.4.1a). Nucleosome production, which had been significant in the spinal cord at 4 weeks also still elevated at 8 weeks (Fig. 3.8.4.1b). Contrary to expectation, the nucleosome ELISA detected no significant difference in the hippocampus at either 4, or 8 weeks (Fig. 3.8.4.2).

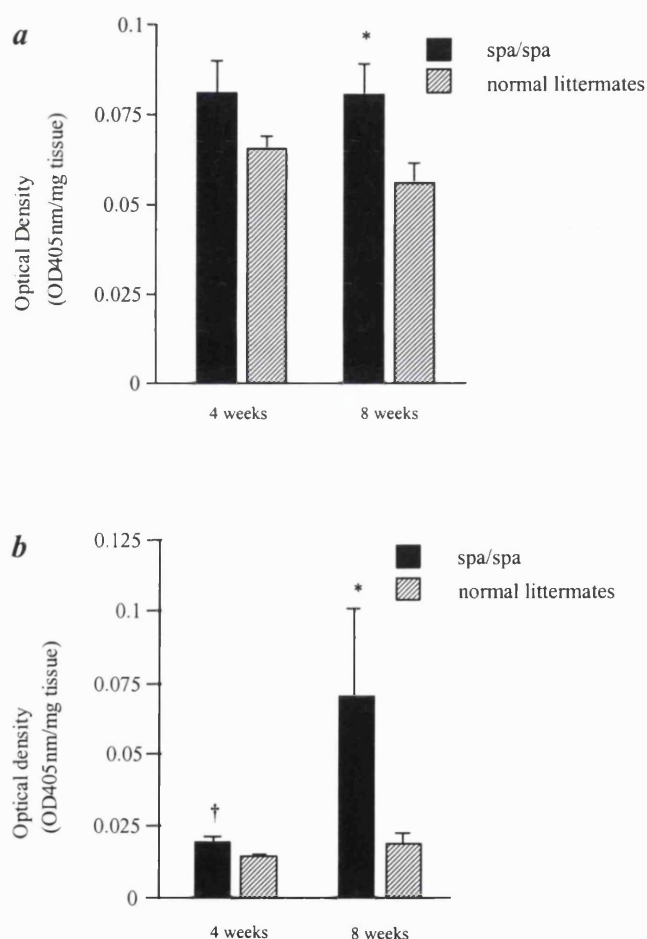


Figure 3.8.4.1 Change in DNA degradation in discrete brain regions of *spa/spa* rats between 4 and 8 weeks of age. Panel **a**. shows the DNA cleavage in the cerebellum of *spa/spa* rats (solid bars) versus phenotypically normal littermates (hatched bars) as measured by production of DNA-histone complexes arising from internucleosomal DNA cleavage. Panel **b**. shows the DNA cleavage for the spinal cord. * $p < 0.05$, or † $p < 0.01$ vs. vehicle by Mann-Whitney U-test. Bars depict mean \pm s.e.m.. $n = 11$ in the 4 week groups and $n = 8$ at 8 weeks.

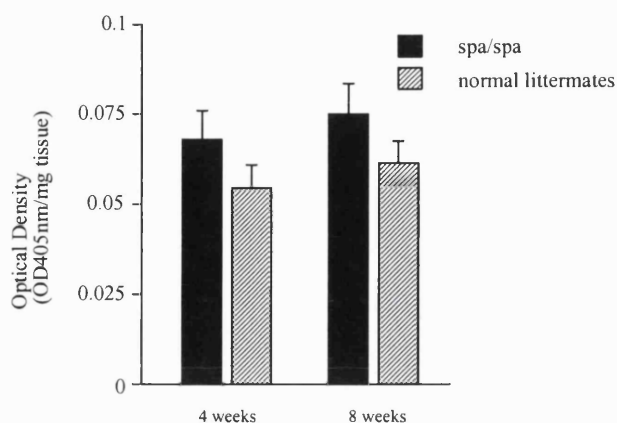


Figure 3.8.4.2 Change in DNA degradation in the hippocampus of *spa/spa* rats between 4 and 8 weeks of age. The histogram shows the DNA cleavage in *spa/spa* rats (solid bars) versus phenotypically normal littermates (hatched bars) as measured by production of DNA-histone complexes arising from internucleosomal DNA cleavage. Bars depict mean \pm s.e.m., $n=11$ in the 4 week groups and $n=8$ at 8 weeks.

3.8.5 TUNEL staining in the cerebellum of *spa/spa* rats

Since the ELISA data suggested ongoing specific DNA cleavage in regions associated with the neurological symptoms in *spa/spa* rats, and TUNEL positivity in Purkinje neurons of the cerebellum had been previously reported (Pikula *et al.*, 1998), TUNEL staining was carried out in the cerebellum of 4 week old *spa/spa* rats. Whilst TUNEL-positivity was seen in the cerebellum, the positive cells were not Purkinje neurons, but astrocytes situated within the Purkinje cell layer (Fig. 3.8.5.1). The TUNEL controls (Fig. 3.8.5.2) clearly demonstrate the specificity of the staining for cleaved DNA, as shown by the positive staining of naturally occurring apoptosis in epithelial cells of the choroid plexus (Fig. 3.8.5.2).

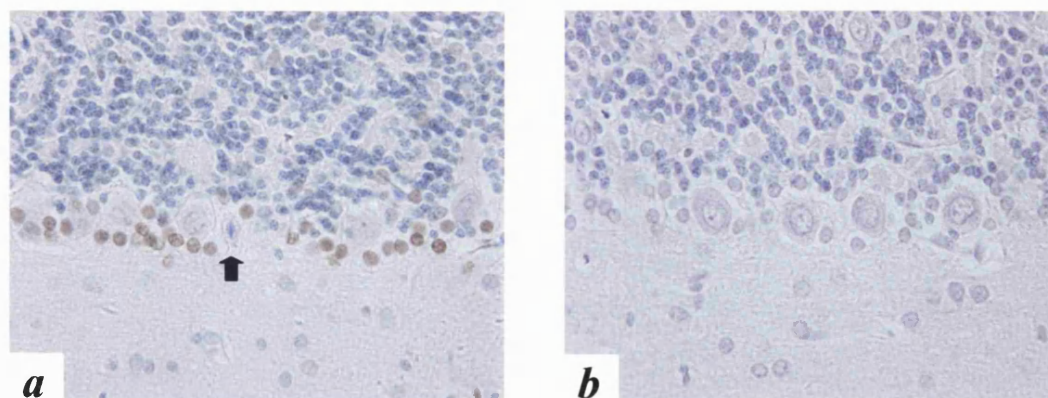


Figure 3.8.5.1 TUNEL staining in the cerebellum of 4 week old *spa/spa* rats. Panel *a* shows that Purkinje cells, even those undergoing degeneration (arrow) are free from TUNEL staining, whilst the nuclei of adjacent astrocytes are clearly positive. Panel *b* shows the lack of positive TUNEL staining in the cerebellum of phenotypically-normal littermates and the reduced number of astrocytes. Magnification: x40.

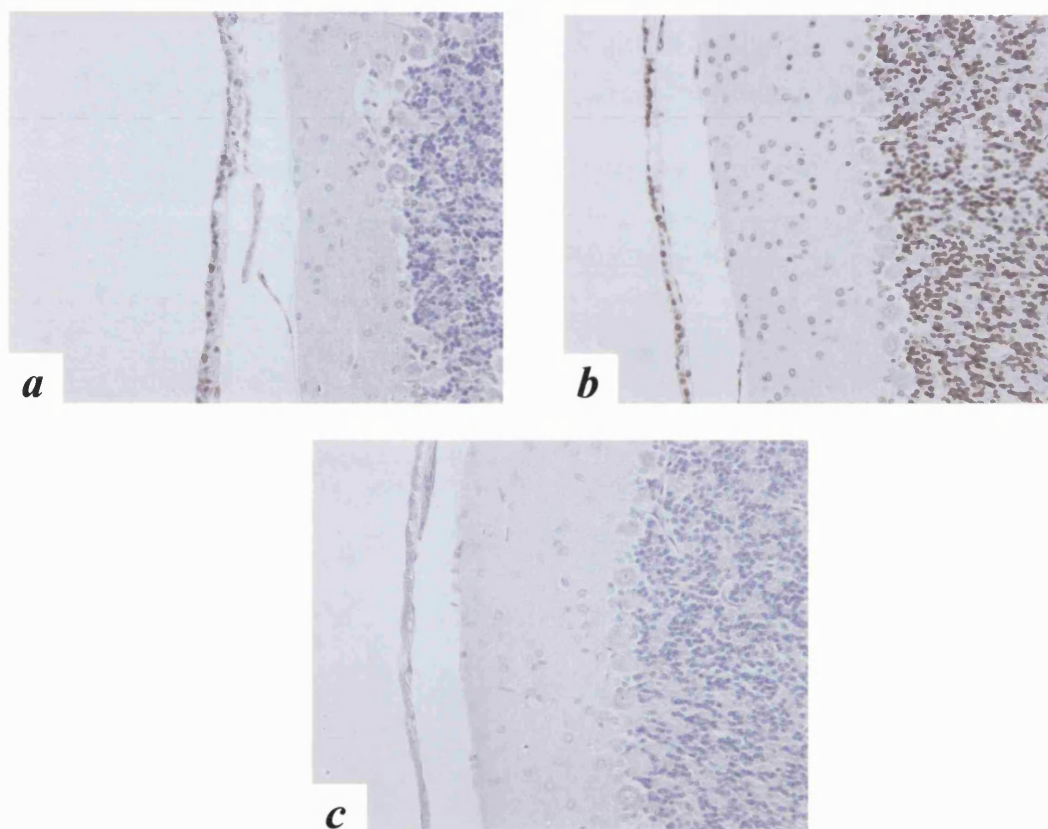


Figure 3.8.5.2 TUNEL staining controls in phenotypically normal *spa/spa* littermates, demonstrating the specificity of staining in control rat brain. Panels depict part of the choroid plexus of the third ventricle and a portion of Purkinje cell layer in the cerebellum. Panel *a* shows normal staining. The choroid plexus is positive for TUNEL, as expected given the turnover of epithelial cells, whilst the cerebellum is free of staining. Panel *b* shows a positive control in the presence of the DNA cleaving enzyme, DNAase I. Panel *c* is the negative control in the absence of the primary reaction mixture, tdT. Magnification: x20.

Neuronal loss was clearly evident in the *spa/spa* animals, as demonstrated by the gaps seen in the cerebellar Purkinje cell layer in Fig. 3.8.5.1 (and previously reported in the literature (Wagemann *et al.*, 1991; Müller *et al.*, 1998)), however, this cell loss did not appear to involve the specific internucleosomal DNA cleavage associated with the classical apoptotic cell death pathway. Therefore, the morphology of neuronal death was examined in more detail in order to determine the nature of cell death.

3.8.6 Light microscopy in *spa/spa* CNS tissue

Three regions were used to investigate the nature of neuronal death. The cerebellum and spinal cord have both previously been shown to exhibit neuronal cell death at 4 weeks of age in mutant animals (Wagemann *et al.*, 1991; Müller *et al.*, 1998), whilst degeneration in the hippocampus typically begins at around 6 weeks (Wagemann *et al.*, 1991; Müller *et al.*, 1998). Indeed, toluidine blue and silver stain revealed ongoing degeneration in the cerebellum and spinal cord at 4 weeks (Fig. 3.8.6.1 and Fig. 3.8.6.2, respectively), whilst the hippocampus CA3 region appeared normal (Fig. 3.8.6.3). In the cerebellum, the Purkinje cells could clearly be seen undergoing condensation of the cytoplasm and nucleoplasm (Fig. 3.8.6.1c and d) resulting in an increase in the staining intensity and shrinkage of the neurons. The motor neurons in the ventral horn of the lumbar spinal cord underwent a similar cell shrinkage with a concomitant increase in staining intensity (Fig. 3.8.6.2). In this instance, the neurons also appear to pull away from the extracellular matrix as they condense leaving a halo around the neurons (Fig. 3.8.6.1c and d). Phenotypically-normal littermates demonstrated no abnormal morphology in the cerebellum, or spinal cord (Fig. 3.8.6.1a and b; Fig. 3.8.6.2a and b).

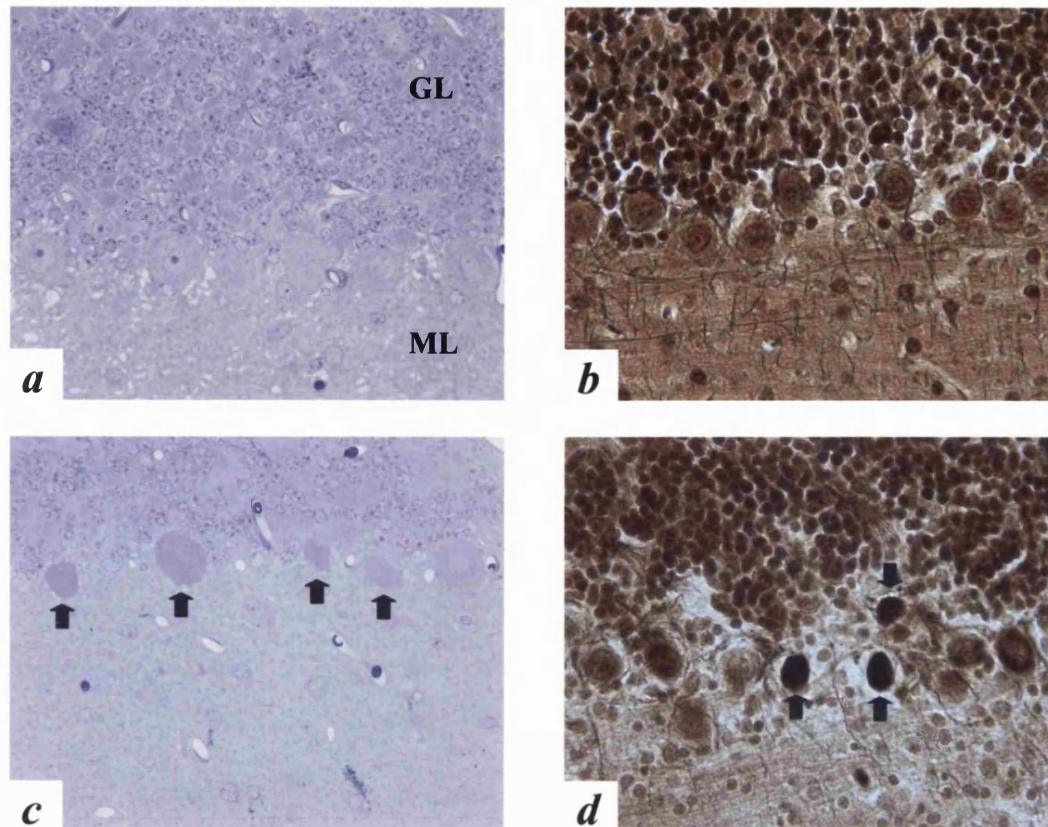


Figure 3.8.6.1 Purkinje cell degeneration in the cerebellum of *spa/spa* rats at 4 weeks of age. Panels **a** and **c** show toluidine blue staining of cerebellar tissue in littermate control and *spa/spa* rat, respectively. In **c**, degenerating neurons (arrows) appear darker and condensed compared with normal Purkinje cells. Panels **b** and **d** show silver staining in control littermate and *spa/spa* rat, respectively. In **d**, the silver stain is taken up much more by degenerating Purkinje cells (arrows). GL – Granule layer; ML – Molecular Layer. Magnification: x40.

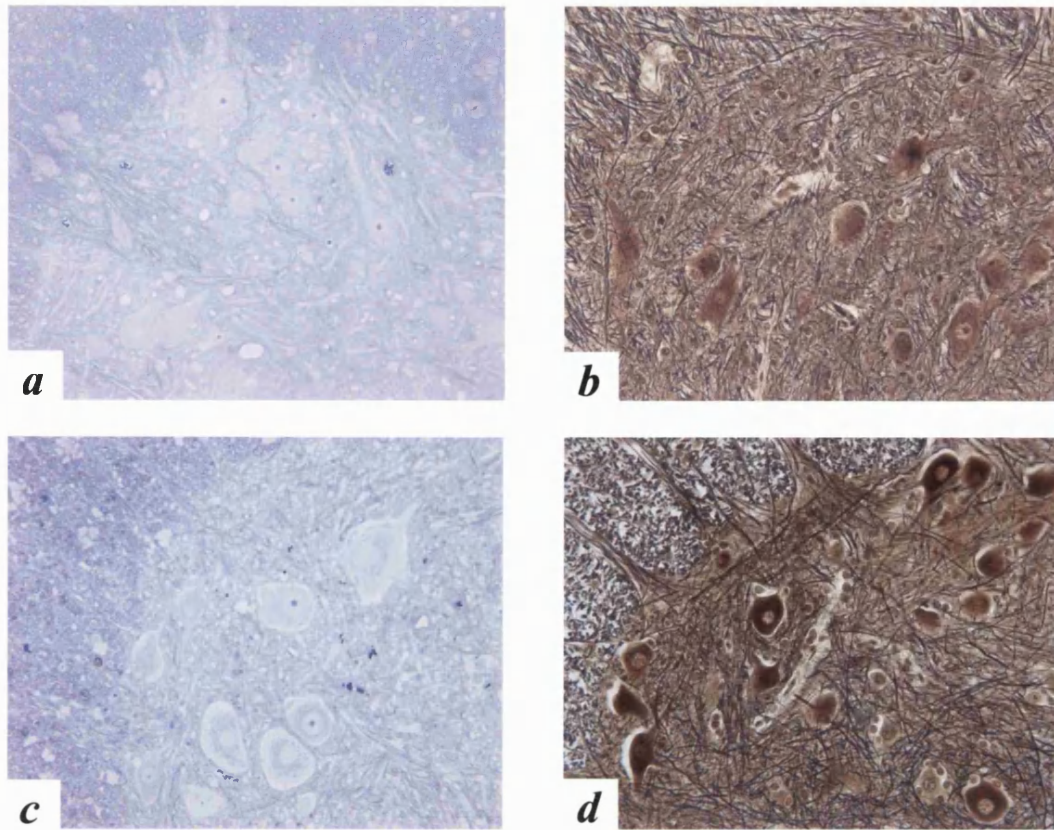


Figure 3.8.6.2 Motor neuron degeneration in the lumbar spinal cord, ventral horn of 4 week old *spa/spa* rats. Panels **a** and **c** shows toluidine blue staining in littermate control and *spa/spa* rat, respectively, which demonstrates how the neurons appear to shrink and pull away from the extracellular matrix in the mutant animal. Panels **c** and **d** shows how condensing motor neurons stain more intensely with silver as they begin degenerate compared with morphologically-normal neurons in the spinal cord from another *spa/spa* rat. Magnification: x20.

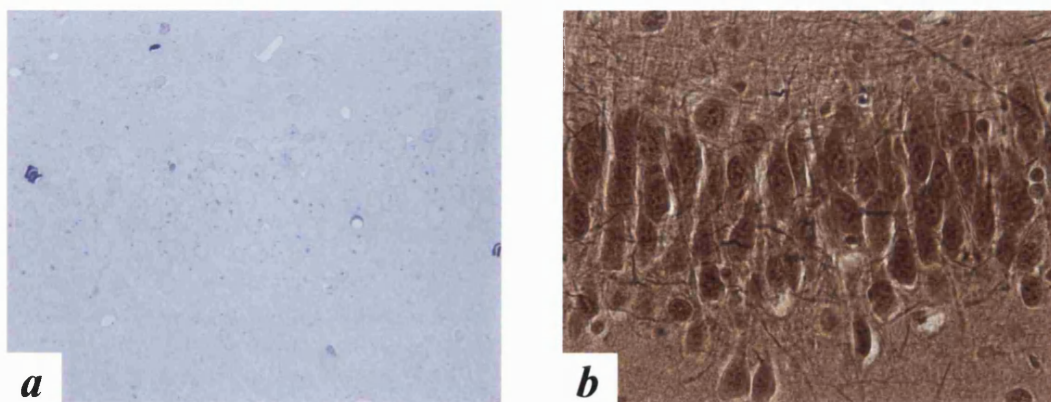


Figure 3.8.6.3 Hippocampal CA3 pyramidal neurons exhibit normal morphology in a 4 week old *spa/spa* rat. In panel **a** sections are stained with toluidine blue. Panel **b** shows silver staining. Magnification: x40.

At 8 weeks of age the degeneration in the cerebellum and spinal cord was still evident. In addition, neurodegeneration was now clearly visible in the hippocampal CA3 subfield (Fig. 3.8.6.4b). Again, by light microscopy, the neurons showed condensation of the nucleoplasm and cytoplasm, which appeared as an intense stain in toluidine blue-stained, plastic-embedded semithin sections (Fig. 3.8.6.4b).

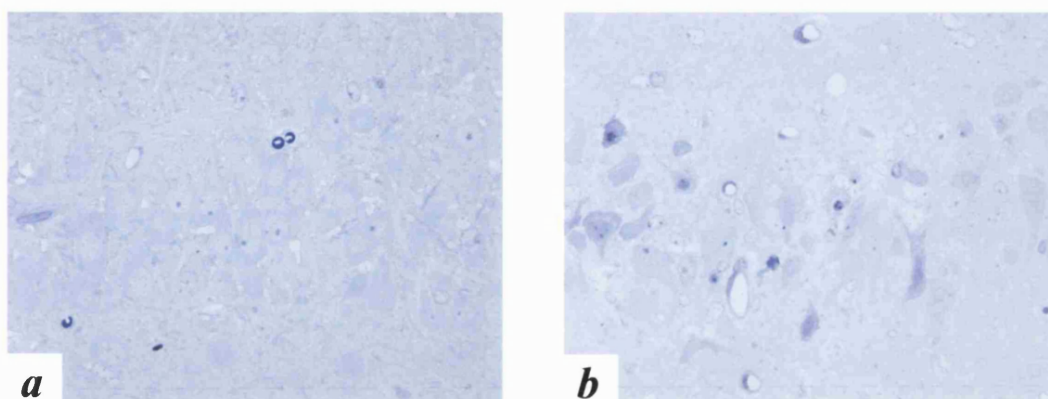


Figure 3.8.6.4 Degeneration in the hippocampal CA3 subfield of an 8 week old *spa/spa* rat. Sections are stained with toluidine blue. Panel *a* shows the normal CA3 subfield from a littermate control, whilst panel *b* demonstrates the degeneration in the same subfield of a *spa/spa* rat. Magnification: x40.

3.8.7 Electron microscopy in *spa/spa* rats

Whilst light microscopy was able to show the ongoing degeneration in the neuronal populations of interest, it gave little information about the cellular events taking place during the death process. In order to investigate this process in more detail, sections taken from the *spa/spa* rat were examined by electron microscopy. Hundreds of fields were examined from *spa/spa* rats at 4 and 8 weeks of age and the following composites were obtained for each of the three regions studied showing the process of degeneration

in each of the neuronal populations. No pathology was seen in phenotypically-normal littermates in any of the regions investigated.

3.8.7.1 Purkinje cell degeneration in the cerebellum of *spa/spa* rats

The process of Purkinje cell degeneration is depicted in the series of electron micrographs in Figure 3.8.7.1. The first sign of degeneration was that as the neurons began to shrink, they became more electron dense, as can be seen from the darkening in Figure 3.8.7.1b and c. The first structural changes to occur were folding of the cytosolic and nuclear membranes and intense chromatin condensation, but never margination as described in classical developmental apoptosis (Fig. 3.8.7.1b). This was followed by dilation of the Golgi and endoplasmic reticulum. There also appeared to be an apparent loss of ribosomes from the rough endoplasmic reticulum. Certainly, very little rough endoplasmic reticulum was seen in the later stages of degeneration and ribosomal-like structures were visible throughout the cytoplasm. As the process continued, the Purkinje cells shrunk further and became even more electron dense (Fig. 3.8.7.1c). Mitochondrial swelling was also observed late in the degenerative process.

Figure 3.8.7.1c represents the most advanced stage of cell death seen in the cerebellum. Membrane blebbing, or the formation of apoptotic bodies was never seen. The degeneration was always associated with an increased number of astrocytes (Fig. 3.8.5.1) and extension of astrocyte processes within the Purkinje cell layer (Fig. 3.8.7.1c) as has been previously reported in these animals (Wagemann *et al.*, 1995). No microglia, macrophages or other inflammatory cells were ever seen in the cerebellum during degeneration as would be expected if the ultimate cell fate was lysis. In fact, the cytoplasmic membrane remained intact throughout the whole death process.

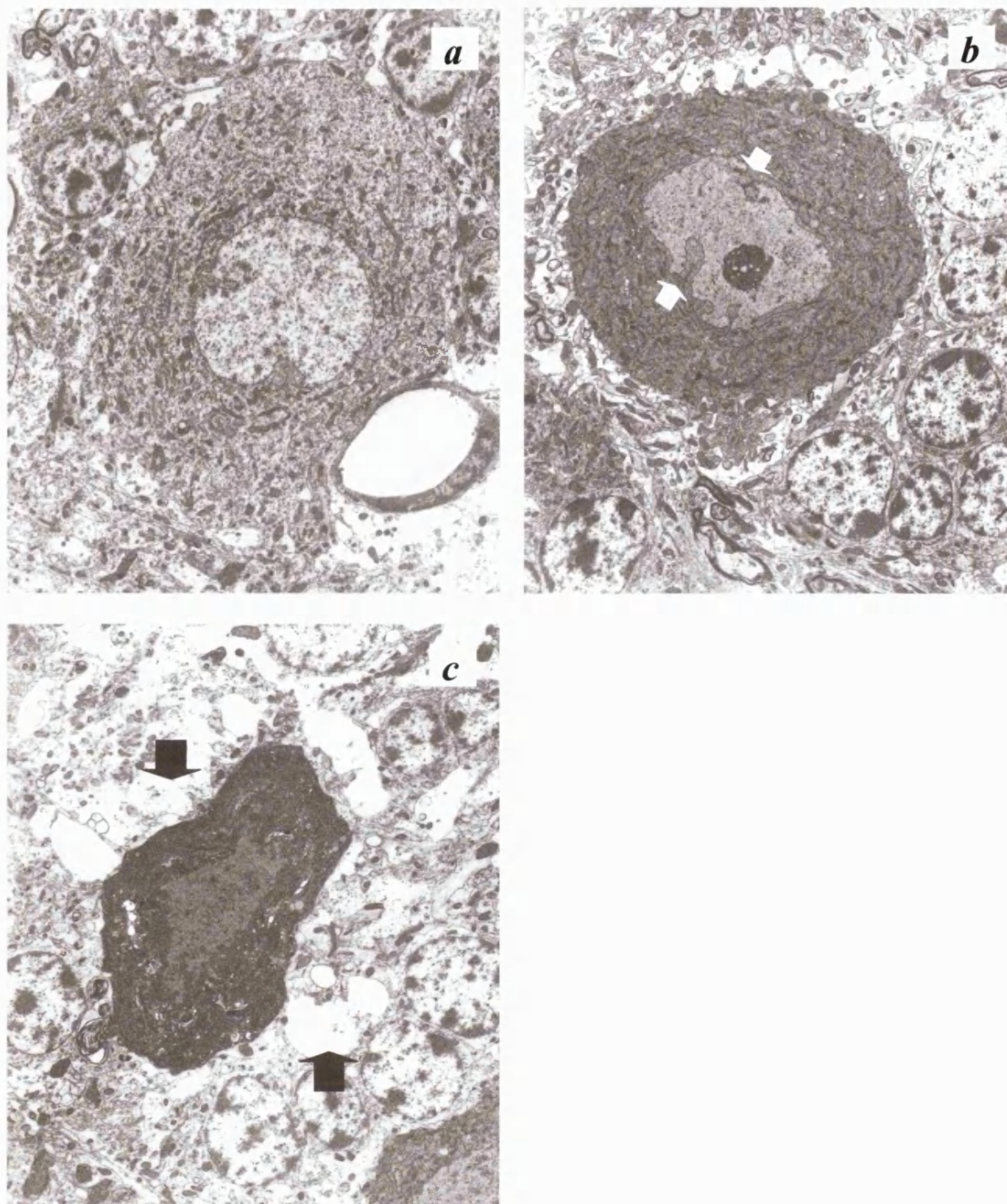


Figure 3.8.7.1 Electron micrographs depicting the stages of Purkinje cell degeneration in 4 week old *spa/spa* rats. Panel *a* shows a healthy Purkinje neuron for comparison. Panel *b* shows a Purkinje cell in the early stages of degeneration. The membranes become invaginated (arrows) and the cell becomes electron dense. Panel *c* represents the most advanced stage of Purkinje cell degeneration seen in the *spa/spa* rat. Note the presence of extensive astroglial processes (arrows) Magnification: x2500.

3.8.7.2 Motor neuron degeneration in the ventral horn of the lumbar spinal cord in *spa/spa* rats

Motor neuron degeneration in the ventral horn of the lumbar spinal cord of *spa/spa* rats followed a similar pattern to that described for the Purkinje cells above. Figure 3.8.7.2 depicts a series of electron micrographs representing the stages of degeneration in the spinal cord. Figure 3.8.7.2a shows the morphology of a healthy α -motor neuron. The cytoplasm was opaque and rich in mitochondria, with a normal microtubule network. Degenerating neurons initially darkened in colour as their affinity for osmium increased and they became more electron dense (Fig. 3.8.7.2b). The nucleoplasm and cytoplasm condensed and chromatin in the nucleus began to clump. At this stage, intracellular organelles remained intact as did the microtubule network (Fig. 3.8.7.2b). However, as the neurons degenerated further, the nuclear envelope became invaginated and the Golgi apparatus and endoplasmic reticulum began to open. The microtubule network also disappeared, whilst mitochondria, having retained a normal appearance until the final stages of degeneration, appeared swollen (Fig. 3.8.7.2c). This represents the final stage of α -motor neuron degeneration that was observed in the spinal cord of the *spa/spa* rat. As with the Purkinje cells, membrane blebbing and apoptotic bodies were never seen, neither was any disruption to the cytoplasmic membrane.

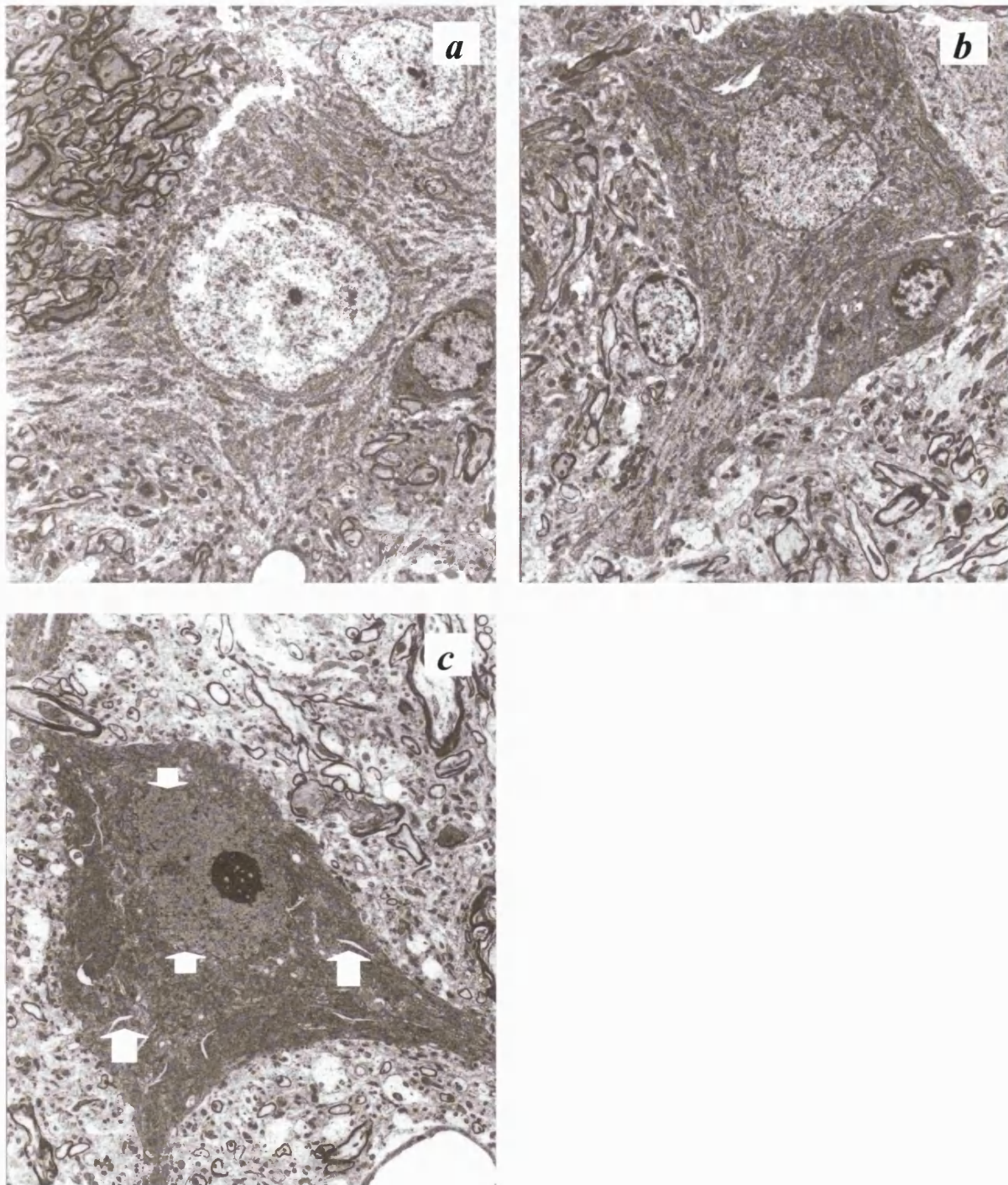


Figure 3.8.7.2 Electron micrographs depicting the process of α -motor neuron degeneration in the ventral horn of the lumbar spinal cord in 4 week old *spa/spa* rats. Panel *a* shows a healthy motor neuron. In *b*, the neuron is in the early stages of degeneration with a darkened, condensed appearance. Panel *c* represents the most advanced stage of degeneration seen in the spinal cord. The Golgi network and endoplasmic reticulum have begun to swell (large arrows) and the nuclear membrane has become invaginated (small arrows). Magnification: x2000.

3.8.7.3 Pyramidal cell death in the hippocampal CA3 subfield of *spa/spa* rats.

Degeneration of hippocampal pyramidal cells was restricted entirely to the CA3 subfield. The onset of neuronal death was much later than that of Purkinje cells and α -motor neurons as described above. Typically, CA3 neurons begin to die at around 6 weeks of age as described by Müller *et al.* (1998) and, indeed, no pathology was observed in the hippocampus of the *spa/spa* rat at 4 weeks of age (Fig. 3.8.6.3). Therefore, 8 week old *spa/spa* rats were used for ultrastructural examination.

In hippocampal CA3 pyramidal cells, several neurons were found in a more advanced stage of degeneration than described for the Purkinje cells, or α -motor neurons. Figure 3.8.7.3.1 demonstrates the process of neurodegeneration in the hippocampus. Healthy pyramidal cells, as seen previously, had a rounded nuclear morphology and an opaque cytoplasm (Fig. 3.8.7.3.1a). With the onset of cell death the neurons began to condense, as they developed a higher affinity for osmium, the chromatin aggregated and the Golgi apparatus and endoplasmic reticulum became swollen (Fig. 3.8.7.3.1b). The next stage of degeneration consisted of further condensation with folding of the nuclear and cytoplasmic membranes. Furthermore, spiral-like formations appeared in the cytoplasm, possibly arising from swelling of the Golgi and endoplasmic reticulum (Fig. 3.8.7.3.1c). The final stage of degeneration in the hippocampus saw the nucleus still distinguishable, but the cytoplasm had completely disassembled into tiny vesicle (Fig. 3.8.7.3.1d). Astrocyte processes were extensive in the region and appeared to surround the vesicles (Fig. 3.8.7.3.1d and Fig. 3.8.7.3.2; stage 3 neuron). Indeed, astrocyte processes in the vicinity of the dying neuron could be seen to contain cellular debris (Fig. 3.8.7.3.1d and Fig. 3.8.7.3.2).

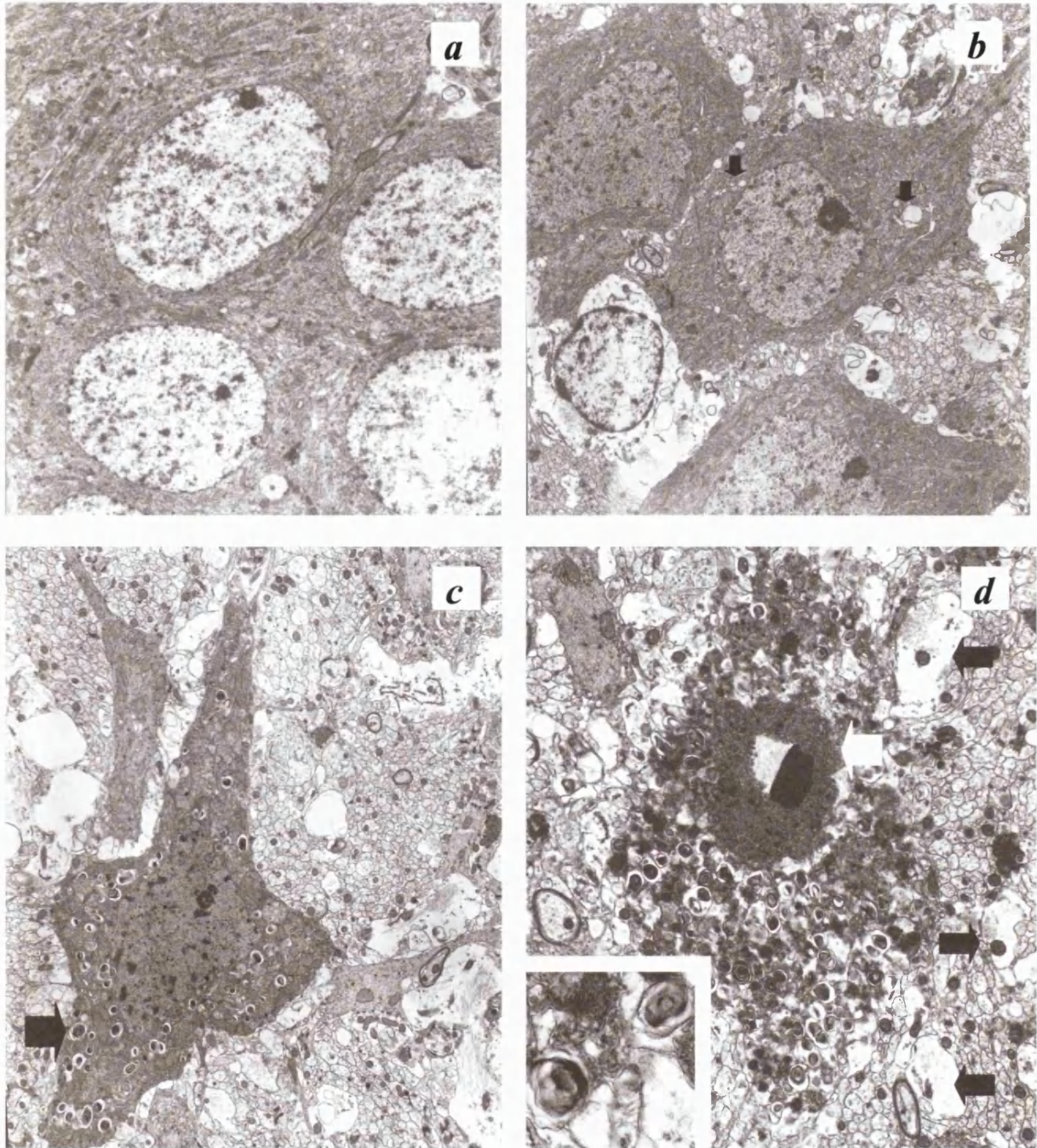


Figure 3.8.7.3.1 Neurodegeneration in the CA3 subfield of *spa/spa* rat hippocampus at 8 weeks of age. Panel *a* shows a normal pyramidal neuron. Panel *b* shows pyramidal neurons during an early stage of degeneration (stage 1). The neurons appear dark and condensed with compacted chromatin and Golgi/endoplasmic reticulum swelling (arrows). In *c*, the neuron is even more condensed with folding of the cytoplasmic and nuclear membranes and the appearance of spiral formations in the cytoplasm (large arrow; stage 2). Panel *d* shows extremely advanced degeneration of pyramidal neurons. The nucleus is highly condensed, although still discernable (large arrow), but the cytoplasm has now completely fractionated into tiny spiral-like vesicles (see inset; stage 3). Astrocyte processes in the vicinity contain cellular debris (dark arrows). Magnifications: *a* and *b* x2500; *c* x 4000; and *d* x6000 (inset *d* x25000).

Figure 3.8.7.3.2 illustrates the whole process in a single field. Pyramidal neurons can be seen at each stage of degeneration with the accompanying astrogliosis and extension of astrocyte processes.

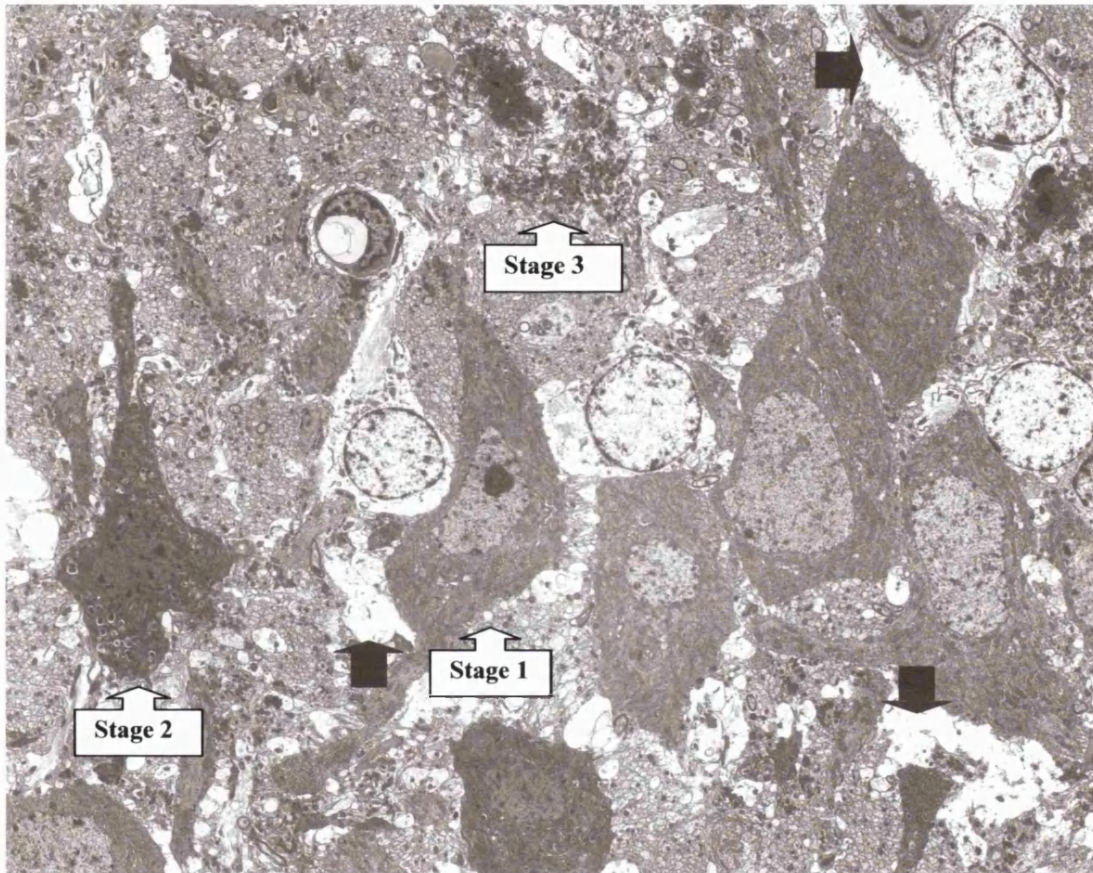


Figure 3.8.7.3.2 Degeneration of the hippocampal CA3 region in an 8 week old *spa/spa* rat. The three stages of degeneration are clearly visible as indicated by the numbered arrows corresponding with the stages described above (Fig. 3.8.7.3.1), along with the extensive astrocyte processes (large arrows). Magnification: x1200.

3.9 Discussion

The results presented in this chapter represent the first ultrastructural description of the morphological changes accompanying neuronal death in the *spa/spa* rat. The dominant features of the neuronal death process are (i) early nuclear and cytoplasmic condensation, associated with an enhanced affinity for toluidine blue and osmium, with nuclear and cytoplasmic membrane folding, (ii) chromatin condensation, but not margination, and (iii) late swelling of the mitochondria, Golgi network and endoplasmic reticulum. Whilst this form of neuronal death shares many of the characteristics of apoptosis, including cell condensation and aggregation of nuclear chromatin, there are several important distinctions. Apoptotic body formation, cytoplasmic, or nuclear membrane blebbing and chromatin margination, critical defining features of apoptosis, were never seen. In addition, the vacuolisation of the Golgi and endoplasmic reticulum and mitochondrial swelling are not seen in classical apoptosis. The loss of ribosomes from rough endoplasmic reticulum is a common feature of apoptosis, but in the apoptotic pathway, the free ribosomes aggregate in the cytosol, whereas in *spa/spa* neuronal death they are dispersed throughout the cytoplasm (Wyllie *et al.*, 1980).

Apoptosis can be further defined on the basis of the biochemical processes taking place inside the cell. One of the primary biochemical hallmarks of apoptosis is internucleosomal DNA fragmentation resulting in the formation of characteristic DNA ladders on agarose gels (Wyllie, 1980). DNA cleavage occurs early in the apoptotic process, concomitant with the appearance of condensed chromatin, but prior to apoptotic body formation. The DNA nucleosome ELISA employed in these studies offers a more specific measure of this internucleosomal cleavage than standard TUNEL, or *in situ* nick end labelling (ISNEL) techniques, by detecting DNA–nucleosome complexes, rather than

the exposed terminal of cleaved DNA alone. The use of the ELISA also allowed quantification of the extent of “apoptotic” degeneration in a given brain region enabling the correlation of regions of degeneration with the phenotype of the *spa/spa* animal.

The spastic phenotype in *spa/spa* rat develops over a lifespan of around 10 weeks. The earliest observable symptoms, of head and forelimb tremor, occur at 4 weeks of age and have been attributed to the onset of Purkinje cell loss in the cerebellum resulting in a loss of fine motor control (Wagemann *et al.*, 1991). The nucleosome ELISA data supported active DNA cleavage in this region at 8 weeks, although the difference between mutant and littermate just failed to reach significance at 4 weeks. Interestingly, the data also showed that DNA cleavage was present in the striatum at 4 weeks. Therefore, degeneration of striatal neurons may also contribute to the early impairment in fine motor control. Striatal degeneration has not previously been reported in the *spa/spa* rat, although increased GFAP staining has been described in sub-cortical regions and the presence of astrocytes has been correlated with neurodegeneration (Wagemann *et al.*, 1995). The striatum also forms part of the neurocircuitry involved in the control of anxiety and disturbances in these pathways, either neurochemical, or physical (lesions), are associated with this disorder (Ninan, 1999). This may be of relevance to the *spa/spa* rat as they exhibit anxiety early in life, as demonstrated by a reduced time spent in the centre of the cage during locomotor activity assessment (Müller *et al.*, 1998), thus, striatal damage may contribute to this.

By 4 weeks of age, increased muscle tone is already evident in the *spa/spa* rat and correlates with the appearance of degenerating primary motor neurons (Müller *et al.*, 1998). The data from the nucleosome ELISA also indicated degeneration in the spinal cord at this time, which was still evident at 8 weeks. Furthermore, DNA cleavage was

also detected in the pons, a region rich in motor neuron cell bodies and pathways involved in motor function and may, therefore, contribute to the *spa/spa* phenotype.

The distribution of the DNA cleavage signal in the cortical regions was stronger, and significant, in rostral regions and low towards the frontal cortex. Cortical damage has not been previously reported in the *spa/spa* rat, but is potentially of interest as the occipital cortex contains a number of visual centres. Neuronal loss in the visual centres of the occipital cortex might account for the anecdotal personal observation of impaired visual processing in *spa/spa* rat relative to phenotypically-normal littermates (the *spa/spa* rats appear to spend more time in exploration and are not as responsive to external movements). Neuronal projections from the olfactory bulb to the piriform cortex, may provide a link between the elevated nucleosome signals in the olfactory bulb and the occipital cortex and the subsequent development of the *spa/spa* phenotype (Cooper *et al.*, 1994).

Caspase-3 activity is an additional biochemical marker widely used as an indicator of apoptotic activity (Fernandes-Alnemri *et al.*, 1994). In the present studies, the caspase-3 activity was not significantly elevated in every region positive for nucleosome cleavage activity, however, there was a trend toward significance in the regions of particular interest. The low signal was not entirely unexpected since caspase-3 activity in any one cell is transient, therefore the signal from any given population during the weeks of protracted degeneration may not be sufficient to produce a measurable increase. The relative weakness of the signals in the nucleosome ELISA and the caspase-3 assay in the majority of brain regions is contrasted by the strong signals obtained from the olfactory bulb, an area of high apoptotic turnover (neuroepithelial cells typically have a lifespan of

around one month; Deckner *et al.*, 1997; Hayward and Morgan, 1995). This highlights the low incidence of programmed cell death in other regions of the adult CNS.

The data from the hippocampus emphasised the problems associated with using a biochemical assay to detect a signal from a small number of degenerating cells within a tissue mass. CA3 pyramidal neurons are known to undergo degeneration in the later stages of the mutant rats lifespan (Wagemann *et al.*, 1991), but the nucleosome ELISA and caspase-3 activity were not significantly different from control littermates at either 4, or 8 weeks even though CA3 degeneration was clearly evident at 8 weeks, as revealed by the morphological studies. It may be that, in this instance, given the small volume of tissue available from dissection of the hippocampus, the assays were not sensitive enough to detect any change in levels of DNA cleavage or caspase-3 activity, especially as this region already seems to have a strong background nucleosome signal. This high background signal could originate from the large astrocyte population present in the region (Wagemann *et al.*, 1995) and therein lies the second problem with biochemical assessments of cell death in tissue samples.

The nucleosome ELISA and caspase-3 activity assay are useful in highlighting possible areas of degeneration, but provide little information about which cells are responsible for the signal. When TUNEL was assessed in the cerebellum, it showed that the DNA cleavage products were present in astrocytes rather than neurons. Astrocytes were not seen undergoing apoptosis, at the ultrastructural level, and TUNEL-positive astrocytes did not have an apoptotic morphology, although the staining had a largely nuclear location. It is possible that the astrocytes were in the early stages of apoptosis, alternatively, the signal could have been produced by DNA degradation products from

the phagocytosis of degenerating neurons. A lack of apoptotic astrocytes has also been described by Turmaine *et al.* in a mouse model of Huntington's disease, in which the Purkinje neurons undergo a similar form of cell death to that described here (Turmaine *et al.*, 2000), although they were able to find the occasional apoptotic astrocyte late in disease (Turmaine M, personal communication).

Although the TUNEL data suggest that the ELISA signal may not be arising from neuronal death, but from astrocytes found in the vicinity, this in itself may be an indicator of ongoing degeneration of neurons. Previous studies in the *spa/spa* rat have shown that neurodegeneration in these animals is always associated with astrogliosis (Wagemann *et al.*, 1995) and also revealed increased glial fibrillary acidic protein (GFAP) reactivity in those regions undergoing degeneration described in the present studies. In addition, degeneration in these particular regions could be expected to produce the symptoms which are, indeed, part of the *spa/spa* phenotype as described above. If astrocytes, and not neurons, are responsible for the nucleosome ELISA signal, this could also explain why the signal does not increase significantly between 4 and 8 weeks as the astrocyte population is likely to remain constant.

Since TUNEL positive neurons were not seen, this suggests that internucleosomal DNA fragmentation, one of the major biochemical characteristics of apoptotic cell death, does not form part of the death pathway involved in neuronal death in the *spa/spa* rat. Combined with the differences seen in the morphology of degenerating neurons from the classical apoptotic morphology, this indicates that neurons in the *spa/spa* rat are dying by an alternative form of programmed cell death.

The morphological and biochemical observations described in *spa/spa* rat neuronal degeneration are in agreement with a number of other descriptions of “dark cell neurodegeneration” in different adult systems (Turmaine *et al.*, 2000; Liposits *et al.*, 1997; Lin *et al.*, 1999). These authors describe a process of programmed cell death in adult brains with important distinctions from the current biochemical and morphological classifications of apoptosis, namely darkening of neurons with cytoplasmic and nuclear shrinkage, chromatin condensation, but not margination, and the appearance of intracellular vacuoles arising from the Golgi or the endoplasmic reticulum. Sperandio *et al.* (2000) have been able to reproduce these characteristics in an *in vitro* model in non-neuronal cells, which may prove useful in further evaluating whether this represents a continuum between necrosis and apoptosis, or a distinct form of programmed cell death.

The formation of apoptotic bodies is the main defining feature of apoptosis (Kerr *et al.*, 1972), however, this characteristic was not described by the authors above. Although no apoptotic bodies were seen in “dark cell degeneration” or in *spa/spa* rat neuronal degeneration, it is possible that this is because the cell debris was cleared before the appearance of bodies. As already stated, astrogliosis, as a result of either proliferation or recruitment, was present in the areas of neurodegeneration in the *spa/spa* rat, which could underlie the rapid phagocytosis of apoptotic debris. Certainly a glial response to this form of neurodegeneration has been reported by other authors (Turmaine *et al.*, 2000; Liposits *et al.*, 1997).

However, the early features of programmed cell death in the *spa/spa* rat are distinct from apoptotic cell death (the pattern of nuclear condensation in particular), suggesting it is unlikely that the neurons would have gone on to develop an apoptotic appearance had they not been phagocytosed. Moreover, although there were many astrocyte processes

throughout the degenerating regions, astrocytes were never seen engulfing whole neurons as might be expected if phagocytosis was such a prominent feature of cell removal. It is possible that rather than engulfing the whole neuron, astrocytes removed smaller portions as it degenerated and occasionally astrocyte processes were seen to pass through the nucleus and cytoplasm of degenerating neurons. Astrocytes certainly appear to be responsible for the removal of neuronal debris in the later stages of hippocampal CA3 degeneration, as was indicated by cellular debris contained within astrocytes in this area. TUNEL in this region may help to confirm this by detecting the presence of DNA debris within astrocytes. The hippocampus was unusual in that hippocampal CA3 neurons underwent the same early stages of condensation degeneration as the other regions, but subsequently progressed to an autophagic-like phenotype as the cytoplasm disintegrated into small vesicles. This process occurred from within the cell, with the vesicles seemingly derived from the dilated endoplasmic reticulum, or Golgi apparatus. The vesicles did not have the dense lysosomal characteristics of autophagic vesicles, rather they contained what appeared to be membranous whorls. Their appearance is similar to that described during neurodegeneration in leucodystrophy (Lowe *et al.*, 1997). Once the cytoplasm had been packaged in this way, it was removed by astrocytes, which enveloped and digested the cytoplasmic constituents. This occurred in the absence of membrane blebbing, apoptotic body formation, or even disruption of the nuclear membrane and was not seen in the cerebellum and spinal cord. In these latter examples, the dying neurons are more likely removed by the astrocytes before this could happen. The onset of degeneration in the hippocampus is later and the process occurs more rapidly, so astrocytes are possibly unable to clear dying cells fast enough and thus, the later stages of degeneration become apparent.

It is clear that developmental, or pathological degeneration of neurons in the immature CNS meets the current criteria for apoptotic cell death (Dikranian *et al.*, 2001), but there are many examples of neuronal death in the adult being described as apoptotic when often these descriptions rely solely on the presence of TUNEL. In the stroke field, delayed neuronal death in the hippocampus is a phenomenon associated with global forebrain ischaemia and has been described by many as apoptotic primarily on the basis of TUNEL positive staining (Nitatori *et al.*, 1995). However, ultrastructural analysis reveals a very distinct morphological appearance, similar to that seen in *spa/spa* rat (Colbourne *et al.*, 1999). The same is true in focal ischaemia where apoptosis is often described in the penumbral regions of the ischaemic core (Li *et al.*, 1995), but when examined in more detail, death is often morphologically distinct (van Lookeren Campagne and Gill, 1996).

The underlying pathological aetiology of “dark cell degeneration” in both stroke and traumatic brain injury is most likely excitotoxicity and antagonists of AMPA, but not NMDA receptors have been shown to be protective (Pulsinelli *et al.*, 1993; Ikonomidou and Turski, 1996; 1997). Glutamate toxicity potentially underlies many of the examples in which this form of condensation and degeneration of neurons is seen *in vivo* (Turmaine *et al.*, 2000; Liposits *et al.*, 1997; Lin *et al.*, 1999). Furthermore, there is a strong link between the altered expression of the AMPA receptor subunit, GluR2, and neurodegeneration in the *spa/spa* rat (Cohen *et al.*, 1991; Margulies *et al.*, 1993; Müller *et al.*, 1998), which is further supported by the neuroprotection afforded by the AMPA receptor antagonist, MPQX (Müller *et al.*, 1998). Taken together, these data provide a strong link between chronic glutamate exposure, and in particular AMPA receptor activation, and the distinct form of programmed cell death in adult neurons described in these studies.

3.9.1 Conclusions

Firstly, from a technical aspect, these studies emphasise that the reliance on one marker of apoptosis, such as DNA fragmentation, is insufficient for the confirmation of this form of programmed cell death *in vivo*. The nucleosome ELISA is a more specific, quantifiable and highly sensitive measure of the internucleosomal cleavage found in cells undergoing apoptosis, which when combined with standard TUNEL staining and detailed morphological assessment can provide more accurate information about which cells are undergoing apoptotic cell death.

In addition to confirming known regions of neurodegeneration, these data also suggest additional areas in which neuronal death may occur. The nucleosome ELISA detected DNA cleavage in discrete brain structures (for example, the striatum and occipital cortex) in which, if neurodegeneration did occur, one would expect neurological deficits that are consistent with the phenotype present in the *spa/spa* rat.

Finally, the data presented in these studies confirm previous reports which describe the neurodegeneration of cerebellar Purkinje cells, hippocampal CA3 pyramidal neurons and spinal cord α -motor neurons in the *spa/spa* rat (Wagemann *et al.*, 1991; Müller *et al.*, 1998) and extend these observations by dissecting the nature of the neuronal death. In doing so they challenge the description of Purkinje cell death in the cerebellum as apoptotic (Pikula *et al.*, 1997) and raise an interesting question as to the relevance of classical apoptotic cell death in the degeneration of mature neurons in the adult CNS. The data have shown that the death of adult neuronal populations in the *spa/spa* rat, along with many other descriptions of adult neuronal death in the literature, does not conform to the strict morphological and biochemical criteria which define apoptosis.

Therefore, they raise the possibility that adult neuronal programmed cell death represents either a continuum between different forms of cell death (necrosis, apoptosis and autophagy), or a distinct form of programmed cell death (paraptosis).

CHAPTER 4 - Final Conclusions

For many years, studies into the involvement of glutamate receptors in the pathophysiology of neurodegenerative diseases had been limited to their role in acute excitotoxicity. In recent years it has become apparent that glutamate has an important role in many aspects of CNS disorders and not simply neuronal dysfunction. The current dissertation describes the ultrastructural neuropathological and pharmacological consequences of AMPA receptor activation in two models of chronic neurodegenerative disease, experimental autoimmune encephalomyelitis in rodents and the *spa/spa* rat.

In experimental autoimmune encephalomyelitis and multiple sclerosis, the consequences of CNS inflammation to gray matter structure and function had, until recently, been largely neglected. Given that the symptoms of the diseases are neurological and that the rapidity of relapse and remission suggest that demyelination and remyelination are not solely responsible for the neurological deficits, it is perhaps surprising that the neuronal aspects of multiple sclerosis and experimental autoimmune encephalomyelitis are only now being revisited. The study in Chapter 2 is the first description of neuronal cell body loss in the spinal cord of experimental autoimmune encephalomyelitis animals and suggests a potentially important mechanism of neuronal death through a direct interaction with invading leucocytes. Whilst T-cell invasion of neurons appears to be the predominant method of motor neuron loss in this form of experimental autoimmune encephalomyelitis, neuronal swelling, perineuronal oligodendrocyte satellitosis and chromatolysis are all present and indicate neuronal and axonal damage, independent of direct cell infiltration. Thus, a combination of these mechanisms of neuronal death will contribute to the overall loss of neuronal density. The mechanism of the execution stage

of cell death remains unclear as, whilst lymphocytes clearly undergo apoptosis, there was no evidence of neuronal apoptosis.

From the pharmacological studies in Chapter 2 it is clear that AMPA receptor activation is essential in the pathophysiology of disease progression in rodent models of multiple sclerosis. Of major importance is the finding that this inflammatory autoimmune disease can be treated with agents which act independently of immunosuppression, or suppression of inflammation. In addition, AMPA antagonists not only treat the acute neurological aspects of experimental autoimmune encephalomyelitis, but also appear to be able to modify disease progression, by protecting the neurons and oligodendrocytes from the consequences of uncontrolled inflammation in the CNS. This has exciting implications for the therapy of multiple sclerosis, suggesting that neuro-/oligodendrocyte-protective agents, such as the AMPA receptor antagonists, would be mutually beneficial in combination with the currently used immunosuppressive and anti-inflammatory therapies. Experiments are continuing in order to identify anomalies in the glutamatergic system in experimental autoimmune encephalomyelitis and multiple sclerosis tissue, thereby determining the source of glutamate and the mechanism of protection afforded by AMPA receptor antagonists.

Preliminary data from the chronic mouse EAE model, suggests that in the later stages of disease when the lymphocytic component has subsided and the surrounding milieu in gray matter is dominated by the astrocyte, the neurons appear to be undergoing cytoplasmic condensation and darkening in a manner similar to that in the *spa/spa* rat. This is accompanied by a reduction in neuronal density, as assessed by use of the stereological disector. The implication is that in the early phase of disease, when T-cells and macrophages dominate the pathology, the neurons are under direct assault from

inflammatory cells in which AMPA receptor activation plays an important role. In the later stages, when inflammation has subsided and demyelination is prevalent, the neurons are still sensitive to glutamate exposure, as demonstrated by the efficacy of AMPA antagonist treatment during the second phase of disease, but the mechanism of neuronal death is similar to that seen with chronic exposure to cytotoxic glutamate in the *spa/spa* rat. These initial observations will be further investigated by comparative analysis of neuronal and axonal pathology in the primary and chronic phases of experimental autoimmune encephalomyelitis in Biozzi mice.

The potential for AMPA-mediated toxicity is investigated further in Chapter 3 in the context of the classification of neurodegeneration in the *spa/spa* rat. The phenotype in *spa/spa* rat has been attributed to reduced expression of the AMPA receptor subunit, GluR2, which renders AMPA channels permeable to calcium resulting in a potentially fatal over activation of the glutamatergic system. The *spa/spa* phenotype is consistent with observations made following either i.c.v., or p.o. administration of AMPA receptor agonists (increased anxiety, muscle tone and seizure activity lasting from minutes to hours (Turski L *et al.*, 1992; Turski WA *et al.*, 1981; Ikonomidou and Turski, 1997)). Since the *spa/spa* rat is known to have altered AMPA receptor function due to reduced GluR2 expression (Margulies *et al.*, 1993), it is likely that the appearance of the *spa/spa* phenotype and the associated neuropathology are attributable to chronic AMPA receptor activation. Indeed, it has been demonstrated that treatment with the AMPA receptor antagonist, MPQX, protects against neuronal loss in both the hippocampus and cerebellum of *spa/spa* rats (Müller *et al.*, 1998).

Many investigators are quick to describe neuronal death as apoptotic in the setting of chronic neurodegenerative disorders when the cell death they describe clearly does not

meet the morphological and/or biochemical requirements for this classification. In the *spa/spa* rat, where previous reports have readily described the mechanism of cell death as apoptotic, a sequence of neuronal degeneration has been presented which cannot be classified according to the criteria of apoptosis set out by Andrew Wyllie and colleagues. Instead, the final stages of neuronal degeneration show a closer resemblance to the “dark cell degeneration” seen in the adult CNS of Huntington’s disease, its mouse models and in other examples of CNS neurodegeneration. These data suggest that, certainly in *spa/spa* rats and possibly in other systems, adult neurons do not die by apoptosis, but by a morphologically and biochemically distinct form of programmed cell death. Whether this represents a separate form of cell death, or part of a continuum between apoptosis, necrosis and autophagy remains to be determined. Further attempts are being made to identify the aetiology of disease in the *spa/spa* rat.

The physiological, pharmacological and pathological characterisation of glutamate is a constantly evolving field. A glutamatergic component has been proposed, to a greater or lesser extent, in an ever expanding list of neurodegenerative diseases. That glutamate may be involved in such a disparate collection of disorders, with their accompanying pathologies, may seem unlikely. However, the disease context may be critical. Thus, the expression of a particular glutamatergic receptor subtype (eg. AMPA) on a certain neuronal/glial population in an aberrant CNS milieu (eg. inflammation) may generate a disease-specific pathology. Further permutations may be envisaged in situations of dysregulated neurotransmitter, growth factor, protein or energy production leading to a variety of pathologies and neuronal death.

Recently, yet another NMDA receptor has been identified (Nishi *et al.*, 2001), which coupled with the increasing knowledge being gained from the study of metabotropic

glutamate receptor pharmacology and function, indicates an even greater diversification of glutamate signalling. Furthermore, it has been shown that AMPA receptor activation does not have to result in the opening of the channel pore and the flux of cations to elicit an intracellular response. Hayashi *et al.* (1999) have shown that AMPA receptor agonism can result in the activation of the Src kinase family member, Lyn, and subsequently activate the mitogen-activated protein kinase (MAPK) pathway, independent of ion flux. This suggests that in addition to their role as excitatory ionophores, AMPA receptors also have an important, direct role in the regulation of intracellular signalling events, which may also hold true for other classes of glutamate ionotropic receptors. Furthermore, the MAPK family are involved in many intracellular signalling cascades including, the control of gene expression, cell proliferation and programmed cell death (Chang and Karin, 2001). This observation may herald the start of a new era of research into the mechanisms and consequences of chronic glutamate exposure.

References

- Abe T, Sugihara H, Nawa H, Shigemoto R, Mizuno N & Nakanishi S (1992). Molecular characterization of a novel metabotropic glutamate receptor mGluR5 coupled to inositol phosphate/Ca²⁺ signal transduction. *J. Biol. Chem.* **267**:13361-8.
- Adams CWM, Poston RN & Buk SJ (1989). Pathology, histochemistry and immunocytochemistry of lesions in acute multiple sclerosis. *J. Neurol. Sci.* **92**: 291-306.
- Ahmed Z, Gveric D, Pryce G, Baker D, Leonard JP & Cuzner ML (2001). Myelin/axonal pathology in interleukin-12 induced serial relapses of experimental allergic encephalomyelitis in the Lewis rat. *Am. J. Pathol.* **158**:2127-38.
- Ankarcrona M, Dybukt JM, Bonfoco E, Zhivotovsky B, Orrenius S, Lipton SA & Nicotera P (1995). Glutamate-induced neuronal death: a succession of necrosis or apoptosis depending on mitochondrial function. *Neuron* **15**:961-73.
- Anson LC, Chen PE, Wyllie DJA, Colquhoun D & Schoepfer R (1998). Identification of amino acid residues of the NR2A subunit that control glutamate potency in recombinant NR1/NR2A NMDA receptors. *J Neurosci*, **18**:581-9.
- Araque A, Sanzgiri RP, Parpura V & Haydon PG (1999). Astrocyte-induced modulation of synaptic transmission. *Can. J. Physiol. Pharmacol.* **77**:699-706.
- Armstrong N, Sun Y, Chen GQ & Gouaux E (1998). Structure of a glutamate-receptor ligand-binding core in complex with kainate. *Nature*, **395**:913-7.
- Baker D, O'Neill JK, Gschmeissner SE, Wilcox CE, Butter C & Turk JL (1990). Induction of chronic relapsing experimental allergic encephalomyelitis in Biozzi mice. *J. Neuroimmunol.* **28**:261-70.
- Baker D, Pryce G, Croxford JL, Brown P, Pertwee RG, Huffman JW & Layward L (2000). Cannabinoids control spasticity and tremor in a multiple sclerosis model. *Nature* **404**:84-7.

- Bauer J, Bien CG, Deckwerth TL, Deckert M, Wiestler OD, Schramm J, Elger CE & Lassmann H (2001). Destruction of neurons by cytotoxic T cells in Rasmussen's encephalitis. *J. Neuroimmunol.* **118**: 140 (Abst. 428)
- Beal MF (1995). Aging, energy, and oxidative stress in neurodegenerative diseases. *Ann. Neurol.* **38**:357-66.
- Beebe GW, Kurtzke JF, Kurland LT, Auth TL & Nagler B (1967). Studies on the natural history of multiple sclerosis. 3. Epidemiologic analysis of the army experience in World War II. *Neurology* **17**:1-17.
- Beeton C, Barbaria J, Giraud P, Devaux J, Benoliel AM, Gola M, Sabatier JM, Bernard D, Crest M & Beraud E (2001). Selective blocking of voltage-gated K⁺ channels improves experimental autoimmune encephalomyelitis and inhibits T cell activation. *J Immunol.* **166**:936-44.
- Benveniste H, Drejer J, Schousboe A & Diemer NH (1984). Elevation of the extracellular concentrations of glutamate and aspartate in rat hippocampus during transient cerebral ischemia monitored by intracerebral microdialysis. *J. Neurochem.* **43**:1369-74.
- Berger T, Weerth S, Kojima K, Linington C, Wekerle H & Lassmann H (1997). Experimental autoimmune encephalomyelitis: the antigen specificity of T lymphocytes determines the topography of lesions in the central and peripheral nervous system. *Lab. Invest.* **76**:355-64.
- Bernard A & Khrestchatisky M (1994). Assessing the extent of RNA editing in the TMII regions of GluR5 and GluR6 kainate receptors during rat brain development. *J. Neurochem.* **62**:2057-60.
- Bettler B & Mulle C (1995). Review: neurotransmitter receptors. II. AMPA and kainate receptors. *Neuropharmacology* **34**:123-39.

Bettler B, Boulter J, Hermans-Borgmeyer I, O'Shea-Greenfield A, Deneris ES, Moll C, Borgmeyer U, Hollmann M & Heinemann S (1990). Cloning of a novel glutamate receptor subunit, GluR5: expression in the nervous system during development. *Neuron*, **5**:583-95.

Bettler B, Egebjerg J, Sharma G, Pecht G, Hermans-Borgmeyer I, Moll C, Stevens CF & Heinemann S (1992). Cloning of a putative glutamate receptor: a low affinity kainate-binding subunit. *Neuron*, **8**:257-65.

Bezzi P, Domercq M, Brambilla L, Galli R, Schols D, De Clercq E, Vescovi A, Bagetta G, Kollias G, Meldolesi J & Volterra A (2001). CXCR4-activated astrocyte glutamate release via TNF α : amplification by microglia triggers neurotoxicity. *Nat. Neurosci.* **4**:702-10.

Bhakoo KK & Pearce D (2000). *In vitro* expression of N-acetyl aspartate by oligodendrocytes: implications for proton magnetic resonance spectroscopy signal *in vivo*. *J. Neurochem.* **74**:254-62.

Bigge CF (1999). Ionotropic glutamate receptors. *Current Opinion in Chemical Biology*, **3**:441-7.

Birken DL & Oldendorf WH (1989). N-acetyl-L-aspartic acid: a literature review of a compound prominent in 1H-NMR spectroscopic studies of brain. *Neurosci. Biobehav. Rev.* **13**:23-31.

Bitsch A, Kuhlmann T, Da Costa C, Bunkowski S, Polak T & Bruck W (2000a). Tumour necrosis factor alpha mRNA expression in early multiple sclerosis lesions: correlation with demyelinating activity and oligodendrocyte pathology. *Glia* **29**:366-75.

Bitsch A, Schuchardt J, Bunkowski S, Kuhlmann T & Bruck W (2000b). Acute axonal injury in multiple sclerosis. Correlation with demyelination and inflammation. *Brain* **123**:1174-83.

- Bittigau P, Sifringer M, Pohl D, Stadthaus D, Ishimaru M, Shimizu H, Ikeda M, Lang D, Speer A, Olney JW & Ikonomidou C (1999). Apoptotic neurodegeneration following trauma is markedly enhanced in the immature brain. *Ann. Neurol.* **45**:724-35.
- Bjartmar C & Trapp BD (2001). Axonal and neuronal degeneration in multiple sclerosis: mechanisms and functional consequences. *Curr. Opin. Neurol.* **14**:271-8.
- Bjartmar C, Kidd G, Mork S, Rudick R & Trapp BD (2000). Neurological disability correlates with spinal cord axonal loss and reduced N-acetyl aspartate in chronic multiple sclerosis patients. *Ann. Neurol.* **48**:893-901.
- Bleakman D & Lodge D (1998). Neuropharmacology of AMPA and kainate receptors. *Neuropharmacology* **37**:1187-204.
- Bochet P, Audinat E, Lambolez B, Crepel F, Rossier J, Iino M, Tsuzuki K & Ozawa S (1994). Subunit composition at the single-cell level explains functional properties of a glutamate-gated channel. *Neuron* **12**:383-8.
- Bolton C & Paul C (1997). MK-801 limits neurovascular dysfunction during experimental allergic encephalomyelitis. *J. Pharmacol. Exp. Ther.* **282**:397-402.
- Bolton C, O'Neill JK, Allen SJ & Baker D (1997). Regulation of chronic relapsing experimental allergic encephalomyelitis by endogenous and exogenous glucocorticoids. *Int. Arch. Allergy Immunol.* **114**:74-80.
- Bonfoco E, Krainc D, Ankarcrona M, Nicotera P & Lipton SA (1995). Apoptosis and necrosis: two distinct events induced, respectively, by mild and intense insults with N-methyl-D-aspartate or nitric oxide/superoxide in cortical cell cultures. *Proc. Natl. Acad. Sci. USA* **92**:7162-6
- Boulter J, Hollmann M, O'Shea-Greenfield A, Hartley M, Deneris E, Maron C & Heinemann S (1990). Molecular cloning and functional expression of glutamate receptor subunit genes. *Science*, **249**:1033-7.

- Bowie D, Lange GD & Mayer ML (1998). Activity-dependent modulation of glutamate receptors by polyamines. *J. Neurosci.* **18**:8175-85.
- Bradford HF, Bennett GW & Thomas AJ (1973). Depolarizing stimuli and the release of physiologically active amino acids from suspensions of mammalian synaptosomes. *J Neurochem*, **21**:495-505.
- Bradley WG (1998). Recent views on amyotrophic lateral sclerosis with emphasis on electrophysiological studies. *Muscle Nerve* **10**:490-502.
- Bredesen DE (1995). Neural apoptosis. *Ann. Neurol.* **38**:839-51.
- Brorson JR, Manzillo PA, Gibbons SJ & Miller RJ (1995). AMPA receptor desensitization predicts the selective vulnerability of cerebellar Purkinje cells to excitotoxicity. *J. Neurosci.* **15**:4515-24.
- Brosnan CF, Selmaj K, Raine CS (1988). Hypothesis: A role for tumor necrosis factor in immune-mediated demyelination and its relevance to multiple sclerosis. *J. Neuroimmunol.* **18**:87-94.
- Brown AM, Westenbroek RE, Catterall WA & Ransom BR (2001). Axonal L-type Ca²⁺ channels and anoxic injury in rat CNS white matter. *J. Neurophysiol.* **85**:900-11.
- Brück W, Schmied M, Suchanek G, Bruck Y, Breitschopf H, Poser S, Piddlesden S & Lassmann H (1994). Oligodendrocytes in the early course of multiple sclerosis. *Ann. Neurol.* **35**:65-73.
- Bruijn LI, Becher MW, Lee MK, Anderson KL, Jenkins NA, Copeland NG, Sisodia SS, Rothstein JD, Borchelt DR, Price DL & Cleveland DW (1997). ALS-linked SOD1 mutant G85R mediates damage to astrocytes and promotes rapidly progressive disease with SOD1-containing inclusions. *Neuron* **18**:327-38.
- Brunson KL, Khanna A, Cromwell HC & Cohen RW (2001). Effect of the Noncompetitive NMDA Antagonists MK-801 and Ketamine on the Spastic Han-Wistar Mutant: A Rat Model of Excitotoxicity. *Dev. Neurosci.* **23**:31-40.

-
- Brusa R, Zimmermann F, Koh DS, Feldmeyer D, Gass P, Seeburg PH & Sprengel R (1995). Early-onset epilepsy and postnatal lethality associated with an editing-deficient GluR-B allele in mice. *Science* **270**:1677-80.
- Burnashev N, Monyer H, Seeburg PH & Sakmann B (1992b). Divalent ion permeability of AMPA receptor channels is dominated by the edited form of a single subunit. *Neuron*, **8**:189-98.
- Burnashev N, Schoepfer R, Monyer H, Ruppersberg JP, Gunther W, Seeburg PH & Sakmann B (1992a). Control by asparagine residues of calcium permeability and magnesium blockade in the NMDA receptor. *Science*, **257**:1415-9.
- Burnashev N, Villarroel A & Sakmann B (1996). Dimensions and ion selectivity of recombinant AMPA and kainate receptor channels and their dependence on Q/R site residues. *J Physiol (Lond)*, **496**:165-173.
- Burnashev N, Zhou Z, Neher E & Sakmann B (1995). Fractional calcium currents through recombinant GluR channels of the NMDA, AMPA and kainate receptor types. *J Physiol (Lond)*, **485**:403-18.
- Bursch W, Ellinger A, Gerner C, Frohwein U & Schulte-Hermann R (2000). Programmed cell death (PCD). Apoptosis, autophagic PCD, or others? *Ann. N.Y. Acad. Sci.* **926**:1-12.
- Cammer W, Tansey FA & Brosnan CF (1990). Reactive gliosis in the brains of Lewis rats with experimental allergic encephalomyelitis. *J. Neuroimmunol.* **27**:111-20.
- Carlson NG, Howard J, Gahring LC, Rogers SW (2000). RNA editing (Q/R site) and flop/flip splicing of AMPA receptor transcripts in young and old brains. *Neurobiol. Aging* **21**:599-606.
- Carnegie PR, Dunkley PR, Kemp BE & Murray AW (1974). Phosphorylation of selected serine and threonine residues in MBP by endogenous and exogenous protein kinases. *Nature* **249**:147-50.

-
- Chalk JB, McCombe PA, Smith R & Pender MP (1994). Clinical and histological findings in proteolipid protein-induced experimental autoimmune encephalomyelitis (EAE) in the Lewis rat. Distribution of demyelination differs from that in EAE induced by other antigens. *J. Neurol. Sci.* **123**:154-61.
- Chang L & Karin M (2001). Mammalian MAP kinase signalling cascades. *Nature* **410**:37-40.
- Charcot M (1868). Histologie de la sclerose en plaques. *Gaz. Hosp.* **141**:554-5.
- Charriaut-Marlangue C, Aggoun-Zouaoui D, Represa A & Ben-Ari Y (1996). Apoptotic features of selective neuronal death in ischemia, epilepsy and gp 120 toxicity. *Trends Neurosci.* **19**:109-14.
- Chittajallu R, Braithwaite SP, Clarke VR & Henley JM (1999). Kainate receptors: subunits, synaptic localization and function. *Trends Pharmacol. Sci.* **20**:26-35.
- Choi DW & Rothman SM (1990). The role of glutamate neurotoxicity in hypoxic-ischemic neuronal death. *Annu. Rev. Neurosci.* **13**:171-82.
- Choi DW (1987). Ionic dependence of glutamate neurotoxicity in cortical cell culture. *J Neurosci*, **7**:369-379.
- Choi DW (1988). Calcium-mediated neurotoxicity: relationship to specific channel types and role in ischemic damage. *Trends Neurosci.* **11**:465-9.
- Ciabarra AM, Sullivan JM, Gahn LG, Pecht G, Heinemann S & Sevarino KA (1995). Protein, Nucleotide Cloning and characterization of chi-1: a developmentally regulated member of a novel class of the ionotropic glutamate receptor family. *J Neurosci*, **15**:6498-508.
- Clarke PG (1990). Developmental cell death: morphological diversity and multiple mechanisms. *Anat. Embryol. (Berl)* **181**:195-213.

-
- Clegg A, Bryant J & Milne R (2000). Disease-modifying drugs for multiple sclerosis: a rapid and systematic review. *Health Technol. Assess.* **4**:i-iv, 1-101.
- Cleveland DW & Rothstein JD (2001). From Charcot to Lou Gehrig: Deciphering selective motor neuron death in ALS. *Nat. Rev. Neurosci.* **2**:806-819.
- Cohen RW, Fisher RS, Duong T, Handley VW, Campagnoni AT, Hull CD, Buchwald NA & Levine MS (1991). Altered excitatory amino acid function and morphology of the cerebellum of the spastic Han-Wistar rat. *Brain Res. Mol. Brain Res.* **11**:27-36.
- Colbourne F, Sutherland GR & Auer RN (1999). Electron microscopic evidence against apoptosis as the mechanism of neuronal death in global ischemia. *J. Neurosci.* **19**:4200-10.
- Collingridge GL & Bliss TV (1995). Memories of NMDA receptors and LTP. *Trends Neurosci.* **18**:54-6.
- Collins GG & Buckley KS (1989). Antagonism of monosynaptic excitations in the mouse olfactory cortex slice by 6,7-dinitroquinoxaline-2,3-dione. *Neuropharmacology* **28**:1123-8
- Conn PJ & Pin JP (1997). Pharmacology and functions of metabotropic glutamate receptors. *Annu. Rev. Pharmacol. Toxicol.* **37**:205-37.
- Cooper HM, Parvopassu F, Herbin M & Magnin M (1994). Neuroanatomical pathways linking vision and olfaction in mammals. *Psychoneuroendocrinology* **19**:623-39.
- Corriveau RA, Huh GS & Shatz CJ (1998). Regulation of class I MHC gene expression in the developing and mature CNS by neural activity. *Neuron* **21**:505-520.
- Coyle JT & Schwarcz R (1976). Lesion of striatal neurones with kainic acid provides a model for Huntington's chorea. *Nature* **263**:244-6.
- Croucher MJ, Collins JF & Meldrum BS (1982). Anticonvulsant action of excitatory amino acid antagonists. *Science* **216**:899-901.

- Cruz-Orive LM & Weibel ER (1990). Recent stereological methods for cell biology: a brief survey. *Am. J. Physiol.* **258**:L148-56.
- Cuzner ML & Smith T (1995). Immune responses in the central nervous system in inflammatory demyelinating disease. In: Rothwell NJ. *Immune responses in the nervous system*. 1st Edition, Bios Scientific Publishers. 117-42.
- Cuzner ML, Hayes GM, Newcombe J & Woodroffe MN (1988). The nature of inflammatory components during demyelination in multiple sclerosis. *J. Neuroimmunol.* **20**:203-9.
- Dal Canto MC & Lipton HL (1980). Schwann cell remyelination and recurrent demyelination in the central nervous system of mice infected with attenuated Theiler's virus. *Am. J. Pathol.* **98**:101-22.
- Dalmau J, Gultekin HS & Posner JB (1999). Paraneoplastic neurologic syndromes: pathogenesis and physiopathology. *Brain Pathol.* **9**:275-84.
- Das S, Sasaki YF, Rothe T, Premkumar LS, Takasu M, Crandall JE, Dikkes P, Conner DA, Rayudu PV, Cheung W, Chen HS, Lipton SA & Nakanishi N. (1998) Increased NMDA current and spine density in mice lacking the NMDA receptor subunit NR3A. *Nature*, **393**:377-81.
- Davie CA, Hawkins CP, Barker GJ, Brennan A, Tofts PS, Miller DH & McDonald WI (1994). Serial proton magnetic resonance spectroscopy in acute multiple sclerosis lesions. *Brain* **117**:49-58.
- Davie CA, Silver NC, Barker GJ, Tofts PS, Thompson AJ, McDonald WI & Miller DH (1999). Does the extent of axonal loss and demyelination from chronic lesions in multiple sclerosis correlate with the clinical subgroup? *J. Neurol. Neurosurg. Psychiatry* **67**:710-5.
- De Groot CJ & Woodroffe MN (2001). The role of chemokines and chemokine receptors in CNS inflammation. *Prog. Brain Res.* **132**:533-44.

-
- Deckner M-L, Risling M & Frisén J (1997). Apoptotic death of olfactory sensory neurons in the adult rat. *Exp. Neurol.* **143**:132-40.
- DiFiglia M (1990). Excitotoxic injury of the neostriatum: a model for Huntington's disease. *Trends Neurosci.* **13**:286-9.
- Dikranian K, Ishimaru MJ, Tenkova T, Labruyere J, Qin YQ, Ikonomidou C & Olney JW (2001). Apoptosis in the *in vivo* mammalian forebrain. *Neurobiol. Dis.* **8**:359-79.
- Dingledine R, Borges K, Bowie D & Traynelis SF (1999). The glutamate receptor ion channels. *Pharmacol Revs.* **51**:7-61.
- Dunkley PR & Carnegie PR (1974). Amino acid sequence of the smaller basic protein from rat brain myelin. *Biochem. J.* **141**:243-55.
- Duvoisin RM, Zhang C & Ramonell K (1995). A novel metabotropic glutamate receptor expressed in the retina and olfactory bulb. *J. Neurosci.* **15**:3075-83.
- Ebers GC (1984). Oligoclonal banding in MS. *Ann. NY Acad. Sci.* **436**:206-12.
- Egebjerg J & Heinemann SF (1993). Ca²⁺ permeability of unedited and edited versions of the kainate selective glutamate receptor GluR6. *Proc. Natl. Acad. Sci. USA.* **90**:755-9.
- Egebjerg J, Bettler B, Hermans-Borgmeyer I & Heinemann S (1991). Cloning of a cDNA for a glutamate receptor subunit activated by kainate but not AMPA. *Nature*, **351**:745-8.
- European Study Group on interferon beta-1b in secondary progressive MS (1998). Placebo-controlled multicentre randomised trial of interferon beta-1b in treatment of secondary progressive multiple sclerosis. *Lancet* **352**:1491-7.
- Evangelou N, Esiri MM, Smith S, Palace J & Matthews PM (2000). Quantitative pathological evidence for axonal loss in normal appearing white matter in multiple sclerosis. *Ann. Neurol.* **47**:391-5.

Faden AI & Simon RP (1988). A potential role for excitotoxins in the pathophysiology of spinal cord injury. *Ann. Neurol.* **23**:623-6.

Faden AI, Demediuk P, Panter SS & Vink R (1989). The role of excitatory amino acids and NMDA receptors in traumatic brain injury. *Science* **244**:798-800.

Fazakerley JK, Khalili-Shirazi A & Webb HE (1988). Semliki Forest virus (A7[74]) infection of adult mice induces an immune-mediated demyelinating encephalomyelitis. *Ann. N Y Acad. Sci.* **540**:672-3.

Fazekas F, Deisenhammer F, Strasser-Fuchs S, Nahler G & Mamoli B (1997). Randomised placebo-controlled trial of monthly intravenous immunoglobulin therapy in relapsing-remitting multiple sclerosis. Austrian Immunoglobulin in Multiple Sclerosis Study Group. *Lancet* **349**:589-93.

Feldmeyer D, Kask K, Brusa R, Kornau HC, Kolhekar R, Rozov A, Burnashev N, Jensen V, Hvalby O, Sprengel R & Seeburg PH (1999). Neurological dysfunctions in mice expressing different levels of the Q/R site-unedited AMPAR subunit GluR-B. *Nat. Neurosci.* **2**:57-64.

Ferguson B, Matyszak MK, Esiri MM & Perry VH (1997). Axonal damage in acute multiple sclerosis lesions. *Brain* **120**:393-9.

Fernandes-Alnemri T, Litwack G & Alnemri ES (1994). CPP32, a novel human apoptotic protein with homology to *Caenorhabditis elegans* cell death protein Ced-3 and mammalian interleukin-1 beta-converting enzyme. *J. Biol. Chem.* **269**:30761-4.

Fine SM, Angel RA, Perry SW, Epstein LG, Rothstein JD, Dewhurst S & Gelbard HA (1996). Tumor necrosis factor alpha inhibits glutamate uptake by primary human astrocytes. Implications for pathogenesis of HIV-1 dementia. *J. Biol. Chem.* **271**:15303-6.

Flanagan EM, Erickson JB, Viveros OH, Chang SY & Reinhard JF Jr (1995). Neurotoxin quinolinic acid is selectively elevated in spinal cords of rats with experimental allergic encephalomyelitis. *J. Neurochem.* **64**:1192-6.

- Flugel A, Berkowicz T, Ritter T, Labeur M, Jenne DE, Li Z, Ellwart JW, Willem M, Lassmann H & Wekerle H (2001). Migratory activity and functional changes of green fluorescent effector cells before and during experimental autoimmune encephalomyelitis. *Immunity* **14**:547-60.
- Flugel A, Schwaiger FW, Neumann H, Medana I, Willem M, Wekerle H, Kreutzberg GW & Graeber MB (2000). Neuronal FasL induces cell death of encephalitogenic T lymphocytes. *Brain Pathol.* **10**:353-64.
- Flugel A, Willem M, Berkowicz T & Wekerle H (1999). Gene transfer into CD4⁺ T lymphocytes: green fluorescent protein-engineered, encephalitogenic T cells illuminate brain autoimmune responses. *Nat. Med.* **5**:843-7.
- Fray AE, Ince PG, Banner SJ, Milton ID, Usher PA, Cookson MR & Shaw PJ (1998). The expression of the glial glutamate transporter protein EAAT2 in motor neuron disease: an immunohistochemical study. *Eur. J. Neurosci.* **10**:2481-9.
- Fu L, Matthews PM, De Stefano N, Worsley KJ, Narayanan S, Francis GS, Antel JP, Wolfson C & Arnold DL (1998). Imaging axonal damage of normal-appearing white matter in multiple sclerosis. *Brain* **121**:103-13.
- Gähring LC, Rogers SW & Twyman RE (1997). Autoantibodies to glutamate receptor subunit GluR2 in nonfamilial olivopontocerebellar degeneration. *Neurology* **48**:494-500.
- Gähring LC, Twyman RE, Greenlee JE & Rogers SW (1995). Autoantibodies to neuronal glutamate receptors in patients with paraneoplastic neurodegenerative syndrome enhance receptor activation. *Mol. Med.* **1**:245-53.
- Geiger JR, Melcher T, Koh DS, Sakmann B, Seeburg PH, Jonas P & Monyer H (1995). Relative abundance of subunit mRNAs determines gating and Ca²⁺ permeability of AMPA receptors in principal neurons and interneurons in rat CNS. *Neuron* **15**:193-204.
- Genain CP, Cannella B, Hauser SL & Raine CS (1999). Identification of autoantibodies associated with myelin damage in multiple sclerosis. *Nat. Med.* **5**:170-5.

- Glees & Marsland (1954). *J. Neuropath. Exp. Neurol.* **13**:587.
- Gold R, Buttgerit F & Toyka KV (2001). Mechanism of action of glucocorticosteroid hormones: possible implications for therapy of neuroimmunological disorders. *J. Neuroimmunol.* **117**:1-8.
- Gold R, Hartung HP & Toyka KV (2000). Animal models for autoimmune demyelinating disorders of the nervous system. *Mol. Med. Today* **6**:88-91.
- Gong C, Berent A, Golovoy D, Slusher B & Russell JW (2000). Inhibition of NAALADase protects neurons against glucose-induced programmed cell death in models of diabetic neuropathy. *Soc. Neurosci. Abst.* **26**:Poster 227.20.
- Goto K, Ishige A, Sekiguchi K, Iizuka S, Sugimoto A, Yuzurihara M, Aburada M, Hosoya E & Kogure K (1990). Effects of cycloheximide on delayed neuronal death in rat hippocampus. *Brain Res.* **534**:299-302.
- Greenamyre JT & Porter RH (1994). Anatomy and physiology of glutamate in the CNS. *Neurology* **44**:S7-13.
- Greenamyre JT & Young AB (1989). Excitatory amino acids and Alzheimer's disease. *Neurobiol. Aging* **10**:593-602.
- Greengard P, Jen J, Nairn AC & Stevens CF (1991). Enhancement of the glutamate response by cAMP-dependent protein kinase in hippocampal neurons. *Science*, **253**:1135-8.
- Han Y, He T, Huang D, Pardo CA & Ransohoff RM (2001). TNF- α mediates SDF-1 α -induced NF- κ B activation and cytotoxic effects in primary astrocytes. *J. Clin. Invest.* **108**:425-435.
- Hardin-Pouzet H, Krakowski M, Bourbonniere L, Didier-Bazes M, Tran E & Owens T (1997). Glutamate metabolism is down-regulated in astrocytes during experimental allergic encephalomyelitis. *Glia* **20**:79-85.

- Hayahsi T (1954). Effects of sodium glutamate on the nervous system. *Keio J Med*, **3**:183-92.
- Hayashi T, Umemori H, Mishina M & Yamamoto T (1999). The AMPA receptor interacts with and signals through the protein tyrosine kinase Lyn. *Nature* **397**:72-6.
- Haydon PG (2001). GLIA: listening and talking to the synapse. *Nat. Rev. Neurosci.* **2**:185-93.
- Hayward MD & Morgan JI (1995). The olfactory system as a model for the analysis of the contribution of gene expression to programmed cell death. *Chem. Senses* **20**:261-9.
- He XP, Patel M, Whitney KD, Janumpalli S, Tenner A & McNamara JO (1998). Glutamate receptor GluR3 antibodies and death of cortical cells. *Neuron* **20**:153-63.
- Headley PM & Grillner S (1990). Excitatory amino acids and synaptic transmission: the evidence for a physiological function. *Trends Pharmacol. Sci.* **11**:205-11.
- Hengartner MO (2000). The biochemistry of apoptosis. *Nature* **407**:770-6.
- Henson PM, Bratton DL & Fadok VA (2001). Apoptotic cell removal. *Curr. Biol.* **11**:R795-805.
- Herb A, Burnashev N, Werner P, Sakmann B, Wisden W & Seeburg PH (1992). The KA-2 subunit of excitatory amino acid receptors shows widespread expression in brain and forms ion channels with distantly related subunits. *Neuron*, **8**:775-85.
- Hermann GE, Rogers RC, Bresnahan JC & Beattie MS (2001). Tumor necrosis factor-alpha induces cFOS and strongly potentiates glutamate-mediated cell death in the rat spinal cord. *Neurobiol. Dis.* **8**:590-9.
- Higuchi M, Maas S, Single FN, Hartner J, Rozov A, Burnashev N, Feldmeyer D, Sprengel R & Seeburg PH (2000). Point mutation in an AMPA receptor gene rescues lethality in mice deficient in the RNA-editing enzyme ADAR2. *Nature* **406**:78-81.

-
- Hollmann M & Heinemann S (1994). Cloned glutamate receptors. *Annu Rev Neurosci*, **17**:31-108.
- Hollmann M, Hartley M & Heinemann S (1991). Ca^{2+} permeability of KA-AMPA-gated glutamate receptor channels depends on subunit composition. *Science*, **252**:851-3.
- Hollmann M, O'Shea-Greenfield A, Rogers SW & Heinemann S (1989). Cloning by functional expression of a member of the glutamate receptor family. *Nature*, **342**:643-8.
- Honegger CG, Krenger W & Langemann H (1989). Changes in amino acid contents in the spinal cord and brainstem of rats with experimental autoimmune encephalomyelitis. *J. Neurochem.* **53**:423-7.
- Houamed KM, Kuijper JL, Gilbert TL, Haldeman BA, O'Hara PJ, Mulvihill ER, Almers W & Hagen FS (1991). Cloning, expression, and gene structure of a G protein-coupled glutamate receptor from rat brain. *Science*, **252**:1318-21.
- Hughes D, Raine CS & Field EJ (1968). Invasion of neurones *in vitro* by non immune lymphocytes. An electron microscopic study. *Br. J. Exp. Pathol.* **49**:356-9.
- Hugon J, Vallat JM, Spencer PS, Leboutet MJ & Barthe D (1989). Kainic acid induces early and delayed degenerative neuronal changes in rat spinal cord. *Neurosci. Lett.* **104**:258-62.
- Huitinga I, van Rooijen N, de Groot CJ, Uitdehaag BM & Dijkstra CD (1990). Suppression of experimental allergic encephalomyelitis in Lewis rats after elimination of macrophages. *J. Exp. Med.* **172**:1025-33.
- Humble JG, Jayne WHW & Pulvertaft RJV (1956). Biological interaction between lymphocytes and other cells. *Br. J. Haemat.* **2**:183-8.
- Hume RI, Dingledine R & Heinemann SF (1991). Identification of a site in glutamate receptor subunits that controls calcium permeability. *Science*, **253**:1028-31.

-
- Ikeda K, Nagasawa M, Mori H, Araki K, Sakimura K, Watanabe M, Inoue Y & Mishina M. (1992). Cloning and expression of the epsilon 4 subunit of the NMDA receptor channel. *FEBS Lett*, **313**:34-8.
- Ikonomidou C & Turski L (1996). Prevention of trauma-induced neurodegeneration in infant and adult rat brain: glutamate antagonists. *Metab. Brain Dis.* **11**:125-41.
- Ikonomidou C & Turski L (1997). Pharmacology of the AMPA antagonist 2,3-dihydroxy-6-nitro-7-sulfamoylbenzo-(F)-quinoxaline. *Ann. N. Y. Acad. Sci.* **825**:394-402.
- Ikonomidou C, Bosch F, Miksa M, Bittigau P, Vockler J, Dikranian K, Tenkova TI, Stefovskaja V, Turski L & Olney JW (1999). Blockade of NMDA receptors and apoptotic neurodegeneration in the developing brain. *Science* **283**:70-4.
- Ikonomidou C, Qin Qin Y, Labruyere J & Olney JW (1996). Motor neuron degeneration induced by excitotoxin agonists has features in common with those seen in the SOD-1 transgenic mouse model of amyotrophic lateral sclerosis. *J. Neuropathol. Exp. Neurol.* **55**:211-224.
- Ince P, Stout N, Shaw P, Slade J, Hunziker W, Heizmann CW & Baimbridge KG (1993). Parvalbumin and calbindin D-28k in the human motor system and in motor neuron disease. *Neuropathol. Appl. Neurobiol.* **19**:291-9.
- Jahr CE & Stevens CF (1990a). A quantitative description of NMDA receptor-channel kinetic behavior. *J Neurosci*, **10**:1830-7.
- Jahr CE & Stevens CF (1990b). Voltage dependence of NMDA-activated macroscopic conductances predicted by single-channel kinetics. *J Neurosci*, **10**:3178-82.
- Jarrard LE & Meldrum BS (1993). Selective excitotoxic pathology in the rat hippocampus. *Neuropathol. Appl. Neurobiol.* **19**:381-9.

Johnson KP, Brooks BR, Cohen JA, Ford CC, Goldstein J, Lisak RP, Myers LW, Panitch HS, Rose JW & Schiffer RB (1995). Copolymer 1 reduces relapse rate and improves disability in relapsing-remitting multiple sclerosis: results of a phase III multicenter, double-blind placebo-controlled trial. The Copolymer 1 Multiple Sclerosis Study Group. *Neurology* **45**:1268-76.

Jonas P, Racca C, Sakmann B, Seeburg PH & Monyer H (1994). Differences in Ca²⁺ permeability of AMPA-type glutamate receptor channels in neocortical neurons caused by differential GluR-B subunit expression. *Neuron* **12**:1281-9.

Kamboj RK, Schoepp DD, Nutt S, Shekter L, Korczak B, True RA, Zimmerman DM & Wosnick MA (1992). Molecular structure and pharmacological characterization of humEAA2, a novel human kainate receptor subunit. *Mol. Pharmacol.* **42**:10-5.

Kamboj SK, Swanson GT & Cull-Candy SG (1995). Intracellular spermine confers rectification on rat calcium-permeable AMPA and kainate receptors. *J. Physiol.* **486**:297-303.

Keinänen K, Wisden W, Sommer B, Werner P, Herb A, Verdoorn TA, Sakmann B & Seeburg PH (1990). A family of AMPA-selective glutamate receptors. *Science*, **249**:556-60.

Kerlero de Rosbo N, Bernard CC, Simmons RD & Carnegie PR (1985). Concomitant detection of changes in MBP and permeability of blood-spinal cord barrier in acute experimental autoimmune encephalomyelitis by electroimmunoblotting. *J. Neuroimmunol.* **9**:349-61.

Kerlero de Rosbo N, Milo R, Lees MB, Burger D, Bernard CC & Ben-Nun A (1993). Reactivity to myelin antigens in multiple sclerosis. Peripheral blood lymphocytes respond predominantly to myelin oligodendrocyte glycoprotein. *J. Clin. Invest.* **92**:2602-8.

Kerr JF, Wyllie AH & Currie AR (1972). Apoptosis: a basic biological phenomenon with wide-ranging implications in tissue kinetics. *Br. J. Cancer* **26**:239-57.

- Kieseier BC, Storch MK & Hartung HP (2000). Toxic effector molecules in the pathogenesis of immune-mediated disorders of the central nervous system. *J. Neural Transm. Suppl* **59**:69-80.
- Kleckner NW & Dingledine R (1988). Requirement for glycine in activation of NMDA-receptors expressed in *Xenopus* oocytes. *Science*, **241**:835-7.
- Klivenyi P, Kekesi K, Juhasz G & Vecsei L (1997). Amino acid concentrations in cerebrospinal fluid of patients with multiple sclerosis. *Acta. Neurol. Scand.* **95**:96-8.
- Koenig H, Trout JJ, Goldstone AD & Lu CY (1992). Capillary NMDA receptors regulate blood-brain barrier function and breakdown. *Brain Res.* **588**: 297-303.
- Koh JY & Choi DW (1988). Zinc alters excitatory amino acid neurotoxicity on cortical neurons. *J Neurosci*, **8**:2164-71.
- Köhler M, Burnashev N, Sakmann B & Seeburg PH (1993). Determinants of Ca²⁺ permeability in both TM1 and TM2 of high affinity kainate receptor channels: diversity by RNA editing. *Neuron*, **10**:491-500.
- Kojima K, Wekerle H, Lassmann H, Berger T & Linington C (1997). Induction of experimental autoimmune encephalomyelitis by CD4⁺ T cells specific for an astrocyte protein, S100 beta. *J. Neural. Transm. Suppl.* **49**:43-51.
- Kornek B, Storch MK, Bauer J, Djamshidian A, Weissert R, Wallstroem E, Stefferl A, Zimprich F, Olsson T, Linington C, Schmidbauer M & Lassmann H (2001). Distribution of a calcium channel subunit in dystrophic axons in multiple sclerosis and experimental autoimmune encephalomyelitis. *Brain* **124**:1114-24.
- Kreutzberg GW, Blakemore WF & Graeber MB (1997). Cellular pathology of the central nervous system. In: Graham DI & Lantos PL. *Greenfield's Neuropathology*. 6th Edition, Arnold. **Vol. 1**:85-156.

Kuner R, Groom A, Bresink I, Müller G, Kornau H-C, Sprengel R, Ikonomidou C, Catania MV, Seeburg P & Turski L. Motoneuron disease in mice with extended Q/R site editing of AMPA receptor subunit GluR-B. *In preparation*.

Kurtzke JF & Hyllested K (1987). Multiple sclerosis in the Faroe Islands. III. An alternative assessment of the three epidemics. *Acta Neurol. Scand.* **76**:317-39.

Kurtzke JF (1997). The epidemiology of Multiple Sclerosis. In: Raine CS, McFarland HF & Tourtellotte WW. *Multiple Sclerosis: Clinical and pathogenetic basis*. 1st Edition, Chapman & Hall. 91-139.

Kurtzke JF, Beebe GW & Norman JE (1979). Epidemiology of multiple sclerosis in U.S. veterans: 1. Race, sex, and geographic distribution. *Neurology* **29**:1228-35.

Kutsuwada T, Kashiwabuchi N, Mori H, Sakimura K, Kushiya E, Araki K, Meguro H, Masaki H, Kumanishi T, Arakawa M, *et al.* (1992). Molecular diversity of the NMDA receptor channel. *Nature*, **358**:36-41.

Kwak S & Nakamura R (1995). Acute and late neurotoxicity in the rat spinal cord *in vivo* induced by glutamate receptor agonists. *J. Neurol. Sci.* **129 Suppl**:99-103.

Lassmann H & Bauer J (2001). Cytotoxic T-lymphocytes in human inflammatory brain diseases. *J. Neuroimmunol.* **118**:7 (Abst. IS13)

Lassmann H (1998). Pathology of multiple sclerosis. In: Compston A, Ebers G, Lassmann H, McDonald I, Matthews B, Wekerle H. *McAlpine's Multiple Sclerosis*, 3rd Edition. Churchill Livingstone, 323-58.

Launes J, Siren J, Viinikka L, Hokkanen L & Lindsberg PJ (1998). Does glutamate mediate brain damage in acute encephalitis? *Neuroreport* **9**:577-81.

Lee MA, Blamire AM, Pendlebury S, Ho KH, Mills KR, Styles P, Palace J & Matthews PM (2000). Axonal injury or loss in the internal capsule and motor impairment in multiple sclerosis. *Arch. Neurol.* **57**:65-70.

- Leigh PN & Meldrum BS (1996). Excitotoxicity in ALS. *Neurology* **47**:S221-7.
- Leist M, Single B, Castoldi AF, Kuhnle S & Nicotera P (1997). Intracellular adenosine triphosphate (ATP) concentration: a switch in the decision between apoptosis and necrosis. *J. Exp. Med.* **185**:1481-6.
- Li S & Stys PK (2000). Mechanisms of ionotropic glutamate receptor-mediated excitotoxicity in isolated spinal cord white matter. *J. Neurosci.* **20**:1190-8.
- Li Y, Sharov VG, Jiang N, Zaloga C, Sabbah HN & Chopp M (1995). Ultrastructural and light microscopic evidence of apoptosis after middle cerebral artery occlusion in the rat. *Am. J. Pathol.* **146**:1045-51.
- Lin TY, Wang SM, Fu WM, Chen YH & Yin HS (1999). Toxicity of tunicamycin to cultured brain neurons: ultrastructure of the degenerating neurons. *J. Cell Biochem.* **74**:638-47.
- Linda H, Hammarberg H, Piehl F, Khademi M & Olsson T (1999). Expression of MHC class I heavy chain and beta2-microglobulin in rat brainstem motoneurons and nigral dopaminergic neurons. *J. Neuroimmunol.* **101**:76-86.
- Linington C, Berger T, Perry L, Weerth S, Hinze Selch D, Zhang Y, Lu HC, Lassmann H & Wekerle H (1993). T cells specific for the myelin oligodendrocyte glycoprotein mediate an unusual autoimmune inflammatory response in the central nervous system. *Eur. J. Immunol.* **23**:1364-72.
- Linington C, Bradl M, Lassmann H, Brunner C & Vass K (1988). Augmentation of demyelination in rat acute allergic encephalomyelitis by circulating mouse monoclonal antibodies directed against a myelin/oligodendrocyte glycoprotein. *Am. J. Pathol.* **130**:443-54.
- Linington C, Morgan BP, Scolding NJ, Wilkins P, Piddlesden S & Compston DA (1989). The role of complement in the pathogenesis of experimental allergic encephalomyelitis. *Brain* **112**:895-911.

- Liposits Z, Kallo I, Hrabovszky E & Gallyas F (1997). Ultrastructural pathology of degenerating "dark" granule cells in the hippocampal dentate gyrus of adrenalectomized rats. *Acta. Biol. Hung.* **48**:173-87.
- Lloyd KG (1977). CNS compensation to dopamine neuron loss in Parkinson's disease. *Adv. Exp. Med. Biol.* **90**:255-66.
- Losseff NA & Miller DH (1998). Measures of brain and spinal cord atrophy in multiple sclerosis. *J. Neurol. Neurosurg. Psychiatry* **64 Suppl 1**:S102-5
- Lowe J, Lennox G & Leigh PN (1997). Disorders of movement and system degenerations. In: Graham DI & Lantos PL. *Greenfield's Neuropathology*. 6th Edition, Arnold. **Vol. 2**:281-366.
- Lucas DR & Newhouse JP (1957). The toxic effect of sodium L-glutamate on the inner layers of the retina. *AMA Arch Ophthalmol*, **58**:193-201.
- Ludolph AC, Meyer T & Riepe MW (2000). The role of excitotoxicity in ALS – What is the evidence? *J. Neurol.* **247**:17-16.
- Ludwin SK (1979). The perineuronal satellite oligodendrocyte. A role in remyelination. *Acta Neuropathol. (Berl)* **47**:49-53.
- Ludwin SK (1984). The function of perineuronal satellite oligodendrocytes: an immunohistochemical study. *Neuropathol. Appl. Neurobiol.* **10**:143-9.
- MacPhee IA, Antoni FA & Mason DW (1989). Spontaneous recovery of rats from experimental allergic encephalomyelitis is dependent on regulation of the immune system by endogenous adrenal corticosteroids. *J. Exp. Med.* **169**:431-45.
- Magnuson DS, Trinder TC, Zhang YP, Burke D, Morassutti DJ & Shields CB (1999). Comparing deficits following excitotoxic and contusion injuries in the thoracic and lumbar spinal cord of the adult rat. *Exp. Neurol.* **156**:191-204.

- Majno G & Joris I (1995). Apoptosis, oncosis, and necrosis. An overview of cell death. *Am. J. Pathol.* **146**:3-15.
- Maragos WF, Greenamyre JT, Penney JB & Young AB (1987). Glutamate dysfunction in Alzheimer's disease: A hypothesis. *Trends Neurosci.* **10**:65-8.
- Margulies JE, Cohen RW, Levine MS & Watson JB (1993). Decreased GluR2(B) receptor subunit mRNA expression in cerebellar neurons at risk for degeneration. *Dev. Neurosci.* **15**:110-20.
- Mason D, MacPhee I & Antoni F (1990). The role of the neuroendocrine system in determining genetic susceptibility to experimental allergic encephalomyelitis in the rat. *Immunology* **70**:1-5.
- Masu M, Tanabe Y, Tsuchida K, Shigemoto R & Nakanishi S (1991). Sequence and expression of a metabotropic glutamate receptor. *Nature*, **349**:760-5.
- Matthews PM (1999). Axonal loss and demyelination in multiple sclerosis. *J. Neurol. Neurosurg. Psychiatry* **67**:708-9.
- Matute C (1998). Characteristics of acute and chronic kainate excitotoxic damage to the optic nerve. *Proc. Natl. Acad. Sci. USA.* **95**:10229-34.
- Matute C, Sanchez-Gomez MV, Martinez-Millan L & Miledi R (1997). Glutamate receptor-mediated toxicity in optic nerve oligodendrocytes. *Proc. Natl. Acad. Sci. USA* **94**:8830-5.
- Mayer ML, Westbrook GL & Guthrie PB (1984). Voltage-dependent block by Mg^{2+} of NMDA responses in spinal cord neurones. *Nature*, **309**:261-3.
- McDonald JW, Althomsons SP, Hyrc KL, Choi DW & Goldberg MP (1998). Oligodendrocytes from forebrain are highly vulnerable to AMPA/kainate receptor-mediated excitotoxicity. *Nat. Med.* **4**:291-7.

- McFarland HF, Martin R & McFarlin (1997). Genetic influences in multiple sclerosis. In: Raine CS, McFarland HF & Tourtellotte WW. *Multiple Sclerosis: Clinical and pathogenetic basis*. 1st Edition, Chapman & Hall. 205-19.
- McGlade-McCulloh E, Yamamoto H, Tan SE, Brickey DA, Soderling TR (1993). Phosphorylation and regulation of glutamate receptors by calcium/calmodulin-dependent protein kinase II. *Nature*. **362**:640-2.
- Medana I, Martinic MA, Wekerle H & Neumann H (2001). Transection of major histocompatibility complex class I-induced neurites by cytotoxic T lymphocytes. *Am. J. Pathol.* **159**:809-15.
- Meguro H, Mori H, Araki K, Kushiya E, Kutsuwada T, Yamazaki M, Kumanishi T, Arakawa M, Sakimura K & Mishina M (1992). Functional characterization of a heteromeric NMDA receptor channel expressed from cloned cDNAs. *Nature*, **357**:70-4.
- Meldrum B (1993). Amino acids as dietary excitotoxins: a contribution to understanding neurodegenerative disorders. *Brain Res. Rev.* **18**:293-314.
- Millefiorini E, Gasperini C, Pozzilli C, D'Andrea F, Bastianello S, Trojano M, Morino S, Morra VB, Bozzao A, Calo' A, Bernini ML, Gambi D & Prencipe M (1997). Randomized placebo-controlled trial of mitoxantrone in relapsing-remitting multiple sclerosis: 24-month clinical and MRI outcome. *J. Neurol.* **244**:153-9.
- Mix E, Correale J, Olsson T, Solders G & Link H (1992). Calcium antagonists suppress experimental allergic neuritis (EAN). *J. Autoimmun.* **5**:69-82.
- Momiyama A, Feldmeyer D & Cull-Candy SG (1996). Identification of a native low-conductance NMDA channel with reduced sensitivity to Mg²⁺ in rat central neurones. *J. Physiol (Lond)*, **494**:479-92.
- Monyer H, Sprengel R, Schoepfer R, Herb A, Higuchi M, Lomeli H, Burnashev N, Sakmann B & Seeburg PH (1992). Heteromeric NMDA receptors: molecular and functional distinction of subtypes. *Science*, **256**:1217-21.

- Mori H, Masaki H, Yamakura T & Mishina M (1992). Identification by mutagenesis of a Mg^{2+} -block site of the NMDA receptor channel. *Nature*, **358**:673-5.
- Moriyoshi K, Masu M, Ishii T, Shigemoto R, Mizuno N & Nakanishi S. (1991). Molecular cloning and characterization of the rat NMDA receptor. *Nature*, **354**:31-7.
- Mothet J-P, Parent AT, Wolosker H, Brady RO, Linden DJ, Ferris CD, Rogawski MA & Snyder SH (2000). D-Serine is an endogenous ligand for the glycine site of the N-methyl-D-aspartate receptor. *Proc. Natl. Acad. Sci. USA*, **97**:4926-4931.
- Müller G, Endermann U, Bresink I and Turski L (1998). Glutamate in neurodegenerative disorders: Phenotype resulting from decreased expression of GluR-B subunit mRNA in rats. In: Seeburg PH, Turski L & Bresink I. *Excitatory amino acids: From genes to therapy*. Springer Verlag. 109-126.
- Nakajima Y, Iwakabe H, Akazawa C, Nawa H, Shigemoto R, Mizuno N & Nakanishi S (1993). Molecular characterization of a novel retinal metabotropic glutamate receptor mGluR6 with a high agonist selectivity for L-2-amino-4-phosphonobutyrate. *J. Biol. Chem.* **268**:11868-73.
- Nakanishi S (1992). Molecular diversity of glutamate receptors and implications for brain function. *Science* **258**:597-603.
- Nakanishi N, Shneider NA & Axel R (1990). A family of glutamate receptor genes: evidence for the formation of heteromultimeric receptors with distinct channel properties. *Neuron*, **5**:569-81.
- Neumann H, Cavalié A, Jenne DE & Wekerle H (1995). Induction of MHC class I genes in neurons. *Science* **269**:549-552.
- Neusch C, Rozengurt N, Jacobs RE, Lester HA & Kofuji P (2001). Kir4.1 potassium channel subunit is crucial for oligodendrocyte development and *in vivo* myelination. *J. Neurosci.* **21**:5429-38.

- Nicoletti F, Bruno V, Copani A, Casabona G & Knopfel T (1996). Metabotropic glutamate receptors: a new target for the therapy of neurodegenerative disorders? *Trends Neurosci.* **19**:267-71.
- Nicotera P, Ankarcrona M, Bonfoco E, Orrenius S & Lipton SA (1997). Neuronal necrosis and apoptosis: two distinct events induced by exposure to glutamate or oxidative stress. *Adv. Neurol.* **72**:95-101.
- Nikam SS & Kornberg BE (2001). AMPA receptor antagonists. *Curr. Med. Chem.* **8**:155-70.
- Ninan PT (1999). The functional anatomy, neurochemistry, and pharmacology of anxiety. *J. Clin. Psychiatry* **60 Suppl 22**:12-7.
- Nishi M, Hinds H, Lu HP, Kawata M & Hayashi Y (2001). Motoneuron-Specific Expression of NR3B, a Novel NMDA-Type Glutamate Receptor Subunit That Works in a Dominant-Negative Manner. *J. Neurosci.* **21**:RC185.
- Nisim AA, Hernandez CM & Cohen RW (1999). The neuroprotective effects of non-NMDA antagonists in the cerebellum of the spastic Han Wistar mutant. *Dev. Neurosci.* **21**:76-86.
- Nitatori T, Sato N, Waguri S, Karasawa Y, Araki H, Shibanaï K, Kominami E & Uchiyama Y (1995). Delayed neuronal death in the CA1 pyramidal cell layer of the gerbil hippocampus following transient ischemia is apoptosis. *J. Neurosci.* **15**:1001-11.
- Noda M, Nakanishi H, Nabekura J & Akaike N (2000). AMPA-kainate subtypes of glutamate receptor in rat cerebral microglia. *J. Neurosci.* **20**:251-8.
- Nowak L, Bregestovski P, Ascher P, Herbert A & Prochiantz A (1984). Magnesium gates glutamate-activated channels in mouse central neurones. *Nature*, **307**:462-5.
- Okamoto N, Hori S, Akazawa C, Hayashi Y, Shigemoto R, Mizuno N & Nakanishi S (1994). Molecular characterization of a new metabotropic glutamate receptor mGluR7 coupled to inhibitory cyclic AMP signal transduction. *J. Biol. Chem.* **269**:1231-6.

- Olney JW (1969a). Glutamate-induced retinal degeneration in neonatal mice. Electron microscopy of the acutely evolving lesion. *J Neuropathol Exp Neurol*, **28**:455-474.
- Olney JW (1969b). Brain lesions, obesity and other disturbances in mice treated with monosodium glutamate. *Science*, **164**:719-721.
- Olney JW (1971). Glutamate-induced neuronal necrosis in the infant mouse hypothalamus. An electron microscopic study. *J. Neuropathol. Exp. Neurol.* **30**:75-90.
- Olney JW, Ho OL & Rhee V (1971). Cytotoxic effects of acidic and sulphur containing amino acids on the infant mouse central nervous system. *Exp Brain Res*, **14**:61-76.
- Ozawa K, Suchanek G, Breitschopf H, Bruck W, Budka H, Jellinger K & Lassmann H (1994). Patterns of oligodendroglia pathology in multiple sclerosis. *Brain* **117**:1311-22.
- Pang Z & Geddes JW (1997). Mechanisms of cell death induced by the mitochondrial toxin 3-nitropropionic acid: acute excitotoxic necrosis and delayed apoptosis. *J. Neurosci.* **17**:3064-73.
- Paolillo A, Coles AJ, Molyneux PD, Gawne-Cain M, MacManus D, Barker GJ, Compston DA & Miller DH (1999). Quantitative MRI in patients with secondary progressive MS treated with monoclonal antibody Campath 1H. *Neurology* **53**:751-7.
- Parpura V, Basarsky TA, Liu F, Jefinija K, Jefinija S & Haydon PG (1994). Glutamate-mediated astrocyte-neuron signalling. *Nature* **369**:744-7.
- Paschen W, Dux E & Djuricic B (1994). Developmental changes in the extent of RNA editing of glutamate receptor subunit GluR5 in rat brain. *Neurosci. Lett.* **174**:109-12.
- Paschen W, Schmitt J, Dux E & Djuricic B (1995). Temporal analysis of the upregulation of GluR5 mRNA editing with age: regional evaluation. *Dev. Brain Res.* **86**:359-63.
- Paterson PY (1960). Transfer of allergic encephalomyelitis in rats by means of lymph node cells. *J. Exp. Med.* **111**:119-33.

-
- Patneau DK & Mayer ML (1990). Structure-activity relationships for amino acid transmitter candidates acting at N-methyl-D-aspartate and quisqualate receptors. *J Neurosci*, **10**:2385-99.
- Patneau DK, Wright PW, Winters C, Mayer ML & Gallo V (1994). Glial cells of the oligodendrocyte lineage express both kainate- and AMPA-preferring subtypes of glutamate receptor. *Neuron* **12**:357-71.
- Paty DW & Li DK (1993). Interferon beta-1b is effective in relapsing-remitting multiple sclerosis. II. MRI analysis results of a multicenter, randomized, double-blind, placebo-controlled trial. UBC MS/MRI Study Group and the IFN β Multiple Sclerosis Study Group. *Neurology* **43**:662-7.
- Paxinos G & Watson C (1998). The rat brain in stereotaxic coordinates. Fourth Edition. Academic Press, London.
- Pellegrini-Giampietro DE, Zukin RS, Bennett MV, Cho S & Pulsinelli WA (1992). Switch in glutamate receptor subunit gene expression in CA1 subfield of hippocampus following global ischemia in rats. *Proc. Natl. Acad. Sci. USA* **89**:10499-503.
- Pender MP (1987). Demyelination and neurological signs in experimental allergic encephalomyelitis. *J. Neuroimmunol.* **15**:11-24.
- Pender MP (1988). The pathophysiology of MBP-induced acute experimental allergic encephalomyelitis in the Lewis rat. *J. Neurol. Sci.* **86**:277-89.
- Pender MP, Nguyen KB, McCombe PA & Kerr JF (1991). Apoptosis in the nervous system in experimental allergic encephalomyelitis. *J. Neurol. Sci.* **104**:81-7.
- Petralia RS, Wang YX, Mayat E & Wenthold RJ (1997). Glutamate receptor subunit 2-selective antibody shows a differential distribution of calcium-impermeable AMPA receptors among populations of neurons. *J. Comp. Neurol.* **385**:456-76.

-
- Piani D, Frei K, Do KQ, Cuenod M & Fontana A (1991). Murine brain macrophages induced NMDA receptor mediated neurotoxicity *in vitro* by secreting glutamate. *Neurosci. Lett.* **133**:159-62.
- Pikula AA, Rhee KD, Morin AM, Cohen RW (1998). Apoptosis: A suspected mechanism of neuronal degeneration in the *Spastic Han Wistar* rat. *Soc. Neurosci. Abstr.* **23**:Poster 17.13.
- Pin JP & Duvoisin R (1995). The metabotropic glutamate receptors: structure and functions. *Neuropharmacology* **34**:1-26.
- Pitt D, Werner P & Raine CS (2000). Glutamate excitotoxicity in a model of multiple sclerosis. *Nat. Med.* **6**:67-70.
- Pittermann W, Sontag K-H, Wand P, Papp K & Deerberg F (1976). Spontaneous occurrence of spastic paresis in Han:Wistar rats. *Neurosci. Lett.* **2**: 45-49.
- Plaitakis A (1990). Glutamate dysfunction and selective motor neuron degeneration in amyotrophic lateral sclerosis: a hypothesis. *Ann. Neurol.* **28**:3-8.
- Plaut GS (1987). Effectiveness of amantadine in reducing relapses in multiple sclerosis. *J. R. Soc. Med.* **80**:91-3.
- Pollak Y, Ovadia H, Goshen I, Gurevich R, Monsa K, Avitsur R, Yirmiya R (2000). Behavioral aspects of experimental autoimmune encephalomyelitis. *J. Neuroimmunol.* **104**:31-6.
- Pollard H, Heron A, Moreau J, Ben-Ari Y & Khrestchatisky M (1993). Alterations of the GluR-B AMPA receptor subunit flip/flop expression in kainate-induced epilepsy and ischemia. *Neuroscience* **57**:545-54.
- Portera-Cailliau C, Price DL & Martin LJ (1997). Non-NMDA and NMDA receptor-mediated excitotoxic neuronal deaths in adult brain are morphologically distinct: further evidence for an apoptosis-necrosis continuum. *J. Comp. Neurol.* **378**:88-104.

-
- Prineas JW, Barnard RO, Kwon EE, Sharer LR & Cho ES (1993). Multiple sclerosis: remyelination of nascent lesions. *Ann. Neurol.* **33**:137-51.
- Pulsinelli W, Sarokin A & Buchan A (1993). Antagonism of the NMDA and non-NMDA receptors in global versus focal brain ischemia. *Prog. Brain. Res.* **96**:125-35.
- Quarles RH (1997). Glycoproteins of myelin sheaths. *J. Mol. Neurosci.* **8**:1-12.
- Raine CS (1997). The neuropathology of multiple sclerosis. In: Raine CS, McFarland HF & Tourtellotte WW. *Multiple Sclerosis: Clinical and pathogenetic basis*. 1st Edition, Chapman & Hall. 151-71.
- Raine CS, Scheinberg L & Waltz JM (1981). Multiple sclerosis. Oligodendrocyte survival and proliferation in an active established lesion. *Lab. Invest.* **45**:534-46.
- Reddy H, Narayanan S, Matthews PM, Hoge RD, Pike GB, Duquette P, Antel J & Arnold DL (2000). Relating axonal injury to functional recovery in MS. *Neurology* **54**:236-9.
- Rivera-Quinones C, McGavern D, Schmelzer JD, Hunter SF, Low P & Rodriguez M (1998). Absence of neurological deficits following extensive demyelination in a class I-deficient murine model of multiple sclerosis. *Nat. Med.* **4**:187-93.
- Rivers TM, Sprunt DH & Berry GP (1933). Observations on attempts to produce acute disseminated encephalomyelitis in monkeys. *J. Exp. Med.* **58**:39-53.
- Robbins J (1959). The excitation and inhibition of crustacean muscle by amino acids. *J. Physiol*, **148**:39-50.
- Roberts PJ & Keen P (1973). Uptake of (¹⁴ C)glutamate into dorsal and ventral roots of spinal nerves of the rat. *Brain Res.* **57**:234-8.
- Roberts PJ & Mitchell JF (1972). The release of amino acids from the hemisectioned spinal cord during stimulation. *J. Neurochem.* **19**:2473-81.

- Roberts PJ (1995). Pharmacological tools for the investigation of metabotropic glutamate receptors (mGluRs): Phenylglycine derivatives and other selective antagonists – an update. *Neuropharmacology* **34**:813-9.
- Rogawski MA & Donevan SD (1999). AMPA receptors in epilepsy and as targets for antiepileptic drugs. *Adv. Neurol.* **79**:947-63.
- Rogers SW, Andrews PI, Gahring LC, Whisenand T, Cauley K, Crain B, Hughes TE, Heinemann SF & McNamara JO (1994). Autoantibodies to glutamate receptor GluR3 in Rasmussen's encephalitis. *Science* **265**:648-51.
- Rothstein JD, Van Kammen M, Levey AI, Martin LJ & Kuncl RW (1995). Selective loss of glial glutamate transporter GLT-1 in amyotrophic lateral sclerosis. *Ann. Neurol.* **38**:73-84.
- Sakimura K, Bujo H, Kushiya E, Araki K, Yamazaki M, Yamazaki M, Meguro H, Warashina A, Numa S & Mishina M (1990). Functional expression from cloned cDNAs of glutamate receptor species responsive to kainate and quisqualate. *FEBS Lett.* **272**:73-80.
- Sakimura K, Morita T, Kushiya E & Mishina M (1992). Primary structure and expression of the gamma 2 subunit of the glutamate receptor channel selective for kainate. *Neuron.* **8**:267-74.
- Saugstad JA, Kinzie JM, Mulvihill ER, Segerson TP & Westbrook GL (1994). Cloning and expression of a new member of the L-2-amino-4-phosphonobutyric acid-sensitive class of metabotropic glutamate receptors. *Mol. Pharmacol.* **45**:367-72.
- Saugstad JA, Kinzie JM, Shinohara MM, Segerson TP & Westbrook GL (1997). Cloning and expression of rat metabotropic glutamate receptor 8 reveals a distinct pharmacological profile. *Mol. Pharmacol.* **51**:119-25.
- Scaravilli F, An SF, Groves M & Thom M (1999). The neuropathology of paraneoplastic syndromes. *Brain Pathol.* **9**:251-60.

Schiffer HH, Swanson GT & Heinemann SF (1997). Rat GluR7 and a carboxy-terminal splice variant, GluR7b, are functional kainate receptor subunits with a low sensitivity to glutamate. *Neuron*, **19**:1141-6.

Schmied M, Breitschopf H, Gold R, Zischler H, Rothe G, Wekerle H & Lassmann H (1993). Apoptosis of T lymphocytes in experimental autoimmune encephalomyelitis. Evidence for programmed cell death as a mechanism to control inflammation in the brain. *Am. J. Pathol.* **143**:446-52.

Schmitt J, Dux E, Gissel C & Paschen W (1996). Regional analysis of developmental changes in the extent of GluR6 mRNA editing in rat brain. *Dev. Brain Res.* **91**:153-7.

Schoepp DD, Jane DE & Monn JA (1999). Pharmacological agents acting at subtypes of metabotropic glutamate receptors. *Neuropharmacology* **38**:1431-76.

Scholin CA, Gulland F, Doucette GJ, Benson S, Busman M, Chavez FP, Cordaro J, DeLong R, De Vogelaere A, Harvey J, Haulena M, Lefebvre K, Lipscomb T, Loscutoff S, Lowenstine LJ, Marin R 3rd, Miller PE, McLellan WA, Moeller PD, Powell CL, Rowles T, Silvagni P, Silver M, Spraker T, Trainer V & Van Dolah FM (2000). Mortality of sea lions along the central California coast linked to a toxic diatom bloom. *Nature* **403**:80-4.

Schulz JB, Matthews RT, Henshaw DR & Beal MF (1996). Neuroprotective strategies for treatment of lesions produced by mitochondrial toxins: Implications for neurodegenerative diseases. *Neuroscience* **71**:1043-8.

Schweichel JU & Merker HJ (1973). The morphology of various types of cell death in prenatal tissues. *Teratology* **7**:253-66.

Scolding NJ, Morgan BP, Houston WA, Linington C, Campbell AK & Compston DA (1989). Vesicular removal by oligodendrocytes of membrane attack complexes formed by activated complement. *Nature* **339**:620-2.

SPECTRIMS Secondary Progressive Efficacy Clinical Trial of Recombinant Interferon-beta-1a in MS Study Group (2001). Randomized controlled trial of interferon- beta-1a in secondary progressive MS: Clinical results. *Neurology* **56**:1496-504.

Sharrack B, Hughes RA, Morris RW, Soudain S, Wade-Jones O, Barnes D, Brown P, Britton T, Francis DA, Perkin GD, Rudge P, Swash M, Katifi HA, Farmer S & Frankel JP (2000). The effect of oral and intravenous methylprednisolone treatment on subsequent relapse rate in multiple sclerosis. *J. Neurol. Sci.* **173**:73-7.

Shaw PJ & Ince PG (1997), Glutamate, excitotoxicity and amyotrophic lateral sclerosis. *J. Neurol.* **244 Suppl 2**:S3-14.

Shaw PJ (1998). Excitotoxicity, genetics and neurodegeneration in amyotrophic lateral sclerosis. In: Seeburg PH, Turski L & Bresink I. *Excitatory amino acids: From genes to therapy*. Springer Verlag. 65-94.

Shaw PJ, Ince PG, Johnson M, Perry EK & Candy J (1991). The quantitative autoradiographic distribution of [3H]MK-801 binding sites in the normal human spinal cord. *Brain Res.* **539**:164-8.

Sheardown MJ, Nielsen EO, Hansen AJ, Jacobsen P & Honore T (1990). 2,3-Dihydroxy-6-nitro-7-sulfamoyl-benzo(F)quinoxaline: a neuroprotectant for cerebral ischemia. *Science* **247**:571-4.

Shrager P & Novakovic SD (1995). Control of myelination, axonal growth, and synapse formation in spinal cord explants by ion channels and electrical activity. *Brain Res. Dev.* **88**:68-78.

Siesjo BK (1988). Acidosis and ischemic brain damage. *Neurochem. Pathol.* **9**:31-88.

Simmons RD, Bernard CC, Singer G & Carnegie PR (1982). Experimental autoimmune encephalomyelitis. An anatomically-based explanation of clinical progression in rodents. *J. Neuroimmunol.* **3**:307-18.

Simon JH, Lull J, Jacobs LD, Rudick RA, Cookfair DL, Herndon RM, Richert JR, Salazar AM, Sheeder J, Miller D, McCabe K, Serra A, Champion MK, Fischer JS, Goodkin DE, Simonian N, Lajaunie M, Wende K, Martens-Davidson A, Kinkel RP & Munschauer FE 3rd (2000). A longitudinal study of T1 hypointense lesions in relapsing MS: MSCRG trial of interferon beta-1a. Multiple Sclerosis Collaborative Research Group. *Neurology* **55**:185-92.

Singh VK, Mehrotra S, Narayan P, Pandey CM & Agarwal SS (2000). Modulation of autoimmune diseases by nitric oxide. *Immunol. Res.* **22**:1-19.

Sladeczek F, Pin JP, Recasens M, Bockaert J & Weiss S (1985). Glutamate stimulates inositol phosphate formation in striatal neurones. *Nature*, **317**:717-9.

Slusher BS, Vornov JJ, Thomas AG, Hurn PD, Harukuni I, Bhardwaj A, Traystman RJ, Robinson MB, Britton P, Lu XC, Tortella FC, Wozniak KM, Yudkoff M, Potter BM, Jackson PF Slusher BS, Vornov JJ, Thomas AG, Hurn PD, Harukuni I, Bhardwaj A, Traystman RJ, Robinson MB, Britton P, Lu XC, Tortella FC, Wozniak KM, Yudkoff M, Potter BM & Jackson PF (1999). Selective inhibition of NAALADase, which converts NAAG to glutamate, reduces ischemic brain injury. *Nat. Med.* **5**:1396-402.

Slusher BS, Wozniak KM, Hartman T, Jada P, Chadran M & Dalcanto M (2000). NAALADase inhibition increases survival and delays clinical symptoms in an SOD transgenic model of ALS. *Soc. Neurosci. Abst.* **26**:Poster 43.10.

Smith T, Groom A, Zhu B & Turski L (2000). Autoimmune encephalomyelitis ameliorated by AMPA antagonists. *Nat. Med.* **6**:62-6.

Smith T, Schmied M, Hewson AK, Lassmann H & Cuzner ML (1996). Apoptosis of T cells and macrophages in the central nervous system of intact and adrenalectomized Lewis rats during experimental allergic encephalomyelitis. *J. Autoimmun.* **9**:167-74.

Sobel RA, Tuohy VK, Lu ZJ, Laursen RA & Lees MB (1990). Acute experimental allergic encephalomyelitis in SJL/J mice induced by a synthetic peptide of myelin proteolipid protein. *J. Neuropathol. Exp. Neurol.* **49**:468-79.

- Sommer B, Burnashev N, Verdoorn TA, Keinänen K, Sakmann B & Seeburg PH (1992). A glutamate receptor channel with high affinity for domoate and kainate. *EMBO. J.* **11**:1651-6.
- Sommer B, Keinänen K, Verdoorn TA, Wisden W, Burnashev N, Herb A, Köhler M, Takagi T, Sakmann B & Seeburg PH (1990). Flip and flop: a cell-specific functional switch in glutamate-operated channels of the CNS. *Science*, **249**:1580-5.
- Spencer PS, Roy DN, Ludolph A, Hugon J, Dwivedi MP & Schaumburg HH (1986). Lathyrism: evidence for role of the neuroexcitatory aminoacid BOAA. *Lancet* **2**:1066-7.
- Sperandio S, de Belle I & Bredesen DE (2000). An alternative, nonapoptotic form of programmed cell death. *Proc. Natl. Acad. Sci. USA* **97**:14376-81.
- Sriram S, Stratton CW, Yao S, Tharp A, Ding L, Bannan JD & Mitchell WM (1999). *Chlamydia pneumoniae* infection of the central nervous system in multiple sclerosis. *Ann. Neurol.* **46**:6-14.
- Starck M, Albrecht H, Pollmann W, Straube A & Dieterich M (1997). Drug therapy for acquired pendular nystagmus in multiple sclerosis. *J. Neurol.* **244**:9-16.
- Stauch BL, Robinson MB, Forloni G, Tsai G & Coyle JT (1989). The effects of N-acetylated alpha-linked acidic dipeptidase (NAALADase) inhibitors on [3H]NAAG catabolism *in vivo*. *Neurosci. Lett.* **100**:295-300.
- Stewart GR, Olney JW, Pathikonda M & Snider WD (1991). Excitotoxicity in the embryonic chick spinal cord. *Ann. Neurol.* **30**:758-66.
- Storch MK, Stefferl A, Brehm U, Weissert R, Wallström E, Kerschensteiner M, Olsson T, Linington C & Lassmann H (1998). Autoimmunity to myelin oligodendrocyte glycoprotein in rats mimics the spectrum of multiple sclerosis pathology. *Brain Pathol.* **8**:681-94.

- Stover JF, Lowitzsch K & Kempfski OS (1997a). Cerebrospinal fluid hypoxanthine, xanthine and uric acid levels may reflect glutamate-mediated excitotoxicity in different neurological diseases. *Neurosci. Lett.* **238**:25-8.
- Stover JF, Pleines UE, Morganti-Kossmann MC, Kossmann T, Lowitzsch K & Kempfski OS (1997b). Neurotransmitters in cerebrospinal fluid reflect pathological activity. *Eur. J. Clin. Invest.* **27**:1038-43.
- Sun D, Whitaker JN, Huang Z, Liu D, Coleclough C, Wekerle H & Raine CS (2001). Myelin antigen-specific CD8⁺ T cells are encephalitogenic and produce severe disease in C57BL/6 mice. *J. Immunol.* **166**:7579-87.
- Swanson GT, Feldmeyer D, Kaneda M & Cull-Candy SG (1996). Effect of RNA editing and subunit co-assembly on single-channel properties of recombinant kainate receptors. *J. Physiol.* **492**:129-42.
- Swanson GT, Gereau RW 4th, Green T & Heinemann SF (1997). Identification of amino acid residues that control functional behavior in GluR5 and GluR6 kainate receptors. *Neuron* **19**:913-26
- Tachibana M, Wenthold RJ, Morioka H & Petralia RS (1994). Light and electron microscopic immunocytochemical localization of AMPA-selective glutamate receptors in the rat spinal cord. *J. Comp. Neurol.* **344**:431-54.
- Tanabe Y, Masu M, Ishii T, Shigemoto R & Nakanishi S (1992). A family of metabotropic glutamate receptors. *Neuron*, **8**:169-79.
- Tarnawa I & Vizi ES (1998). 2,3-benzodiazepine AMPA antagonists. *Restor. Neurol. Neurosci.* **13**:41-57.
- Taupin V, Renno T, Bourbonniere L, Peterson AC, Rodriguez M & Owens T (1997). Increased severity of experimental autoimmune encephalomyelitis, chronic macrophage/microglial reactivity, and demyelination in transgenic mice producing tumor necrosis factor-alpha in the central nervous system. *Eur. J. Immunol.* **27**:905-13.

Teitelbaum JS, Zatorre RJ, Carpenter S, Gendron D, Evans AC, Gjedde A & Cashman NR (1990). Neurologic sequelae of domoic acid intoxication due to the ingestion of contaminated mussels. *N. Engl. J. Med.* **322**:1781-7.

Tekkok SB & Goldberg MP (2001). Ampa/kainate receptor activation mediates hypoxic oligodendrocyte death and axonal injury in cerebral white matter. *J. Neurosci.* **21**:4237-48.

The IFN β Multiple Sclerosis Study Group (1993). Interferon beta-1b is effective in relapsing-remitting multiple sclerosis. I. Clinical results of a multicenter, randomized, double-blind, placebo-controlled trial. *Neurology* **43**:655-61.

The IFN β Multiple Sclerosis Study Group and The University of British Columbia MS/MRI Analysis Group (1995). Interferon beta-1b in the treatment of multiple sclerosis: final outcome of the randomized controlled trial. *Neurology* **45**:1277-85.

The Transatlantic Multiple Sclerosis Genetics Cooperative (2001). A meta-analysis of genomic screens in multiple sclerosis. The Transatlantic Multiple Sclerosis Genetics Cooperative. *Mult. Scler.* **7**:3-11.

Tokarev D & Jezova D (1997). Effect of central administration of the non-NMDA receptor antagonist DNQX on ACTH and corticosterone release before and during immobilization stress. *Methods Find. Exp. Clin. Pharmacol.* **19**:323-8.

Trapp BD, Ransohoff R & Rudick R (1999). Axonal pathology in multiple sclerosis: relationship to neurologic disability. *Curr. Opin. Neurol.* **12**:295-302.

Traynelis SF & Cull-Candy SG (1990). Proton inhibition of N-methyl-D-aspartate receptors in cerebellar neurons. *Nature*, **345**:347-50.

Traynelis SF, Hartley M & Heinemann SF (1995). Control of proton sensitivity of the NMDA receptor by RNA splicing and polyamines. *Science*, **268**:873-6.

Turecky L, Liska B & Pechan I (1980). Glycine in the central nervous system in experimental allergic encephalomyelitis. *J. Neurochem.* **35**:735-8.

- Turmaine M, Raza A, Mahal A, Mangiarini L, Bates GP & Davies SW (2000). Nonapoptotic neurodegeneration in a transgenic mouse model of Huntington's disease. *Proc. Natl. Acad. Sci. USA* **97**:8093-7.
- Turski L, Bressler K, Rettig KJ, Loschmann PA & Wachtel H (1991). Protection of substantia nigra from MPP⁺ neurotoxicity by N-methyl-D-aspartate antagonists. *Nature* **349**:414-8.
- Turski L, Huth A, Sheardown M, McDonald F, Neuhaus R, Schneider HH, Dirnagl U, Wiegand F, Jacobsen P & Ottow E (1998). ZK200775: a phosphonate quinoxalinedione AMPA antagonist for neuroprotection in stroke and trauma. *Proc. Natl. Acad. Sci. USA* **95**:10960-5.
- Turski L, Jacobsen P, Honore T & Stephens DN (1992). Relief of experimental spasticity and anxiolytic/anticonvulsant actions of the alpha-amino-3-hydroxy-5-methyl-4-isoxazolepropionate antagonist 2,3-dihydroxy-6-nitro-7-sulfamoylbenzo(F)quinoxaline. *J. Pharmacol. Exp. Ther.* **260**:742-7.
- Turski L, Klockgether T, Turski WA, Schwartz M & Sontag KH (1990). The entopeduncular nucleus regulates muscle tone in genetically spastic rats: role of substance P and gamma-aminobutyric acid. *Brain Res.* **509**:347-50.
- Turski L, Schwarz M, Turski WA, Klockgether T, Sontag KH & Collins JF (1985). Muscle relaxant action of excitatory amino acid antagonists. *Neurosci. Lett.* **53**:321-6.
- Turski WA, Turski L, Czuczwar SJ & Kleinrok Z (1981). (RS)- α -Amino-3-hydroxy-5-methyl-4-isoxazolepropionic acid: wet dog shakes, catalepsy and body temperature changes in rats. *Pharmacol. Biochem. Behav.* **15**:546-9.
- Van Harreveld A & Mendelson M (1959). Glutamate-induced contractions in crustacean muscle. *J Cell Comp Physiol*, **54**:85-94.
- van Lookeren Campagne M & Gill R (1996). Ultrastructural morphological changes are not characteristic of apoptotic cell death following focal cerebral ischaemia in the rat. *Neurosci. Lett.* **213**:111-4.

van Walderveen MA, Barkhof F, Pouwels PJ, van Schijndel RA, Polman CH & Castelijns JA (1999). Neuronal damage in T1-hypointense multiple sclerosis lesions demonstrated *in vivo* using proton magnetic resonance spectroscopy. *Ann. Neurol.* **46**:79-87

Vandenberghe W, Ihle EC, Patneau DK, Robberecht W & Brorson JR (2000). AMPA receptor current density, not desensitization, predicts selective motoneuron vulnerability. *J. Neurosci.* **20**:7158-66.

Verdoorn TA, Burnashev N, Monyer H, Seeburg PH & Sakmann B (1991). Structural determinants of ion flow through recombinant glutamate receptor channels. *Science.* **252**:1715-8.

Vesce S, Bezzi P & Volterra A (1999). The active role of astrocytes in synaptic transmission. *Cell. Mol. Life Sci.* **56**:991-1000.

Villaroya H, Violleau K, Ben Younes-Chennoufi A & Baumann N (1996). Myelin-induced experimental autoimmune encephalomyelitis in Lewis rats: Tumour necrosis factor α levels in serum and cerebrospinal fluid. Immunohistochemical expression in glial cells and macrophages of optic nerve and spinal cord. *J. Neuroimmunol.* **64**:55-61.

Wagemann E, Schmidt-Kastner R, Block F & Sontag KH (1991). Neuronal degeneration in hippocampus and cerebellum of mutant spastic Han-Wistar rats. *Neurosci. Lett.* **121**:102-6.

Wagemann E, Schmidt-Kastner R, Block F & Sontag KH (1995). Altered pattern of immunohistochemical staining for glial fibrillary acidic protein (GFAP) in the forebrain and cerebellum of the mutant spastic rat. *J. Chem. Neuroanat.* **8**:151-63.

Waksman BH (1959). Experimental allergic encephalomyelitis and the 'auto-allergic' diseases. *Int. Arch. Allergy Appl. Immunol.* **14(Suppl)**:1-87.

Wallström E, Diener P, Ljungdahl A, Khademi M, Nilsson CG & Olsson T (1996). Memantine abrogates neurological deficits, but not CNS inflammation, in Lewis rat experimental autoimmune encephalomyelitis. *J. Neurol. Sci.* **137**:89-96.

Waxman SG & Ritchie JM (1993). Molecular dissection of the myelinated axon. *Ann. Neurol.* **33**:121-36.

Weerth S, Berger T, Lassmann H & Linington C (1999). Encephalitogenic and neuritogenic T cell responses to the myelin-associated glycoprotein (MAG) in the Lewis rat. *J. Neuroimmunol.* **95**:157-64.

Weinshenker BG, O'Brien PC, Petterson TM, Noseworthy JH, Lucchinetti CF, Dodick DW, Pineda AA, Stevens LN & Rodriguez M (1999). A randomized trial of plasma exchange in acute central nervous system inflammatory demyelinating disease. *Ann. Neurol.* **46**:878-86.

Werner P, Pitt D & Raine CS (2001). Multiple sclerosis: altered glutamate homeostasis in lesions correlates with oligodendrocyte and axonal damage. *Ann. Neurol.* **50**:169-80.

Werner P, Voigt M, Keinänen K, Wisden W & Seeburg PH (1991). Cloning of a putative high-affinity kainate receptor expressed predominantly in hippocampal CA3 cells. *Nature*, **351**:742-4.

Williams TL, Day NC, Ince PG, Kamboj RK & Shaw PJ (1997). Calcium-permeable alpha-amino-3-hydroxy-5-methyl-4-isoxazole propionic acid receptors: a molecular determinant of selective vulnerability in amyotrophic lateral sclerosis. *Ann. Neurol.* **42**:200-7.

Williams TL, Ince PG, Oakley AE & Shaw PJ (1996). An immunocytochemical study of the distribution of AMPA selective glutamate receptor subunits in the normal human motor system. *Neuroscience* **74**:185-98.

Wofsey AR, Kuhar MJ & Snyder SH (1971). A unique synaptosomal fraction which accumulates glutamic and aspartic acids in brain tissue. *Proc Nat Acad Sci USA*, **68**:1102-6.

Wolosker H, Blackshaw S & Snyder SH (1999). Serine racemase: A glial enzyme synthesizing D-serine to regulate glutamate-N-methyl-D-aspartate neurotransmission. *Proc. Natl. Acad. Sci. USA*, **96**:13409-13414.

Wozniak KM, Callizot N, Poindron P, & Slusher BS (2000). NAALADase inhibition enhances behavioral and morphological recovery following sciatic nerve crush in mice. *Soc. Neurosci. Abst.* **26**:Poster 43.11.

Wyllie AH (1980). Glucocorticoid-induced thymocyte apoptosis is associated with endogenous endonuclease activation. *Nature* **284**:555-6.

Wyllie AH, Beattie GJ & Hargreaves AD (1981). Chromatin changes in apoptosis. *Histochem. J.* **13**:681-92.

Wyllie AH, Kerr JF & Currie AR. (1980). Cell death: the significance of apoptosis. *Int. Rev. Cytol.* **68**:251-306.

Yong VW, Chabot S, Stuve O & Williams G (1998). Interferon beta in the treatment of multiple sclerosis: mechanisms of action. *Neurology* **51**:682-9.

Yoshioka A, Bacskai B & Pleasure D (1996). Pathophysiology of oligodendroglial excitotoxicity. *J. Neurosci. Res.* **46**:427-37.

Yoshioka A, Hardy M, Younkin DP, Grinspan JB, Stern JL & Pleasure D (1995). Alpha-amino-3-hydroxy-5-methyl-4-isoxazolepropionate (AMPA) receptors mediate excitotoxicity in the oligodendroglial lineage. *J. Neurochem.* **64**:2442-8.

Publications Relevant to Thesis

Peer Reviewed Articles

Smith T, **Groom A**, Zhu B & Turski L (2000). Autoimmune encephalomyelitis ameliorated by AMPA antagonists. *Nat. Med.*, **6**:62-66.

Kuner R, **Groom A**, Bresink I, Müller G, Kornau H-C, Sprengel R, Ikonomidou C, Catania MV, Seeburg P & Turski L. Motoneuron disease in mice with extended Q/R site editing of AMPA receptor subunit GluR-B. *In preparation*.

Abstracts

Groom A, Zhu B, Müller G, & Turski L (1998). Neurodegeneration in the brain and spinal cord of genetically determined *spa/spa* rats. *Soc. Neurosci. Abst.* **24**:Poster 569.16.

Smith T, **Groom A** & Turski L (1999). The AMPA antagonist NBQX ameliorates experimental autoimmune encephalomyelitis. *Soc. Neurosci. Abst.* **25**:Poster 17.13.

Groom A, Smith T, Zhu B & Turski L (1999). Spinal motoneurons in experimental autoimmune encephalomyelitis. *Soc. Neurosci. Abst.* **25**:Poster 628.7.